Advanced oxidation processes for water treatment: Reactor design and case studies

Von der Fakultät für Umweltwissenschaften und Verfahrenstechnik der Brandenburgischen Technischen Universität Cottbus zur Erlangung des akademischen Grades eines Doktor-Ingenieurs (Dr.-Ing.)

genehmigte Dissertation

vorgelegt von

M. Sc.

Mohammad Mehrjouei

geboren am 06. September 1977 in Karbala, Iraq

Gutachter: Prof. Dr. Detlev Möller

Gutachter: Prof. Dr. Günter Busch

Tag der mündlichen Prüfung: 22.05.2012

Abstract

The aim of this work was to study in detail the physical-chemical aspects of water and wastewater treatment using different so-called “advanced oxidation systems”. Our target was to construct an annular multiphase falling film reactor with a fixed photocatalyst (TiO_2) and to compare its performance with that of a planar reactor in different chemical oxidation regimes. The annular design of the falling film reactor was prepared for heterogeneous photocatalytic oxidation systems by combining three different phases (solid fixed photocatalyst, falling liquid wastewater and an ozone/oxygen gaseous mixture). UVA light sources were employed for irradiation of the photocatalyst surface.

In the first step, the design, construction and characterisation of the reactor was performed. The next step was the assessment of the performance of the falling film reactor in the decomposition of selected organic chemicals as model compounds. Six different oxidation methods were evaluated for the degradation of model compounds. Photo-oxidation (UVA/O_2), photo-ozonation (UVA/O_3), ozonation (O_3), catalytic ozonation ($TiO2/O_3$), photocatalytic oxidation ($TiO_2/UVA/O_2$) and photocatalytic ozonation ($TiO_2/UVA/O_3$) processes were investigated in this study. It was shown that due to the synergetic effects between ozone molecules and the irradiated surface of TiO_2, photocatalytic ozonation was the most effective oxidation process for the decomposition of model compounds. Oxalic acid, dichloroacetic acid, citric acid, terephthalic acid, p-chlorobenzoic acid, methyl tert-butyl ether, ethyl tert-butyl ether, tert-amyl ethyl ether and tert-butanol were chosen as model compounds.

Two different immobilisation techniques were employed and evaluated for fixing TiO_2 nanoparticles onto the reactor walls. The immobilisation of photocatalysts was performed on

borosilicate glass and polymethylmethacrylate. It was observed that the photoactivity of fixed TiO_2 particles on borosilicate glass was higher than that on polymethylmethacrylate. The stability of immobilised photocatalysts on both substrates was good.

The influences of different experimental parameters, such as the initial concentration of model compounds, ozone concentration, solution pH, temperature and solution recycling rate on the degradation rate and efficiency of the oxidation systems were studied and discussed. In terms of the characterisation of the falling film reactor, different aspects were studied. The thickness and distribution pattern of falling films, the gas washing effects of falling films, the absorption of ozone in the falling films, the adsorption of organic pollutants on the photocatalyst surface, the effect of UVA irradiation on ozone decomposition, etc. were studied in detail.

The concentration of model compounds was determined by ion chromatography (IC), high performance liquid chromatography (HPLC) and headspace techniques. Chemical oxygen demand (COD) was applied to quantify the quality of wastewaters and total organic carbon (TOC) measurements were employed for the determination of model compound mineralisation.

At the end of this study, treatment of real wastewater was performed by means of the falling film reactor as a case study. The real wastewater was produced in a pyrolysis process. More than 30 organic and inorganic compounds were included in the composition of this wastewater. The application of ozone-based advanced oxidation processes showed good results in terms of colour and odour removal of pyrolysis wastewater as well as in terms of decreasing its COD.

List of contents

1. Theoretical

1.1. Introduction

Currently, water plays a significant role in our daily activities. Imagining a world without water available for typical domestic chores (bathing, cooking, cleaning, heating and cooling, etc.) is definitely impossible. Just like power, fuel, raw materials and other vital elements are necessary for a wide variety of manufacturing industries all over the world, even a small shortage of water can affect these processes negatively or completely stop them. It is evident that a lack or insufficiency of water, either from rain sources or brought by irrigation systems to agricultural fields, leads to non-repairable detriments on production rates as well as on the quality of products. Despite this, around $1.26 \cdot 10^9$ km^3 water is spread out over approximately two thirds of the Earth's surface area. This water is continuously recycled between oceans, air and land. Some politicians believe that attaining more water resources will be a strong reason for war between different nations in the future.

As life standards improve, water consumption levels and, as a result, wastewater generation rates are enhanced. Considering the numerous sources of wastewater, such as domestic residences, medical and pharmaceutical departments, agricultural lands, commercial properties, industrial plants, etc., many methods and technologies are being used for the treatment of water and wastewater discharged by these sectors. Based on the level of toxicity, removal complexity and the chemical and biological characteristics of the contaminants in the wastewater, a broad spectrum of techniques have been developed for decontamination processes.

In this study, new modifications on one of the present technologies used in the treatment of water and wastewater, called “advanced oxidation processes (AOPs)”, will be introduced.

1.2. Overview

State of the art decontamination technologies are based on condensation, gas washing, adsorption, bio-filtration as well as thermal or catalytic combustion. As a result, pollution problems are often only shifted from one medium to another because the pollutants are not decomposed (with the exception of combustion) [1].

In comparison with the techniques mentioned above, the employment of new technologies with the generic term “advanced oxidation processes” leads to the decomposition and mineralisation of many groups of organic materials in both the liquid [2] and gas [3] phases. AOPs have attracted significant attention in recent years. Depending on the chemical structure of the pollutant molecules, AOPs mineralise numerous pollutants into ultimately harmless substances like CO_2 and H_2O and therefore avoid the issue of pollution shifting. The particular importance of these technologies appears to be in destroying biologically non-degradable chemical structures as well as ozone-resistant substances such as organic pesticides and herbicides [4-6], aromatic structures [7], organo-halogens [8] and petroleum constituents [9] in wastewaters.

In a general definition, physicochemical procedures which promote in situ generation of free hydroxyl radicals as highly oxidative reagents for the decomposition of pollutants in water or air are described as “advanced oxidation processes”. These oxidation processes basically use three different reagents: ozone, hydrogen peroxide and oxygen in many combinations, either combined with each other or applied with UV irradiation and/or various kinds of catalysts homogeneously and heterogeneously [10]. Due to the generation of increased amounts of OH radicals, combination of two or more AOPs usually leads to higher oxidation rates. With promising results observed on the laboratory scale, compared with conventional water and wastewater treatment methods, these technologies will likely be more essential for real applications in the near future. However, the reactivity of hydroxyl radicals with radical scavengers (carbonate, phosphate, etc.), which exist in real wastewaters, is the main disadvantage of all oxidative degradation processes based on hydroxyl radical reactions [11].

1.2.1. Characteristics of photocatalysts

1.2.1.1. Photoexcitation

One of the outstanding advanced oxidation technologies is the photoexcitation of semiconductor surfaces with ultraviolet-visible radiation, which provides the appropriate band gap energies to generate photoactivated electron-hole pairs; electrons (e^-) migrate to the conductivity band and holes (h^+) are produced in the valance band (Fig. 1.1). The photogenerated electrons and holes are assumed to diffuse to the surface and react with the electrophilic and nucleophilic substances absorbed on the photocatalyst surface, respectively, producing activated and unstable products, A and B (Reactions 1.1 to 1.3).

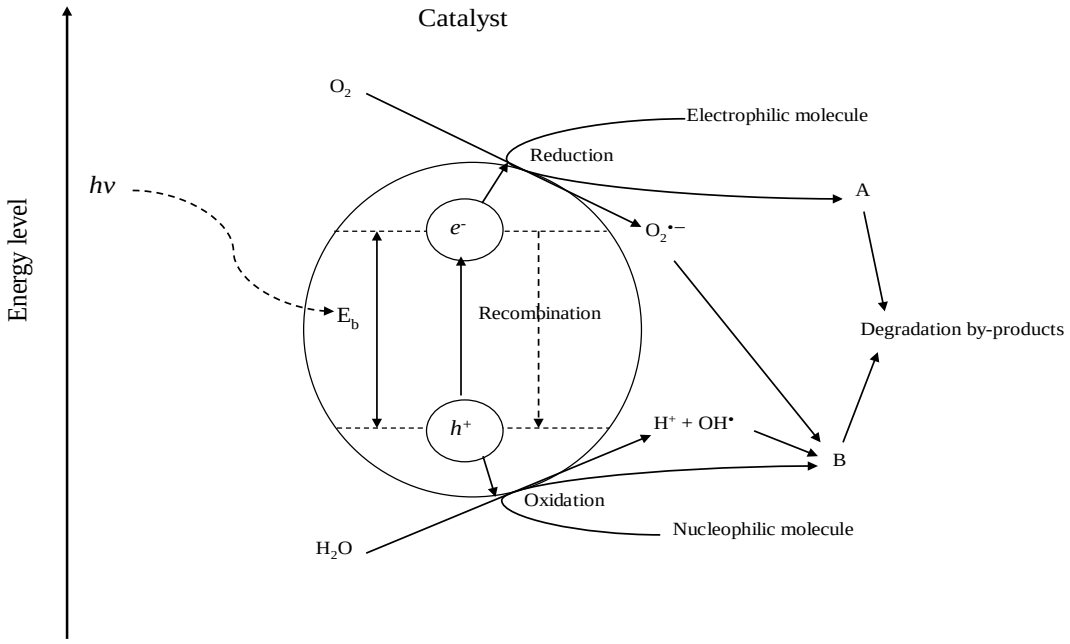

Fig. 1.1. Photogeneration of electron-hole pairs and their oxidative-reductive reactions [12]

$$\text{semiconductor} \xrightarrow{h\nu} \text{electron}^{(-)} + \text{hole}^{(+)} \xrightarrow{\text{recombination}} \text{semiconductor} + \text{heat} \quad (1.1)$$

or {

$$\text{electron}^{(-)} + \text{electrophilic molecule}_{(ads)} \rightarrow \text{Product A} \quad (1.2)$$

$$\text{hole}^{(+)} + \text{nuceophile molecule}_{(ads)} \rightarrow \text{Product B} \quad (1.3)$$

Depending on the variety of molecules adsorbed on the photocatalyst surface and their reaction rates with electron-hole pairs, the generation of more than two intermediates likely occurs as a result of the interaction between the present molecules and these photogenerated species. The mean life of the electron-hole pairs before recombination is on the order of nanoseconds and, unfortunately, this recombination negatively affects the reduction and oxidation reactions on the photocatalyst surface. This event quantitatively decreases the effective interactions and consequently reduces the performance of this technology.

The most interesting approach, highlighting this technology as an effective one, is the generation of hydroxyl radicals via interactions between the photogenerated holes and water molecules adsorbed on the photocatalyst surface. Furthermore, the presence of adsorbed oxygen molecules near the photogenerated electrons leads to the formation of superoxide radical anions ($O_2^{\cdot -}$) and reduces the possibility of electron-hole recombination as a result. These superoxide radical anions either oxidise the pollutant molecules directly or generate further hydroxyl radicals.

Hydroxyl radicals are well-known for being able to either oxidise in the interface as adsorbed species on the photocatalyst surface or to diffuse away into the bulk of the solution and promote oxidation reactions with pollutants therein. It is worth mentioning that, depending upon the conditions, hydroxyl or superoxide radicals, holes, hydrogen peroxide and oxygen molecules can play roles at different levels in the photocatalytic treatment.

1.2.1.2. TiO_2 as a photocatalyst

TiO_2 is a semiconductor most commonly used as a photocatalyst for environmental purification, showing considerable potential in this process [13-15]. This photocatalyst is relatively inexpensive and is commercially available under more than one trademark. Degussa P-25, BDH, Sachtleben Hombikat UV100 and Millennium TiONA PC50 are examples of commercial TiO_2 materials commonly used for scientific investigation [16, 17]. TiO_2 is chemically inert and stable and has relatively low toxicity. This semiconductor mainly occurs in nature in three forms called anatase, rutile and brookite (Fig. 1.2). Anatase seems to be the most photoactive form, while rutile has the most stable structure, such that other forms convert to rutile when heated or processed at temperatures higher than 600°C [18].

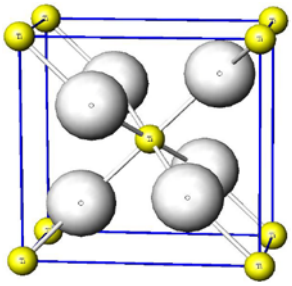

a) Rutile

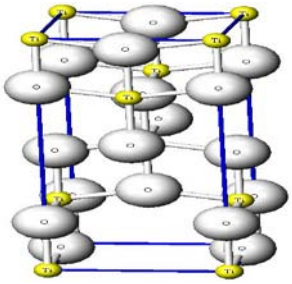

b) Anatase

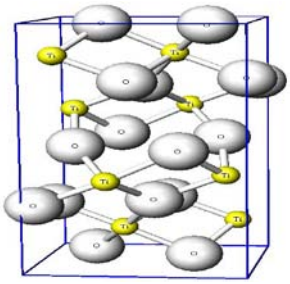

c) Brookite

Fig. 1.2. TiO_2 crystal structures [19]

Fig. 1.3 represents the redox potential for conductivity band electrons and photogenerated holes at the valence band for both rutile and anatase compared to the reduction potential of oxygen and ozone [20]. Considering Fig. 1.3, it is evident that the crystalline structure of TiO_2 determines the band gap energy and, as a result, indicates the light adsorption properties of the semiconductor. Samples of TiO_2 with a mixture of anatase and rutile are more active than both the pure crystalline phases [21]. This increased activity is due to the fact that the photoexcited electrons at conduction band of the anatase part jump to that of the rutile part which is less positive, leading to a decrease in electron-hole recombination and, consequently, an increase in photoactivity [21].

1.2.1.3. Superhydrophilicity

The other unique phenomenon relating to TiO_2 is called “superhydrophilicity”. This photo-induced aspect, which has been well-described by Fujishima et al. [15] leads to high wettability of surfaces coated by TiO_2 particles after UV illumination. In the case of illumination, the photogenerated electrons tend to reduce Ti (IV) cations to the Ti (III) state and the holes oxidise O^{2-} to O_2. Fig. 1.4 shows that the ejection of oxygen molecules creates oxygen vacancies which

then become occupied by H_2O molecules, generating a hydrophilic surface. This character of TiO_2 coatings is considered to be a vital factor for providing suitable falling liquid films in the falling film reactor.

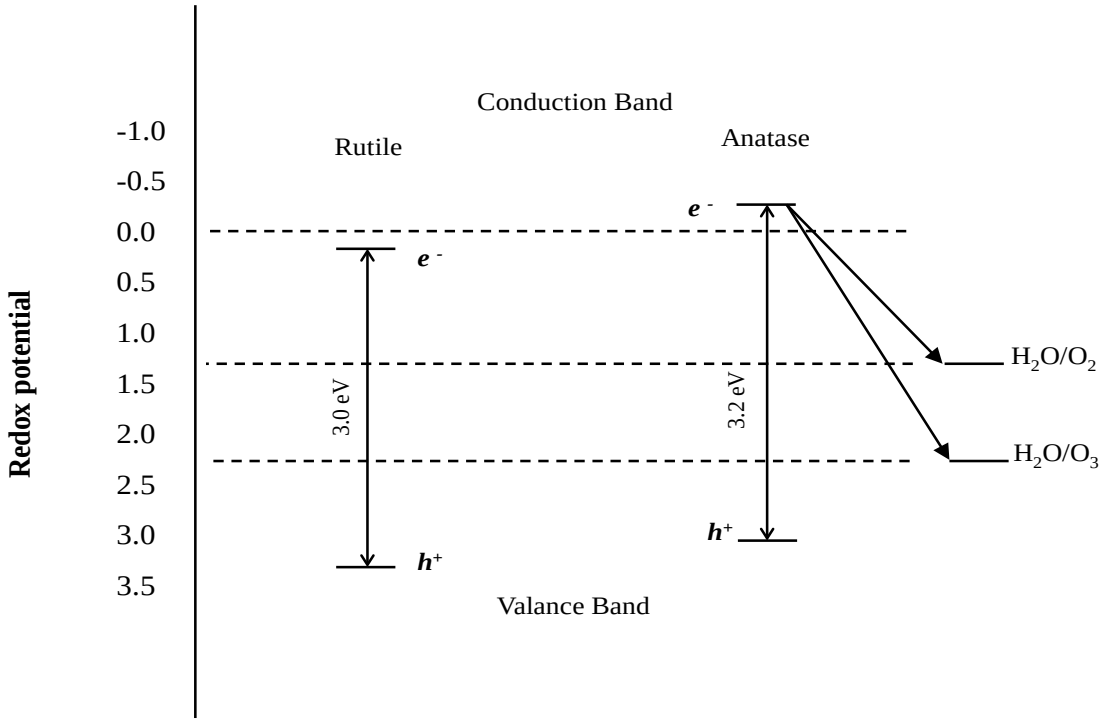

Fig. 1.3. Redox potential of electrons and holes for rutile and anatase [20]

In addition to increased attention to the properties of TiO_2 itself, many studies in the literature have reported improvements in the photoactivity of TiO_2 particles where they have been employed either chemically impregnated (doped) or physically implanted with other materials like carbon atoms [22] or carbon nanotubes [23], transition metal ions [24], noble metals [25], non-metals [26], etc. These modifications are basically made with the aim of (1) widening the wavelength spectrum for photonic activation of TiO_2, especially toward cheap and more available visible wavelengths by narrowing the band gap, (2) stabilising the anatase structure in the catalyst composition, (3) decreasing hole-electron recombination by scavenging excited electrons and/or holes and (4) increasing the adsorption of organic molecules on the catalyst surface by enhancing the specific surface area.

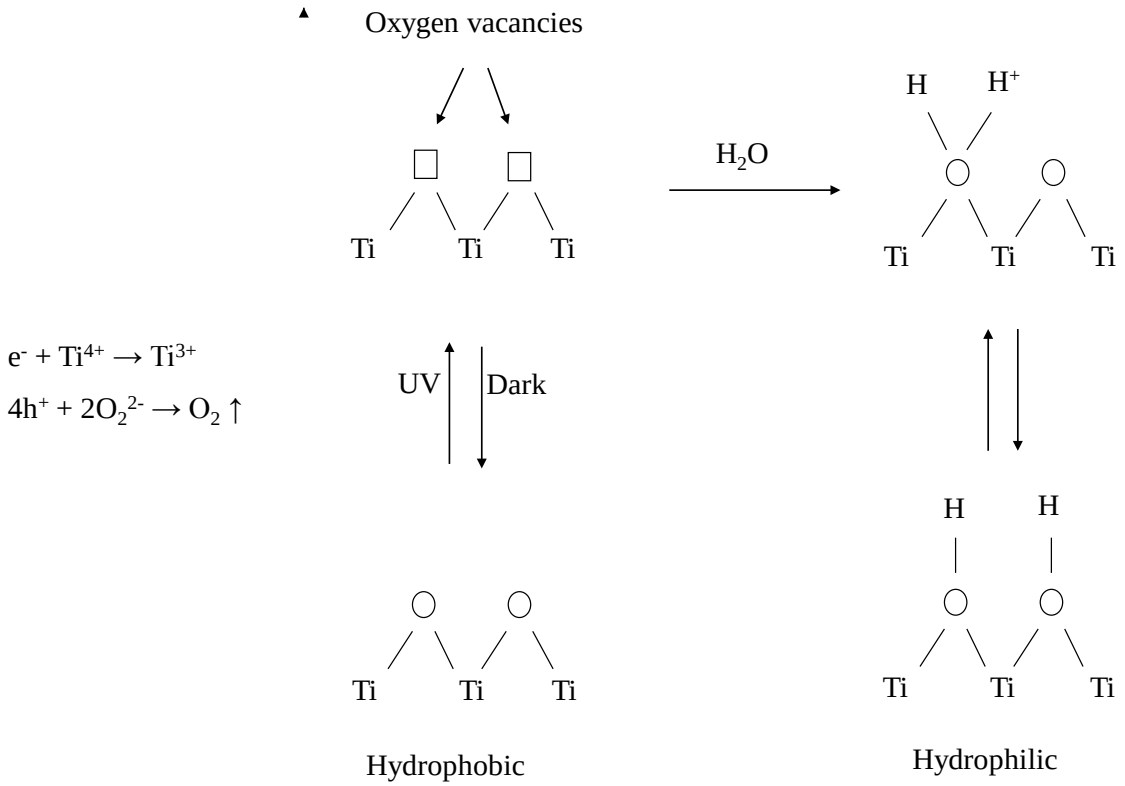

Fig. 1.4. Superhydrophilicity of TiO_2 [15]

1.2.1.4. Application of photocatalysts

Photocatalysts are generally utilised in the treatment of water and wastewater using two approaches. The first approach is the immobilisation of catalyst particles on stable and inert substrates and the second is adding catalyst particles to polluted water and using them in a suspended form. Published reports in recent years show that both techniques still have interest for researchers [27-30].

Unlike systems employing photocatalyst immobilisation setups, which frequently suffer from mass transfer problems, application of a photocatalyst suspended in a liquid solution in a slurry form represents more modified mass transfer conditions; in the latter procedure, the quantities of semiconductor particles involved in the redox processes are usually greater than for immobilised semiconductor systems. The interactions occur in the interfacial region around each particle in suspension, while interactions are assumed to be more limited when the particles are fixed close to each other on supporting materials. However, the need for filtering and recycling

of photocatalyst particles after the treatment and, furthermore, the extinction of UV-vis light due to scattering and adsorption of the radiation by the particles existing in the reaction medium are considered to be two significant disadvantages for suspension applications, leading to less attention to these setups, especially when practical features are being considered.

1.2.2. Ozone and ozonation

1.2.2.1. Ozone properties

Ozone was recognised for the first time in 1840 by a German scientist, Christian Friedrich Schönbein (1799-1868). At that time, he chose the name “ozone” for this unknown gas from the Greek term “ozein” which means “to smell”, which was determined easily by its penetrating odour. Nowadays, this compound has a wide range of applications, for example as a chemical reagent in the synthesis of pharmaceuticals, in lubricants and many other organic compounds, as well as for the purification, decontamination and disinfection of water. Due to its relatively high redox potential (Reaction 1.4), ozone reacts with many categories of organic and inorganic compounds.

$$O_3 + e^- \rightarrow O_2 + O^- \qquad E^0 = 2.08\ V \qquad (1.4)$$

$$HO^\bullet + e^- \rightarrow HO^- \qquad E^0 = 2.8\ V \qquad (1.5)$$

Unlike chlorine, the oxidative reactions between ozone and organic compounds do not usually yield products with higher levels of toxicity in comparison to the initial organic compound. This electrophile agent attacks its target directly via ozone molecules or decomposes to form a more powerful oxidant reagent, the hydroxyl radical (Reaction 1.5), thus indirectly leading to the oxidation process. The mechanism of ozone decomposition, which occurs in a chain procedure, was described by Langlais et al. [31] and is presented briefly in Fig. 1.5. It is assumed that the free radical initiating reaction (generation of the hydroperoxide radical $HO_2^\cdot$ and the superoxide radical ion $^\cdot O_2^-$) is the rate-determining step in this mechanism. The ozone decomposition rate in the aqueous phase strongly depends on pH. Alkaline pH causes an increase in ozone decomposition. Reactions 1.6 and 1.7 compare the ozone decomposition rate at two different pH levels [32].

$O_3 + H_2O \rightarrow 2HO^{\bullet} + O_2$ $\quad k = 1.1 \cdot 10^{-4}\ M^{-1}s^{-1}$ (1.6)

$O_3 + HO^- \rightarrow {}^{\bullet}O_2^- + HO_2^{\bullet}$ $\quad k = 70\ M^{-1}s^{-1}$ (1.7)

Ozone itself is considered to be a highly selective electrophilic molecule, such that the reaction constants for the oxidation of different groups of compounds by ozone are variable over a wide range, from < 0.1 $M^{-1}s^{-1}$ up to about 7·10^9 $M^{-1}s^{-1}$ [33]. The solubility of ozone in water mainly depends on the water temperature and ozone content in the gas phase (Table 1.1). For pure ozone gas, it is 570 $mg.L^{-1}$ at 20°C, about 63 times higher than that for oxygen (9.1 $mg.L^{-1}$).

Table 1.1. Approximate solubility of ozone in water ($mg.L^{-1}$) as a function of ozone concentration in gas and temperature [35]

Temperature, °C	2.5%wt.	5%wt.	10%wt.	100%wt.
0	27.5	54.5	109	1090
10	19.5	39	78	780
20	14.25	28.5	57	570
30	10	20	40	400
40	6.75	13.5	27	270
50	4.75	9.5	19	190
60	3.5	7	14	140

The typical half-life of ozone at ambient temperature is about 3 days in the gaseous phase but only 20±5 min when it is dissolved in deionised water (pH 7); however, depending on the water quality and conditions, the half-life of ozone in aqueous solutions varies from seconds to hours [34]. For this reason, ozone is usually generated in situ and the transportation and storage of this gas make no sense. Furthermore, the low stability of ozone in water, in addition to its high production costs, are two big disadvantages for the application of ozone alone in wastewater treatment.

Since the direct attack of ozone onto organic molecules occurs only at double bands, at more acidic pH levels, where ozone decomposition and the generation of hydroxyl radicals are assumed to be slight, ozone reacts slowly with saturated carboxylic acids and molecules containing inactivated aromatic systems in their molecular structures. Generally, the existence of electron-withdrawing groups (-NO_2, -COOH, -COH, -CN, etc.) in the structure of organic

molecules decreases the rate of ozone attack, while substitution of electron-donating groups (-OH, $-CH_3$, $-NH_2$, etc.) increases the oxidation rate by the direct attack of ozone.

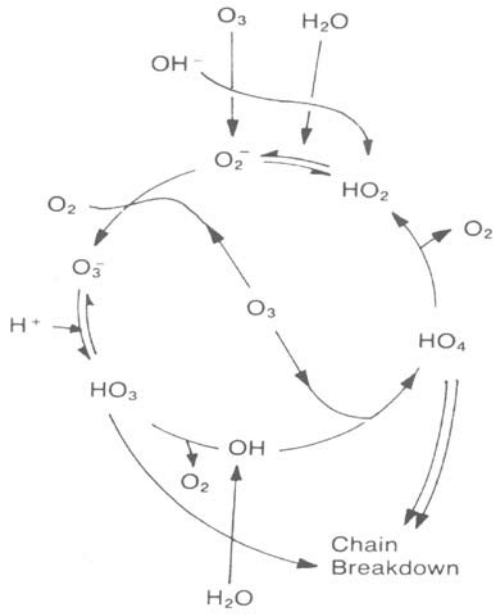

Fig. 1.5. Chain mechanism of ozone decomposition [31]

1.2.2.2. Application of ozone

Regarding the application of ozone, many scientific studies have reported several application conditions dealing with ozone as a disinfection and oxidation agent. Various batch and semi-batch setups and bubble column reactors have been introduced, where various ratios of ozone-oxygen gaseous mixtures are bubbled through the bulk of the wastewater under different experimental conditions and in the presence of numerous categories of auxiliary materials or accelerators which enhance the performance of the ozonation process [36-38].

1.2.3. Combination of TiO_2 and ozone

A quick and simple look at scientific studies reported since the beginning of the 1980s on water and wastewater treatment shows a growing tendency with a remarkable progressive slope in the last 10 years in terms of the development, extension and advancement of new approaches, ideas or designs which aim to solve new problems or to improve the existing methods in this field of

science. In this way, many studies have focused on the enhancement of the efficiency of well-known technologies or the reduction of their costs and other disadvantages by merging them with cheaper, more sustainable and more environmentally friendly methods. One of these ideas is the combination of the oxidative characteristics of ozone and photo-excited semiconductors to obtain a synergistic effect on the decomposition of recalcitrant microorganisms and organic compounds by means of photocatalytic ozonation processes.

Combination of the photocatalytic oxidative features of TiO_2 and the excellent oxidation properties of ozone by photocatalytic ozonation is thought to be a promising technique to improve the oxidation and decomposition conditions of the adsorbed contaminant molecules on the photocatalyst surface. At the same time, the oxidation efficiency of ozone molecules adsorbed on the irradiated semiconductor surface is assumed to be increased compared with the case when ozone is used alone to oxidise pollutants. This effect is mainly attributed to the formation of more reactive but non-selective hydroxyl radicals, which react with almost all organic molecules at a rate on the order of 10^6 - 10^9 $M^{-1}s^{-1}$ [39].

Concerning the application of the TiO_2/UVA/O_3 combination and its synergistic effects on the degradation of contaminant molecules in water, the economic aspects must be highlighted. In addition to energy consumption by the UV lamp, compared to photocatalytic oxidation processes, photocatalytic ozonation requires additional electrical energy for ozone generation. Therefore, at first glance, photocatalytic ozonation seems to be less cost effective from an economical point of view. But, for a better assessment, the specific energy consumption must be calculated, where the consumed energy is apportioned to the amount of decomposed materials. Kopf et al. [20] have shown that the specific energy consumption for the photocatalytic ozonation of monochloroacetic acid and pyridine is much lower than that for photocatalytic oxidation and ozonation. Beltran et al. [40] have expressed the same belief. They have shown that if ozone-based processes are compared for the degradation of sulphamethoxazole, photocatalytic ozonation is the most efficient process regarding ozone uptake. Under their conditions, after 60 min of reaction, ozone consumption was 78, 20, 25 and 10 mg ozone per mg TOC removed for simple ozonation, ozone photolysis, catalytic ozonation and photocatalytic ozonation, respectively. Many studies in the literature have reported assessments of this advanced oxidation technique in the degradation of numerous groups of organic chemicals [41-44].

As far as the combination of fixed-bed TiO_2 nanoparticles photoexcited by UV-vis light and ozone or oxygen is concerned as a photocatalytic oxidation/ozonation system for the decomposition of pollutants existing in water, many partial processes are involved in this procedure. The steps of this heterogeneous oxidation process are illustrated schematically in Fig. 1.6.

The first step consists of the absorption and dissolution of gas molecules of the oxidants (O_2 or O_3) into an aqueous film of polluted water or wastewater. Diffusion steps (2 and 3) occur when molecules of oxidants and pollutants are transported via the hypothetical diffusion layer to the surface of the photocatalyst. The next step is the adsorption of these molecules on the photoactivated surface of catalyst and their further reactions with photogenerated hole-electron pairs (step 4). This step is mostly expressed as being preceded by the generation of non-selective oxidant OH radicals. Afterwards, the oxidation products leave the catalyst surface by moving out of the diffusion layer (steps 5 and 6).

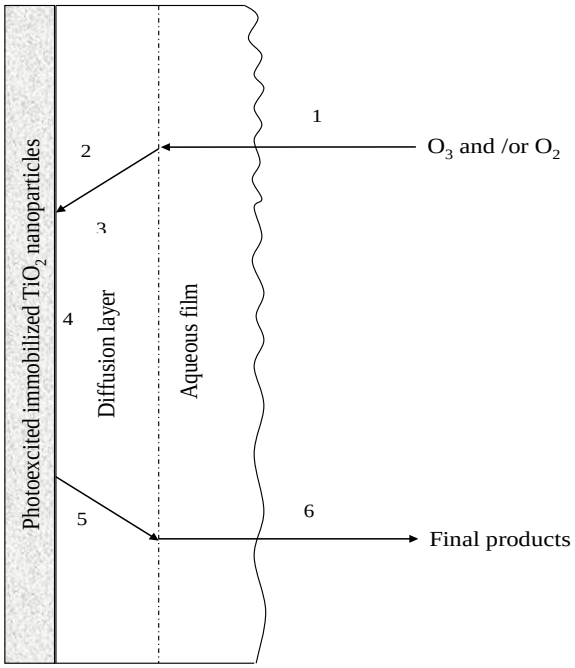

Fig. 1.6. Schematic diagram of the heterogeneous photocatalytic oxidation by means of immobilised TiO_2

It should be mentioned that, in addition to this pathway, other simultaneous events likely occur, such as the direct attack of ozone/oxygen on pollutants in the bulk of the solution or on

the photocatalyst surface and diffusion of generated OH radicals far away from the catalyst surface into the solution medium to mediate the oxidation process therein [45]; however, Turchi and Ollis [46] believe that the latter is impossible.

1.2.3.1. Absorption of gas into liquid

Incorporation of the maximum possible concentration of oxygen or ozone into contaminated water is an important preliminary step which must take place in order to engage the oxidative properties of these molecules for the degradation of contaminants. Various parameters such as the solubility of the gas into liquid, the temperature of the liquid and gas, the pressure of the gas and liquid viscosity affect the absorption level of oxidant gases into water or wastewater and, consequently, the efficiency of oxidation. Relating to falling film reactors, Sisoev et al. [47] reported that the flow of a wavy falling film as well as the structure and frequency of waves intensively affect the mass transfer properties of the system and, as a result, the maximum adsorption flux by influencing the diffusion layer which develops from the film surface. As far as the combination of a liquid falling film and a gas stream is concerned, two directions of movement are possible: co-current and counter-current flow. Akanksha et al. [48] have indicated that shear stress increases the rate of absorption in the case of co-current flow and vice versa for the counter-current condition.

1.2.3.2. Adsorption of molecules on the photocatalyst surface

As far as the adsorption of an organic compound (pollutant) on the photocatalyst surface is concerned as the first step of decomposition, two pathways for oxidation have been proposed. First, a reaction occurs between the active oxidant species, i.e. OH radicals, and the adsorbed contaminant molecule at the surface of the catalyst. This kind of reaction is described by the Langmuir-Hinshelwood (L-H) mechanism. Several studies have been reported in this way, assuming the existence of an adsorption/desorption equilibrium under dark or irradiated conditions [49, 50]. Equation 1.1 shows that, according to the L-H mechanism, the initial oxidation rate (r_0) of any pollutant which is able to be adsorbed on the catalyst surface depends on its initial concentration (C_p); where k_{ads} is the adsorption/desorption constant and k_r

represents the reaction (oxidation) constant. One should take into account that k_{ads} is independent of the photon flux.

$$r_0 = \frac{k_r k_{ads} C_p}{1 + k_{ads} C_p} \qquad \text{(Equation 1. 1)}$$

Based on Equation 1.1, at very low initial concentrations ($1 \gg k_{ads} C_p$), the initial reaction rate will be given by pseudo first-order kinetics with respect to the initial concentration of the pollutant and the equation can be rewritten as $r_0 = k_r k_{ads} C_p$, while at high initial concentrations ($1 \ll k_{ads} C_p$), the reaction rate will be independent of the initial concentration, $r_0 = k_r$. Even though many judgments stand against the use of the L-H mechanistic model because not all assumptions are considered, it is still recommended for its simplicity and its ability to fit experimental results well in heterogeneous photocatalytic processes [51].

The second type of oxidation happens when OH radicals or other active oxidants which are adsorbed at the catalyst surface react with the contaminant in solution. This mechanism is known as the Eley-Rideal (E-R) mechanism [52]. The E-R mechanism is shown by Equation 1.2, where k_r is the reaction (oxidation) rate constant, k_{ads} is the adsorption-desorption constant of the oxidant on the catalyst surface, C_p is the concentration of the pollutant in solution and C_{ox} is the concentration of the oxidant on the surface.

$$r = k_r C_p \frac{k_{ads} C_{ox}}{1 + k_{ads} C_{ox}} \qquad \text{(Equation 1.2)}$$

In this case, depending on the concentration of oxidants, there are two possibilities. At a low concentration of C_{ox} ($1 \gg k_{ads} C_{ox}$), the equation can be rewritten as $r = k_r k_{ads} C_p C_{ox}$. Under these conditions, the reaction rate will be first-order with respect to both pollutants and oxidants. At excess concentrations of C_{ox} ($1 \ll k_{ads} C_{ox}$), the rate will be first-order with respect to the pollutant concentration and independent of the oxidant concentration, $r = k_r C_p$. Beltran et al.

[53] have described the ozonation of oxalic acid on the surface of a TiO_2/Al_2O_3 catalyst by considering an Eley-Rideal mechanism.

Hufschmidt et al. [16] and Brosillon et al. [54] have proposed that the degradation of molecules that are adsorbed poorly or not at all on the catalyst surface is performed by hydroxyl radicals in solution. They believe that these active radicals are able to diffuse away from the semiconductor surface to the solution medium and react with pollutants therein. The kinetic expression of the oxidation process in this case is simply presented by Equation 1.3 as follows:

$$r = k_r C_{OH^\cdot} C_p \qquad \text{(Equation 1.3)}$$

where k_r is the oxidation rate constant, $C_{OH^\cdot}$ is the concentration of hydroxyl radicals and C_p is the pollutant concentration in solution [54]. Moreover, Tatsuma et al. [55] have presented a new aspect called “remote oxidation” where the photocatalytic degradation of some aromatic and aliphatic hydrocarbons in the gas phase can take place at a distance as much as 500 μm away from the TiO_2 surface. Even more interesting is that the reaction rate decreases with distance. They assumed that the organic compounds in the gas phase had been oxygenated and gradually decomposed to CO_2 by active oxygen species ($OH^\bullet$, $HO_2^\bullet$ and H_2O_2) that were produced at the TiO_2 surface and transported to the gas phase.

1.3. Advanced oxidation processes

In the next sections, a concise review is presented on some studies published in recent years. Reviewing these studies, which dealt primarily with the treatment of water and wastewater and investigated the influence of many factors affecting the treatment process, can generate an overview of the principles of four categories of oxidation processes, providing direction for the present study.

1.3.1. Photocatalytic oxidation

This type of advanced oxidation process occurs where a combination of TiO_2, UV light and oxygen is employed for the oxidation and decomposition of an organic compound. Oxygen molecules are adsorbed on UV-illuminated TiO_2 and are involved in a number of reactions.

Zalazar et al. [56] have reported that the existence of adsorbed oxygen molecules and their reaction with photogenerated electrons on the photocatalyst surface is very important, because it decreases the significance of electron-hole recombination and consequently improves the effectiveness of oxidative paths which include photogenerated holes. Degradation of a large number of chemical substances has been investigated by utilising the benefits of photocatalytic oxidation [49; 57-59].

1.3.1.1. Mechanisms of photocatalytic oxidation

The fundamental mechanisms of TiO_2 photocatalysis have been repeatedly postulated and discussed in many studies [15, 60]. Photoexcitation of the TiO_2 surface by photons ($h\nu$) with an energy level providing the band gap energy of TiO_2 causes the generation of holes and electrons on the catalyst surface. After this photogeneration, hole-electron recombination is assumed to take place immediately, releasing a certain amount of energy. Even though, the existence of adsorbed electrophilic and nucleophilic molecules on the surface promotes oxidative-reductive reactions between electrons and electrophilic substances on one side and holes and nucleophilic elements on the other side.

$$TiO_2 + h\nu \rightarrow e^- + h^+ \quad (1.8)$$

$$pH < 7: H_2O_{ads} + h^+ \rightarrow OH^\bullet + H^+ \quad \text{or} \quad pH > 7: OH^-_{ads} + h^+ \rightarrow OH^\bullet \quad (1.9)$$

$$O_{2\,ads} + e^- \rightarrow {}^\bullet O_2^- \quad (1.10)$$

$$R^\bullet + {}^\bullet O_2^- \rightarrow R\text{-}O_2^- + H^+ \rightleftarrows R\text{-}O_2H \quad (1.11)$$

$$R + h^+ (OH^\bullet) \xrightarrow{multistep} CO_2 \quad (1.12)$$

$${}^\bullet O_2^- + H^+ \rightleftarrows HO_2^\bullet \quad (1.13)$$

$$2HO_2^\bullet \rightarrow H_2O_2 + O_2 \quad (1.14)$$

$$H_2O_2 + {}^\bullet O_2^- \rightarrow OH^\bullet + OH^- + O_2 \quad (1.15)$$

$$OH^\bullet + R\text{-}H \rightarrow R^\bullet + H_2O \xrightarrow{multistep} CO_2 \quad (1.16)$$

Through this process, oxygen molecules participate as electron acceptors, producing superoxide radicals (${}^\bullet O_2^-$) (Reaction 1.10). The reaction between oxygen and electrons is relatively slow and could become the controlling step in photocatalytic oxidations. The superoxide radical itself can likely oxidise organic molecules (R) [16] by forming peroxides

which subsequently results in total oxidation (Reactions 1.11 and 1.12), or they may be involved in chain reactions to produce more oxidative OH radicals via the generation of hydrogen peroxide molecules (Reactions 1.13 to 1.15). Depending on the acidity of the reaction medium, holes react with water molecules (acidic conditions) or hydroxide anions (alkaline conditions) to generate the predominant oxidative species, OH radicals (Reaction 1.9). According to Reaction 1.16, hydroxyl radicals attack pollutant molecules to gradually oxidise and decompose them; however, Ishibashi et al. [61] have proposed that the role of holes in the oxidative reactions of TiO_2 is more important than that of hydroxyl radicals.

1.3.1.2. The effect of photocatalyst loads and properties

The degradation of an organic substance at the surface of metal oxide/aqueous electrolyte systems is a complicated phenomenon because it depends on many factors. For effective adsorption, a good interaction between the pollutant molecule and semiconductor surface groups is required. For this reason, the structure and properties of the photocatalyst play a significant role. Gorska et al. [18] have reported that the photocatalytic activity of a series of TiO_2 samples increased as the ratio between TiO_2 crystal lattice oxygen to surface oxygen species decreased. The morphology of the photocatalyst is other decisive parameter. High crystallinity predominantly increases the lifetime of electron-hole pairs, which consequently leads to an enhancement in the performance of oxidation [16]. The content of triple phases of TiO_2 in the crystalline structure mainly indicates its band gap energy, which defines the light absorption properties of the semiconductor as a result. Another significant structural factor is the BET surface area, which represents the porosity of the catalyst. Any increase in the TiO_2 specific surface area increases the adsorption capacity of the pollutant on the catalyst [62]. In addition to the properties of the photocatalyst, its content in the reaction medium has also been found to be important in treatments dealing with photocatalysts. Unlike the efficiency of fixed-bed photocatalyst applications, that of suspended systems has been reported as being dependent on the load of the photocatalyst, such that increasing the concentration of the photocatalyst in the suspension increases the degradation rate of pollutants in slurry utilisations. However, this ascending trend for degradation rate versus catalyst load reaches a maximum point at an adequate amount of catalyst. After this point, increasing the catalyst concentration will not affect the degradation rate or will even show a negative influence on it. Dijkstra et al. [63] have

explained this process by increased light adsorption with increasing catalyst concentration. The maximum point appears when all wavelengths are adsorbed. Any further catalyst load in the reaction medium will result in an increase in light scattering and will consequently cause a decrease in the penetration depth of light.

1.3.1.3. The effect of light intensity

The light intensity of the irradiation source is a principal parameter in photocatalytic processes. It has been reported by Piera et al. [6] that for a photocatalytic oxidation system at intensities less than one sun UVA equivalent (1 $mW.cm^{-2}$ ≈ $4.1 \cdot 10^{15}$ $photons.cm^{-2}.s^{-1}$), the reaction rate is a linear function of light intensity according to first-order kinetics, indicating that the number of photons is a limiting factor for the generation of hole-electron pairs to initiate oxidation. Above one sun UVA equivalent, half-order kinetics apply, which indicates that a higher concentration of hole-electron pairs under greater light intensities leads to increased hole-electron recombination; this becomes the limiting factor for photocatalysis processes under these conditions. At high intensities (> 20 $mW.cm^{-2}$), the reaction rate is independent of intensity [64].

1.3.1.4. The effect of solution pH value

The pH level affects the performance of photocatalytic oxidation in two ways: first, in alkaline media, high levels of hydroxide anions (OH^-) induce the generation of hydroxyl radicals, which come from the reaction of OH^- with holes on the TiO_2 surface. Since hydroxyl radicals are the dominant oxidising species in the photocatalytic process, photocatalytic oxidation is therefore accelerated at solutions with higher pH and vice versa [65]. The second aspect is the electrostatic attractive effects between the charged surface of TiO_2 and pollutant molecules which influence both the adsorption level of these molecules on the catalyst surface and interfacial electron transfer. The most significant factor is the isoelectric point (pH_{iep}) or point of zero charge (pzc). The isoelectric point for any form of TiO_2 is defined as the pH level at which the surface of the catalyst carries neither a negative nor a positive charge. This point for anatase and rutile ranges from 2 to 8.9 as reported by Kosmulski [66]. However, the average pzc of anatase is 5.9 which is slightly higher than that of rutile (5.4) [18]. It is evident that, according to pzc, the surface of the photocatalyst is negatively or positively charged under different pH conditions. As a result, the adsorption of cationic pollutants is accelerated when the surface is negatively charged and, on

the contrary, a positively-charged catalyst surface has a greater tendency to attract anionic compounds.

1.3.2. Ozonation

Reactions of ozone with organic substances mainly lead to the formation of alcohols, aldehydes and carboxylic acids. Due to the low reaction rate of these oxidation by-products with ozone, very slow further oxidation toward total mineralisation by ozone is considered to be the most significant disadvantage of ozonation processes [67]. For this reason, ozonation processes are sometimes considered as pre-treatment oxidation techniques followed by photocatalysis [68], or they are modified by adding other elements (which will be described later), introducing a new method known as catalytic ozonation. In the absence of elements, at pH < 3, ozone molecules mainly attack their nucleophilic target (R) directly (Reactions 1.17 and 1.18), but they gradually and via a chain of reactions (Reactions 1.7 and 1.19 to 1.25) decompose to generate hydroxyl radicals and indirectly oxidise substances under conditions of pH > 3. Under these conditions (pH > 3), the existence of hydroxyl radicals accelerates the decomposition of ozone molecules (Reaction 1.26) [32, 33].

Direct oxidation mechanisms:

$O_3 + R \rightarrow R\text{-}O + O_2$ (1.17)

or

$O_3 + R \rightarrow R^{+\bullet} + {}^{\bullet}O_3^-$ (1.18)

Indirect oxidation mechanisms:

$O_3 + OH^- \rightarrow {}^{\bullet}O_2^- + HO_2^{\bullet}$ (or) $O_2 + HO_2^-$ $k = 70\ M^{-1}s^{-1}$ (1.7)

$O_3 + HO_2^- \rightarrow {}^{\bullet}O_2^- + O_2 + OH^{\bullet}$ $k = 2.8\cdot10^6\ M^{-1}s^{-1}$ (1.19)

$O_3 + HO_2^{\bullet} \rightleftarrows 2O_2 + OH^{\bullet}$ $k = 1.6\cdot10^9\ M^{-1}s^{-1}$ (1.20)

$O_3 + {}^{\bullet}O_2^- \rightarrow {}^{\bullet}O_3^- + O_2$ $k = 1.6\cdot10^9\ M^{-1}s^{-1}$ (1.21)

pH < 8: ${}^{\bullet}O_3^- + H^+ \rightleftarrows HO_3^{\bullet}$ $k_+ = 5\cdot10^{10}\ M^{-1}s^{-1}$ and $k_- = 3.3\cdot10^2\ s^{-1}$ (1.22)

$HO_3^{\bullet} \rightarrow O_2 + OH^{\bullet}$ $k = 1.4\cdot10^5\ s^{-1}$ (1.23)

pH > 8: ${}^{\bullet}O_3^- \rightleftarrows 0^{\bullet -} + O_2$ $k_+ = 2.1\cdot10^3\ s^{-1}s^{-1}$ and $k_- = 3.3\cdot10^9\ s^{-1}$ (1.24)

$0^{\bullet -} + H_2O \rightarrow OH^- + OH^{\bullet}$ $k = 10^8\ s^{-1}$ (1.25)

$O_3 + OH^{\bullet} \rightarrow O_2 + HO_2^{\bullet}$ $k = 10^8\ M^{-1}s^{-1}$ - $2\cdot10^9\ M^{-1}s^{-1}$ (1.26)

By comparing the reaction rate constants for ozone decomposition chain reactions, it is evident that the first attack of ozone molecules on hydroxyl ions is the rate-controlling step in this process.

1.3.2.1. The effect of ozone concentration

Based on Henry's law, in equilibrium between a gaseous mixture containing ozone and a liquid, the ozone concentration in the liquid phase is directly proportional to the concentration of ozone in the gas phase. Therefore, the ozone concentration in both phases is thought to influence the efficiency of an ozonation process. Since the reactions take place in the liquid phase, the concentration therein will be mainly discussed. On one hand, regardless of the direct or indirect attack of ozone on target molecules, Gunten [33] demonstrated that the kinetics of ozone reactions with organic compounds in the liquid phase are typically first-order with respect to ozone, first-order with respect to the compound and second-order overall. Therefore, the decomposition rate of substances is simply demonstrated by Equation 1.4 as follows:

$$r = \frac{dC_p}{dt} = kC_pC_{O_3} \qquad \text{(Equation 1.4)}$$

where k is the ozonation reaction constant, C_p is the concentration of the organic compound and C_{O_3} is the ozone concentration in the liquid phase. On the other hand, Beltran et al. [69] have reported that ozone rapidly accumulates in water and reaches the saturation level in a few minutes, indicating that all ozonation processes in the liquid phase develop in a slow kinetic regime. To conclude, increasing the ozone concentration will cause an increase in the ozonation rate of organic substances [70], but depending on the reactor conditions, after reaching an adequate concentration of ozone, the degradation rate by ozone is assumed to be independent of the ozone concentration in the liquid phase. Volk et al. [71] and Wu et al. [72] observed similar effects of ozone concentration on the degradation of fulvic acid and the decolourisation of textile reactive dye, respectively. Chu et al. [73] observed that the existence of low concentrations of surfactant in the solution medium increases ozone dissolution and, as a consequence, the saturation level of ozone in the solution as well as the indirect generation of hydroxyl radicals is increased.

1.3.2.2. The effect of solution pH on the ozonation rate

The pH value is a key factor for ozone stability in aqueous solutions and also determines the manner in which the ozonation process occurs. A critical pH value is defined for each chemical composition in the liquid phase and is expected to be variable for different solutions. Below the critical pH, oxidation reactions develop via molecular ozone, while above this critical level of pH, hydroxyl radicals mainly handle the oxidation process as the predominant oxidising species. In other words, compared with acidic regimes, under alkaline conditions, hydroxyl anions react as initiators to accelerate ozone decomposition, yielding OH radicals more rapidly; this is why the oxidation process at basic pH proceeds at a faster rate but with relatively low selectivity [73]. However, it should be noted that in special wastewaters, probably due to the presence of traces of impurities in the starting materials, even at pH 2 oxidation mainly develops through indirect oxidation by means of radicals [74].

1.3.2.3. The effect of temperature

Temperature variations influence ozonation systems in two ways, which are usually considered to be opposite to each other. On one hand, with any temperature increase in the solution, the solubility of ozone in the liquid phase decreases, such that negligible ozone solubility in water under conventional conditions has been reported above 43°C. On the other hand, any temperature increase should result in higher reaction rates [75]. Therefore, the observed influence of temperature on ozonation is a consequence of these two effects. However, the existence of other factors (homogeneous and heterogeneous catalysts, illumination, initiators, inhibitors, etc.) in the reaction flux will determine the temperature dependency in a highly complex fashion. In general, the correlation between the reaction rate constant and the temperature is presented by Arrhenius' law (Equation 1.5), where k is the reaction rate, A is the frequency factor, E_A is the activation energy ($J.mol^{-1}$), R is the ideal gas law constant (8.314 $J.mol^{-1}.K^{-1}$) and T is the temperature in K [11]. The frequency factor depends on how often molecules collide and on whether the molecules are properly oriented when they collide [76].

$$k = A\exp\left(-\frac{E_A}{RT}\right) \qquad \text{(Equation 1.5)}$$

For all reactions following Arrhenius' law, a straight line with a slope equal to $-E_A/R$ will be presented by plotting of $\ln k$ versus T^{-1}.

1.3.3. Catalytic ozonation

The modification of oxidative properties of ozone in the presence of various types of catalysts is considered to be one of the most effective AOPs for the removal of a wide variety of organic compounds [77, 78]. Catalytic ozonation can increase the efficiency and decrease the reaction time with respect to separate ozonation and catalytic treatments by affecting the reaction mechanisms [79]. Gracia et al. [80] have reported that the application of catalysts combined with ozone results in a noticeable decrease in ozone consumption by decreasing the reaction time and increasing the efficiency of ozonation.

1.3.3.1. Homogeneous catalytic ozonation

In this process, hydroxyl radicals are usually produced by the decomposition of ozone molecules in the presence of transition metal ions which are available in the bulk solution [81]. Fe(II), Mn(II), Ni(II), Zn(II), Cu(II), Co(II), Cd(II), Ag(I) and Cr(III) are the most commonly used metal ions as catalysts for ozonation [82]. Hordern et al. [32] have reported that the nature of the metal ion used determines the reaction rate, selectivity and the consumption of ozone. Despite the introduction of new catalysts in recent years, the mechanisms of catalytic ozonation are still not clear [67]. However, two major mechanisms are generally described for homogeneous catalytic ozonation; the first is the decomposition of ozone by means of metal ions, followed by the generation of hydroxyl or other free radicals (Reactions 1.27 and 1.28) [6, 81] and the second is the formation of a complex between metal ions and the organic compounds and further oxidation of this complex by ozone which leads to the final products [83, 84].

$$Me^{n+} + O_3 \rightarrow Me\text{-}O^{n+} + O_2 \quad (1.27)$$

$$Me\text{-}O^{n+} + H_2O \rightarrow Me^{n+1} + OH^{\bullet} + OH^{-} \quad (1.28)$$

Catalytic ozonation of oxalic acid via complex formation between ozone and metal ions was proposed by Beltran et al. [85] to proceed as indicated below (Reactions 1.29 to 1.31).

$$Me^{n+} + C_2O_4^{2-} \rightarrow [Me\text{-}\ C_2O_4]^{n-2} + 2O_3 \rightarrow Me^{n+} + 2CO_2 + 2^{\bullet}O_3^{-} \quad (1.29)$$

$$[Me\text{-}\ C_2O_4]^{n-2} + C_2O_4^{2-} \rightarrow [Me\text{-}\ (C_2O_4)_2]^{n-4} + 2O_3 \rightarrow [Me\text{-}\ C_2O_4]^{n-2} + 2CO_2 + 2^{\bullet}O_3^{-} \quad (1.30)$$

$$[Me\text{-}\ (C_2O_4)_2]^{n-4} + C_2O_4^{2-} \rightarrow [Me\text{-}\ (C_2O_4)_3]^{n-6} + 2O_3 \rightarrow [Me\text{-}\ (C_2O_4)_2]^{n-4} + 2CO_2 + 2^{\bullet}O_3^{-} \quad (1.31)$$

The evidence for this mechanism is that the degradation rate was increased with decreasing pH, indicating that the formation of hydroxyl radicals did not play an important role under these conditions. In addition, adding radical scavenger reagents like *tert*-butanol did not affect the efficiency of decomposition, further suggesting no responsibility for hydroxyl radicals in this process.

1.3.3.2. Heterogeneous catalytic ozonation

The decomposition of ozone on the surface of metal oxides such as TiO_2, Al_2O_3 and MnO_2 or supported metals and metal oxides such as Cu-TiO_2, Fe_2O_3/Al_2O_3, Ru-CeO_2, etc. is commonly known as heterogeneous catalytic ozonation. Reports have also been published utilising activated carbons [86] and soils modified with a catalyst [7] combined with ozone as heterogeneous catalysts in recent years. The efficiency of this kind of ozonation depends mainly on the physical and chemical properties (surface area, porosity, density, pore volume, purity, chemical stability, mechanical strength, presence of active surface sites, etc.) of the surface of the metal oxide and the pH of the solution. As mentioned before, pH is one of the most significant variables in the reaction medium which influences the charge and active sites of the catalyst surface and, consequently, its adsorption capacity as well as the mechanisms of ozone decomposition in aqueous solutions [32]. Adsorption of ozone and/or organic compounds on the surface of a catalyst is considered to be a key step for heterogeneous catalytic ozonation. The ability of ozone adsorption on the surface of catalysts and its decomposition to generate active hydroxyl radicals is usually given as a factor determining the activity of catalyst [67]. Based on the type of catalyst used in this process, various mechanisms have been described. Faria et al. [87] have proposed that the adsorption and reaction of ozone on the surface of activated carbons leads to the generation of surface free radicals which are responsible for the degradation of contaminant molecules. Zhang et al. [88] have suggested that the non-associated catalyst surface hydroxyl

groups are active sites for promoting hydroxyl radical generation. Roscoe and Abbatt [89] assumed that ozone molecules are decomposed at the Lewis acid sites of the catalyst. Therefore, higher amounts of Lewis centres on the catalyst surface lead to a higher level of ozone decomposition. To summarise, two major mechanisms have been reported for heterogeneous catalytic ozonation in the literature. The first is the production of hydroxyl radicals by the adsorption of ozone molecules on the catalyst surface and the decomposition of these molecules [90, 91], and the second is the adsorption and decomposition of ozone molecules on the surface of the catalyst, leading to the generation of active oxidative surface-bound O radicals [92, 93].

1.3.4. Photocatalytic ozonation

Because of the electron affinity of ozone compared to oxygen, it can clearly be concluded that photocatalytic ozonation is a different process from photocatalysis in the presence of oxygen and from ozonation in the absence of a photocatalyst. Gilbert [94] have demonstrated that, compared with ozone, a disadvantage of oxygen as an oxidising agent combined with TiO_2 is the slow electron transfer from this photocatalyst to oxygen. In addition, Addamo et al. [95] quantitatively showed that one electron must be trapped by ozone to generate a hydroxyl radical (Reaction 1.32), while three electrons are necessary for the generation of one hydroxyl radical when oxygen acts as the electron acceptor (Reactions 1.10 and 1.13 to 1.15). The major chain reactions of ozone with photogenerated electrons over the surface of a photocatalyst are given in Reactions 1.32 to 1.34. Hydroxyl radicals produced in these chain reactions non-selectively attack target contaminant molecules (R-H) and decompose them.

$$O_3 + e^- \rightarrow {}^{\bullet}O_3^- \quad (1.32)$$

$${}^{\bullet}O_3^- + H^+ \rightarrow HO_3^{\bullet} \quad (1.33)$$

$$HO_3^{\bullet} \rightarrow O_2 + OH^{\bullet} \quad (1.34)$$

$$OH^{\bullet} + R\text{-}H \rightarrow R^{\bullet} + H_2O \xrightarrow{multistep} CO_2 \quad (1.16)$$

Many studies have discussed the synergistic effects of the combination of $TiO_2/UV/O_3$ on the degradation and removal of various substances from aqueous solutions. Ye et al. [96] showed that among six different advanced oxidation processes, $TiO_2/UV/O_3$ was the most efficient for complete mineralisation of 4-chloronitrobenzene. Li et al. [97] and Rajeswari and Kanmani [98]

have also reported similar results for the mineralisation of dibutyl phthalate and carbaryl, respectively, where photocatalytic ozonation was compared with two other advanced oxidation techniques.

As with the previously discussed oxidation processes, many parameters such as pH, solution temperature, ozone content in the gaseous mixture, light intensity, etc. affect the efficiency of photocatalytic ozonation. However, taking into account the different possible setup conditions of photocatalytic ozonation runs, such as reactor design, photocatalyst properties, etc., the effect of variation of these factors might differ slightly in some respects. For example, Müller et al. [99] reported that the best results for the photocatalysis of 2,4-dichlorophenoxyacetic acid were observed under acidic (pH 3) conditions, whereas non-catalytic ozonation of this compound under alkaline (pH 11) conditions delivered the best degradation rates. The degradation rate of this compound by photocatalytic ozonation at pH 7 was 1.5 times faster than the best result of ozonation at pH 11 and more than 3 times faster than that of photocatalysis (i.e. without O_3) at pH 3.

Concerning the effect of ozone concentration on photocatalytic ozonation treatments, Jing et al. [43] showed that increasing the ozone dosage from 20 $mg.h^{-1}$ to 100 $mg.h^{-1}$ reduced the duration of the removal process of dimethyl phthalate by photocatalytic ozonation from 1 h to 30 min and increased the TOC removal by about 20%. It was clearly observed that the effect of an increased ozone dosage on TOC removal was much higher for photocatalytic ozonation compared to ozonation and photo-ozonation. Sanchez et al. [68] also reported that enhancing the ozone flow bubbling through the suspension of TiO_2 in a photocatalytic ozonation setup effectively increased the TOC removal rate of an aniline solution. A similar trend was observed for the effect of the amount of the photocatalyst in the suspension on TOC removal, where tripling the catalyst amount decreased the TOC level by about 15%.

Regarding the influence of temperature, Mehrjouei et al. [44] observed that an increase in temperature from 10^{o}C to 55^{o}C increased the degradation rate of oxalic acid as well as the ozone consumption level in a TiO_2/UVA/O_3 system, while even higher temperatures of up to 70^{o}C had a negative effect and reduced both the degradation rate and ozone consumption level compared to that observed at 55^{o}C.

1.4. General purposes

This study had two main goals. The first goal was the design, construction and characterisation of a multiphase falling film reactor on the laboratory scale capable of combining 1) immobilised TiO_2 particles as the solid phase, 2) ozone or oxygen molecules as the gaseous phase and 3) the wastewater in the form of a falling film as the liquid phase under optimised conditions. The second goal was the evaluation of the performance of this falling film reactor by determining the synergistic effects between ozone, immobilised TiO_2 and near-UV light in the degradation of special compounds as contaminants in water by means of different advanced oxidation processes. Finally, the application of this modular reactor for colour removal and treatment of a real wastewater sample produced in a plastic pyrolysis process was performed as a case study.

1.4.1. Characteristics of the falling film reactor

Despite many investigations reporting numerous variable reactor designs for the degradation and removal of a wide range of chemicals existing in water as contaminant substances, coupling the oxidative properties of immobilised titanium dioxide particles irradiated with near-UV light and ozone/oxygen in a modified falling film reactor is a new idea. The benefits of the application of this reactor are explained as:

- The polluted water falls at certain falling rates on the reactor walls which are coated with TiO_2 particles and irradiated with near-UV light in the presence of ozone or oxygen, generating appropriate thin liquid layers adequate for bringing the three important functions involved (the photo-induced semiconductor surface, wastewater and ozone/oxygen molecules) very close to each other. In this way, optimised and yet uncomplicated conditions will be available for the synergistic oxidation of target pollutant molecules existing in water.
- The ratio of the active photocatalyst surface to wastewater volume for this design is estimated to be around 20000 $m^2.m^{-3}$. This high ratio indicates that the mass transfer properties for this type of reactor are well-modified compared to those of other oxidation systems employing the immobilisation and utilisation of TiO_2 particles as a photocatalyst. The obtained results confirm this claim.
- The design of the falling film reactor provides the possibility of applying and evaluating different advanced oxidation processes, such as catalytic ozonation, photocatalytic oxidation,

photo-ozonation, photocatalytic ozonation and even photo-Fenton oxidation, etc., on demand, thus providing this reactor with multiple functions.

- Enhancement of the contact time between ozone molecules and polluted water in addition to the possible reuse of ozone consequently leads to significant efficiencies in ozone consumption and decreases ozone production costs.
- Oxidation of pollutants even at very low concentrations (removal of volatile organic compounds and odours).
- Movement of falling aqueous films over a fixed-bed photocatalyst improves two factors at the same time; first, it provides better conditions from the mass transfer point of view and second, oxidation by-products are dissolved and washed from the surface of the photocatalyst to avoid its poisoning.
- The unique design of this reactor provides the preliminaries for conjunction to other advanced preparations called dielectric-barrier-discharge (DBD) systems for in situ production of ozone using plasma, which have been described in detail by Obradovic et al. [100] and Kuraica et al. [101].
- Solving the problem of the separation of photocatalyst particles after treatment by immobilisation and at the same time diminishing the mass transfer problems which almost all immobilised photocatalyst systems suffer from was done using a modified design in construction which allows using this reactor for more practical and industrial applications.

The capability of the falling film reactor was evaluated in the oxidation and decomposition of a set of organic chemicals as model compounds. The reasons for the selection of these compounds which are generally categorised in three groups in this study are explained individually below.

1.4.2. Characteristics of the chosen model compounds

1.4.2.1. Group A: aliphatic dicarboxylic and tricarboxylic acids

Oxalic acid

This dicarboxylic acid has been reported by Xiao [102] and Kosanic [103] to be one of the toxic pollutants existing in alumina processing liquors and textile industrial wastewaters, respectively.

Furthermore, oxalate is a detectable intermediate in the mineralisation of many pesticides and other organic compounds [104-106] and, at the same time, it is oxidised directly to CO_2 without the formation of any stable intermediate products [57, 95]. This compound was described by Hoigne and Bader [107] to be recalcitrant to the direct attack of ozone alone, especially at acidic pH. Moreover, this compound was chosen as a model compound in many studies [44, 53, 57, 87, 103]; therefore, it could be considered a good choice to show the benefits of advanced oxidation processes in the falling film reactor.

Dichloroacetic acid (DCAA)

This carcinogenic haloacetic acid [108, 109] is one of the typically disfavoured by-products produced in water disinfection during the chlorination process [110]. The provisional guideline value for announced by the WHO is 0.05 $mg.L^{-1}$ [111]. Dichloroacetic acid is a non-volatile compound [112] and is often found in industrial liquid wastes as a consequence of the destruction of various chlorinated organic compounds such as trichloroacetic acid, trichloroethylene and perchloroethylene [113]. Dichloroacetate also has pharmaceutical applications as an enzyme inhibitor in cancer remediation [114, 115]; therefore, it likely exists in wastewaters produced by some pharmaceutical plants or hospitals [116]. Wang et al. [117] have reported imperceptible decomposition of dichloroacetic acid by ozonation, and it has already described by Volk et al. [71] that saturated aliphatic carboxylic acids are refractory to the direct action of ozone. On this basis, dichloroacetic acid was introduced and investigated as the next model compound in this study by the evaluation of its oxidation behaviours in the falling film reactor under various oxidative conditions.

Citric acid

This tricarboxylic aliphatic acid is mainly used as a natural flavouring and preservative additive in foods and soft drinks. It is also used as an industrial chelating agent in the detergent and food industries [118] to capture metal ions which hinder various processes. New technology was recently developed to use citric acid as a more environmental friendly alternative to nitric acid in the passivation process of stainless steel surfaces. Mazzarino and Piccinini [119] claimed that wastewaters produced by the cleaning process of boilers in power plants contain concentrations of several grams per litre of this carboxylic acid. Many researchers [120, 121] have employed

citric acid as a hole scavenger in the photocatalytic reduction of some toxic metal ions such as Cu(II), Ni(II), Zn(II), Pb(II) and Cr(VI). Furthermore, since citric acid has a saturated aliphatic chemical structure, it is assumed to be highly resistant to electrophilic assault by ozone. It will be presented later that the experimental results are in good agreement with this assumption.

Table 1.2. Basic identifiers of the chosen aliphatic carboxylic acids

Compounds	CAS No.	Chemical structure	Molecular weight, $g.mol^{-1}$	pKa
Oxalic acid dihydrate	144-62-7	$HOOC\text{-}COOH.2H_2O$	126.07	1.23 – 4.27
Dichloroacetic acid	79-43-6	$Cl_2HC\text{-}COOH$	128.94	1.48
Citric acid monohydrate	77-92-9	$HOOC\text{-}CH_2\text{-}C(COOH)(OH)\text{-}CH_2\text{-}COOH.H_2O$	210.14	3.14 – 4.75 – 6.41

1.4.2.2. Group B: Aromatic mono- and dicarboxylic acids

In general, organic substances that do not have strong nucleophilic sites in their chemical structures are oxidised and decomposed slowly by common ozonation processes. In this section, two well-known ozone-recalcitrant aromatic structures [122, 123] were chosen in order to examine the performance of the falling film reactor in the degradation of these compounds by AOPs. Table 1.3 briefly shows some selected physicochemical specifications of these two aromatic carboxylic acids.

p-chlorobenzoic acid (pCBA)

*p*CBA is not typically present in natural water, but since it is used in the manufacture of dyes, adhesives, fungicides and pharmaceuticals, it is present excessively in the wastewater of these industries. It is a common contaminant in the paper mill industry [124]. It was observed by Magara et al. [125] that *p*CBA is an intermediate product during the chlorination of pesticides. This halo-aromatic acid was chosen as a model compound for the AOPs because of its low reactivity with ozone ($k_{O_3,pCBA} \leq 0.5\ M^{-1}s^{-1}$) but high reactivity with hydroxyl radicals ($k_{OH,pCBA} = 5 \cdot 10^9\ M^{-1}s^{-1}$) [126, 127]. Jing et al. [43] have reported pseudo first-order reaction behaviour for *p*CBA reacting with OH radicals using the UV chlorine process.

Terephthalic acid (TPA)

One billion kilograms of this aromatic dicarboxylic acid are produced annually and applied as raw materials in the production of polyester fibres and films, polyethylene terephthalate (PET) bottles, dyes, medicines, pesticides, perfumes, etc. The toxicity of terephthalic acid as a carcinogenic substance in the urinary bladder and as an endocrine disrupting factor have been reported by Cui et al. [128] and Dai et al. [129]. Although TPA wastewater is traditionally treated by biological processes, new studies investigating AOPs for the degradation of this compound have been published [130, 131].

Table 1.3. Identifiers and properties of the chosen aromatic carboxylic acids

Compounds	CAS No.	Chemical structure	Molecular weight, $g.mol^{-1}$	Solubility in water, $g.L^{-1}$	pKa
p-chlorobenzoic acid	74-11-3	$Cl\text{-}C_6H_4\text{-}COOH$	156.57	0.08 (20° C)	3.98
Terephthalic acid	100-21-0	$HOOC\text{-}C_6H_4\text{-}COOH$	166.13	0.017 (25° C)	3.51 – 4.82

1.4.2.3. Group C: Ethers and their by-products

Chemicals of this group are used as oxygenating fuel additives in the formulation of gasoline to raise its octane number by decreasing the aromatic content in the fuel [78]. Nowadays, due to large-scale fuel production and considering that these toxic compounds have been detected in surface and groundwater, increasing interest in effective removal methods for these substances from water are clearly needed. Some physical and chemical characteristics of the compounds in this group are summarised in Table 1.4.

Table 1.4. Some physicochemical properties of the chosen ethers and TBA

Ethers	CAS No.	Chemical structure	Molecular weight, $g.mol^{-1}$	Boiling point, °C	Henry's law constant (at 25° C) [132]
MTBE	1634-04-4	$(CH_3)_3\text{-}C\text{-}O\text{-}CH_3$	88.15	55	$1.23\cdot10^{-1} – 2.40\cdot10^{-2}$
ETBE	637-92-3	$(CH_3)_3\text{-}C\text{-}O\text{-}CH_2\text{-}CH_3$	102.17	70	$1.09\cdot10^{-1}$
TAEE	919-94-8	$CH_3\text{-}CH_2\text{-}C(CH_3)\text{-}O\text{-}CH_2\text{-}CH_3$	116.20	102	N.A.
TBA	75-65-0	$(CH_3)_3\text{-}C\text{-}OH$	74.12	82	$4.25\cdot10^{-4} – 5.93\cdot10^{-4}$

Methyl tert-butyl ether (MTBE)

Among other oxygenates, MTBE is chosen often mainly because of its relatively high cost-effectiveness and better mixing properties with gasoline [133]. MTBE has been determined to be an animal carcinogen [134] and its suspected human carcinogenic potential has been described by Kane and Newton [135]. In 1995, the U.S. Geological Survey reported that MTBE had been detected in shallow urban groundwater [136], and since that time, many efforts have been initiated to investigate possibilities for the removal of this compound from water. Hordern et al. [78] proposed that the slow biodegradation rate of MTBE in aqueous solutions leads to its persistence in water supplies. Acero et al. [137] and Baus et al. [138] reported that the reaction rate of ozone molecules with MTBE is considered to be very low. Based on this information, conventional ozonation cannot effectively remove this compound from water. Therefore, AOPs have been extensively evaluated to improve the degradation process of MTBE [139, 140].

Ethyl tert-butyl ether (ETBE)

This substance is manufactured from ethanol and isobutene. Since ethanol is more expensive than methanol, which is one of raw materials for the production of MTBE, the higher production costs of ETBE have generally inhibited its widespread use [141]. Nevertheless, environmental considerations limit the use of MTBE and attention has been diverted to ethanol-based oxygenates like ETBE and TAEE in recent years.

Tert-amyl ethyl ether (TAEE)

One advantage of ethanol-based oxygenates for gasoline like TAEE compared to MTBE is that ethanol can be produced by fermentation from renewable resources like sugarcane, sugar beet, corn or molasses and also from crop and sugar wastes [142]. For this reason and due to the health risk of using of MTBE as a gasoline additive, it seems that TAEE will be a good alternative to MTBE in the near future [143]. Compared to MTBE, there is more limited information about the degradation properties of TAEE by means of advanced oxidation processes.

Tert-butyl alcohol (TBA)

This compound has been reported as a by-product of the oxidation processes of MTBE and ETBE [13, 137, 138]. Stupp et al. [144] reported that the toxicity and health risks of TBA are as

high as those of MTBE. TBA is a well-known scavenger of OH radicals, since it reacts very rapidly with hydroxyl radicals (bimolecular rate constant, $k_{OH,TBA}$ = 3.6·10^{10} M^{-1}.min^{-1}), but very slowly with ozone ($k_{O_3,TBA}$ = 0.18 M^{-1}.min^{-1}) [131].

2. Experimental

The present work was carried out in six phases: 1) the design and construction of the falling film reactor, 2) immobilisation of photocatalyst nanoparticles on the reactor walls, 3) characterisation of the reactor to determine the optimum working conditions, 4) selection of appropriate organic chemicals to be studied as model compounds, 5) an elementary assessment of the selected model compounds properties and their behaviour under different oxidation conditions using the planar reactor which was prepared for this aim and 6) an intensive and complete study on the degradation of model compounds, including the mechanisms, kinetics, details on the intermediates, behavioural studies and mass transport properties.

2.1. Materials

The most commonly utilised Degussa P-25 TiO_2 nanoparticles consisting of 70% photoactive anatase and 30% thermodynamically stable rutile modified with a BET surface area of 50 $m^2.g^{-1}$ and crystalline size of 30 nm in 0.1 μm diameter aggregates was used as the photocatalyst in this work. This type of TiO_2 was chosen for two reasons:

1) Despite the fact that Degussa P-25 is considered to be non-porous product of TiO_2, it has been determined to be a highly crystalline photocatalyst. Hufschmidt et al. [16] have postulated that high crystallinity enhances the lifetime of electron-hole pairs in the semiconductor and consequently increases the production rate of hydroxyl radicals.
2) Notwithstanding the fact that anatase is the most photoactive form of TiO_2, Bakardjieva et al. [145] and Kawahara et al. [146] have reported that controlling the content of crystalline rutile in the photocatalyst composition improves the photocatalytic decomposition of 4-chlorophenol and acetaldehyde, respectively, compared with experiments in which a pure

anatase phase of TiO_2 was employed for treatment. This development was explained by increasing the charge separation efficiencies due to photo-induced interfacial electron transfer from anatase to rutile [21].

Analytical grades of all model compounds were employed for these experiments. All model compounds investigated in this work were used without any additional pre-treatment or purification. More details and specifications on the selected model compounds are given in Table 2.1.

Table 2.1. Experimental specifications of model compounds

Model compound	Molar mass, g/mol	Purity, %	producer
Oxalic acid	126.07	99.5	Merck , Germany
Dichloroacetic acid	128.94	> 98	Merck , Germany
Citric acid	210.14	99.5	Chem solute, Germany
p-chlorobenzoic acid	156.57	> 97	Fluka, Germany
Terephthalic acid	166.13	> 98	Merck, Germany
MTBE	88.15	> 99	Merck, Germany
ETBE	102.18	> 95	Merck, Germany
TAEE	116.2	98	ABCR, Germany
TBA	74.12	> 99.5	Merck, Germany

Absolute ethanol (C_2H_5OH), M = 46.07 $g.mol^{-1}$ with a purity of > 99.8 % (provided by Chem solute, Germany) was used as the solvent in the preparation of the TiO_2 suspension, while 65% nitric acid (HNO_3; MW = 63.01), which was added after dilution (to 6.5 %) to the TiO_2 slurry for better dispersion conditions was produced by Merck, Germany. Triton X-100 and a phenylmethylpolysiloxane emulsion (Silikophen P 40W), which were employed as a surfactant and binding reagent in the composition of the polysiloxane suspension were manufactured by Merck and Tego Chemie, Germany, respectively.

Two components of KASI ^{R}-GL which were employed as binders in the immobilisation process of TiO_2 nanoparticles on polymethylmethacrylate surfaces were provided by KRD Coatings GmbH, Germany, and added to the composition of the suspension without any

preliminary treatment. In this procedure, 1-methoxy-2-propanol ($CH_3OCH_2CH(OH)CH_3$), supplied by Merck, Germany, was used as the solvent for slurry preparation.

Solutions of 5,5,7-Indigotrisulfonic acid tripotassium salt produced by Sigma-Aldrich GmbH, Germany was used as model compound on demand as well as for the measurement of ozone concentration in the liquid phase.

NaOH (Lachema, Czech Republic) was added to adjust the pH value when required.

Pure dry oxygen specified as > 99.5 vol.% and H_2O < 200 ppmv was delivered by Air Liquide to be used as the feed gas for the ozone generator; pure dry nitrogen, 99.99 vol.%, was prepared by the same company and used on demand. The input gas flow rate in all runs was fixed at 10 $mL.h^{-1}$.

The deionised water used for the preparation of solutions and for washing the reactors was provided by a Seradest SD-2000 deionising column (Seral, Germany) with a conductivity of < 0.1 $\mu S.cm^{-1}$ in the outlet.

2.2. The design and structure of reactors

Two different designs of reactors were used in the present work. Some preliminary investigations concerning immobilisation techniques for TiO_2 as well as the behaviour of model compounds under different oxidation conditions were performed by means of a planar reactor. A polymethylmethacrylate box with a special interior structure and transparent window was used as the planar reactor (Fig. 2.1).

In this design, the photocatalyst particles were immobilised on borosilicate glass sheets, and these sheets were embedded and fixed inside the reactor. The solutions were injected through the bottom inlet to generate a thin liquid layer on the photocatalyst surface and left the reactor from the outlet on the top of the reactor. An optical window allowed UV light irradiation of the photocatalyst surface.

The majority of experiments were carried out using an annular falling-film reactor. In this design, a cylindrical tube with internal and external diameters of 26 mm and 30 mm, respectively, was placed and fixed vertically inside another bigger tube with an internal diameter of 64 mm and external diameter of 68 mm to form an annular space between the two tubes along the length of the reactor (Fig. 2.2).

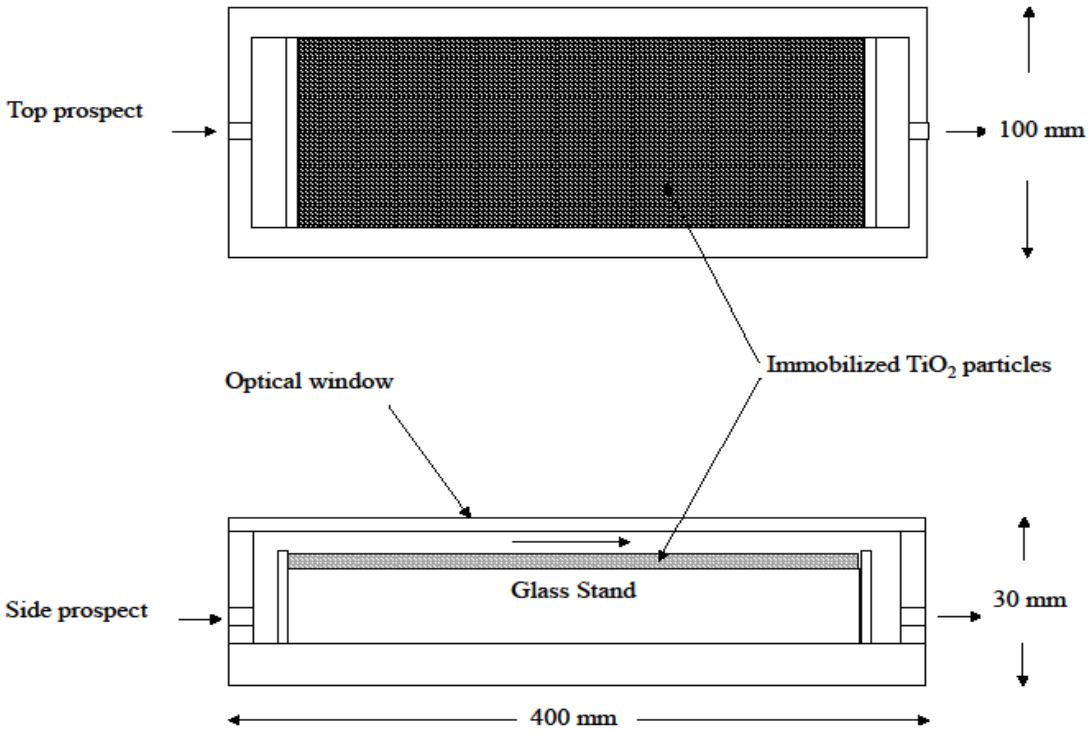

Fig. 2.1. Structure of the planar reactor

The space between the two tubes was used as the reaction medium. Two special caps at the bottom and top of the structure fixed the tubes and closed the system. TiO_2 particles were immobilised on the inner side of the outer tube and the outer side of the inner tube such that all surfaces of the annular space were covered with semiconductor particles. A UV light lamp was located inside the inner tube vertically, thus uniformly irradiating all surfaces of the tube around the source.

2.3. Instruments and devices

In all experiments which needed illumination, UV lamps produced by Narva Lichtquellen GmbH & Co. KG, Germany, model LT 30 W/009, were used as the UV irradiation source. Fig. 2.3 presents the illumination spectrum of this type of lamp with a range of wavelengths from 300 nm to 420 nm and a maximum wavelength at about 360 nm. The incident light intensity of these sources is about 1 $mW.cm^{-2}$. The maintenance of radiation was reported by the manufacturer as being about 85% after 2000 hours.

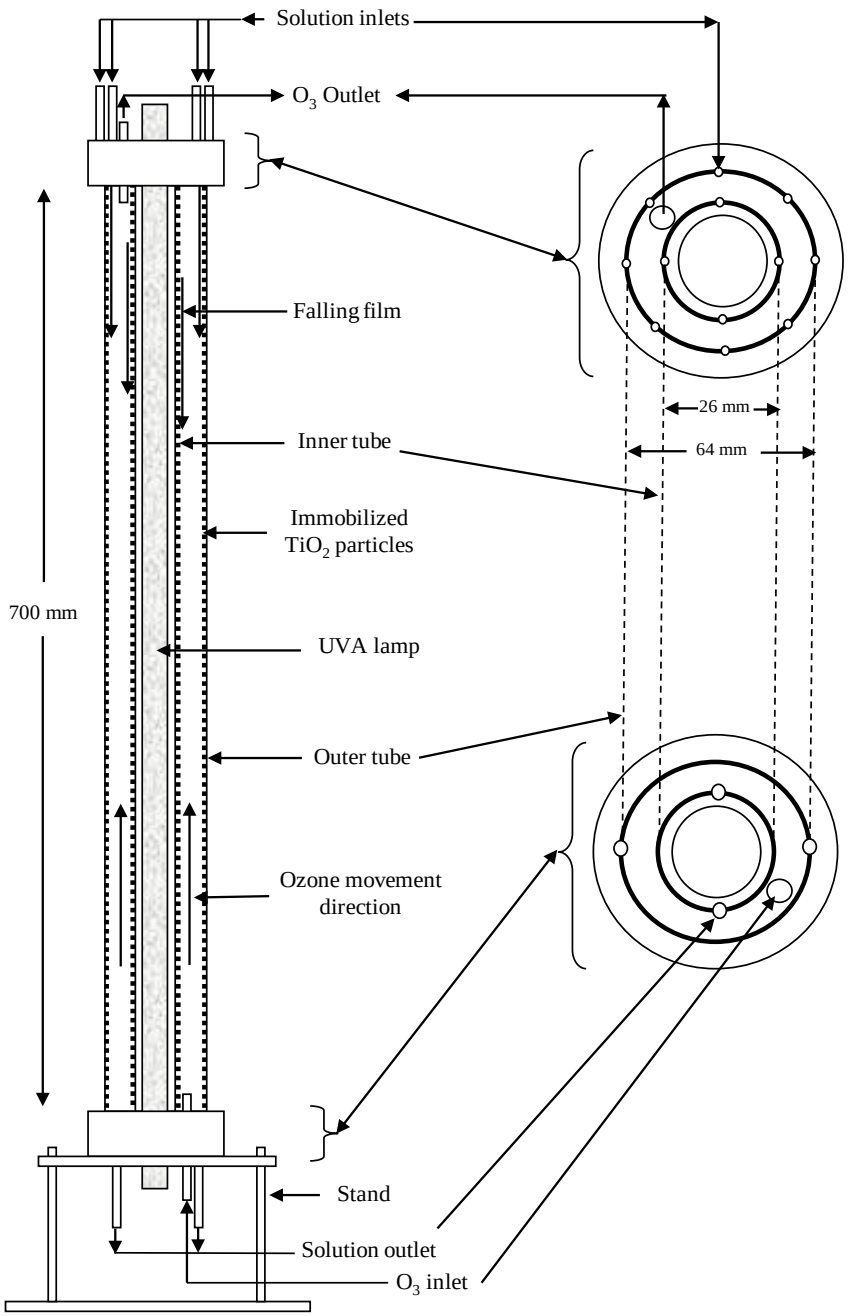

Fig. 2.2. Structure of the annular falling film reactor

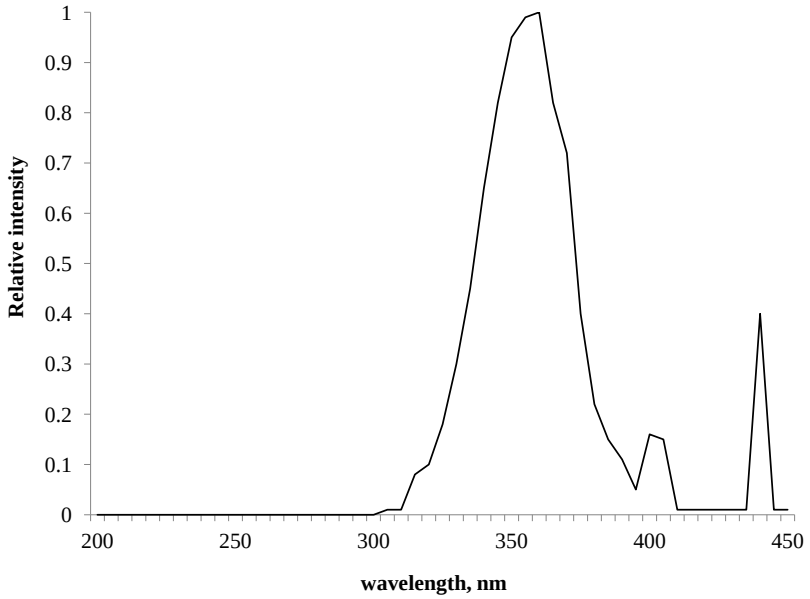

Fig. 2.3. Illumination spectrum of the UVA irradiation source

The ozone generator used in this work was manufactured by Fischer, Germany, model OZ 502/10. This device was able to produce ozone from either pure oxygen or compressed air. By changing the oxygen content of the feed gas, input flow rates and the selected power range of the device, the ozone concentration in the input gaseous mixture was programmable.

An ozone analyser produced by Anseros Ozomat GM, Germany, model RT1 measured the ozone concentration in the gas. This device was also used to determine the steady state conditions of ozone generation after the ozone generator was started.

The solution temperature was fixed at the required temperatures in all treatments, using a thermostatic bath produced by LAUDA, Germany, model B. The solution pH was measured by a pH-196 Microprocessor pH meter supplied by WTW, Germany.

2.4. Installation and setup details

Fig. 2.4 demonstrates the installation details of all equipment involved in experiments carried out by means of (a) the planar reactor and (b) the falling film reactor. In the case of the planar reactor, the solution was ozonised or oxygenised on demand in the ozonation chamber and then recycled through the reactor. The recycling of solutions was performed using a Micropump 75211-15 gear pump. The ozone generator was connected to the inlet of the ozonation chamber,

where the gas mixture bubbled through the liquid and left the chamber from the top outlet. An ozone analyser with the capability of switching between the inlet and outlet of the ozonation chamber was included to continuously detect ozone concentration in the gas phase.

Similar in principle but different in implementation, the falling-film reactor was designed to provide a wide area of photoactivated catalyst in a small space, as well as to bring the three different phases (photocatalyst as the solid, wastewater as the liquid and ozone as the gas) close to each other more effectively. In this way, whilst the stream of liquid was injected into the reactor through small apertures in the top cap to generate falling, thus generating thin layers over the immobilised semiconductor nanoparticles on the vertical walls of the reactor, the direction of gas flow through the reactor could be set in co-current or counter-current form with regard to the liquid stream by replacing the gas inlet and outlet. After passing through the reactor by falling, the solution was transferred to a vessel held in a thermostatic bath to be prepared for injection into the reactor again by means of two membrane pumps. In order to obtain a similar falling rate and similar falling film thickness for both tubes, which were different in size, the first pump recycled the solution for the outer (bigger) tube at relatively higher rates, while recycling of the solution over the inner (smaller) tube was performed separately by the second pump at lower rates.

However, as far as the gas stream was concerned, experiments were done under two conditions. In the case of volatile compounds (ethers), experiments were performed in a closed gaseous system to minimise evaporation influences, while other compounds were investigated under open gaseous systems.

2.5. Immobilisation of the photocatalyst

In order to avoid practical problems which have already been mentioned for slurry applications, TiO_2 nanoparticles were used as immobilised thin films of the photocatalyst. For the planar reactor runs, TiO_2 was deposited and fixed on borosilicate glass plates while for the falling film reactor experiments, the catalyst was immobilised on the interior surfaces of the reactor walls. Associated with catalyst immobilisation on falling film tubes, the deposition of P-25 Degussa powder was carried out on two types of support materials, borosilicate glass and Plexiglas, by means of two different technical procedures.

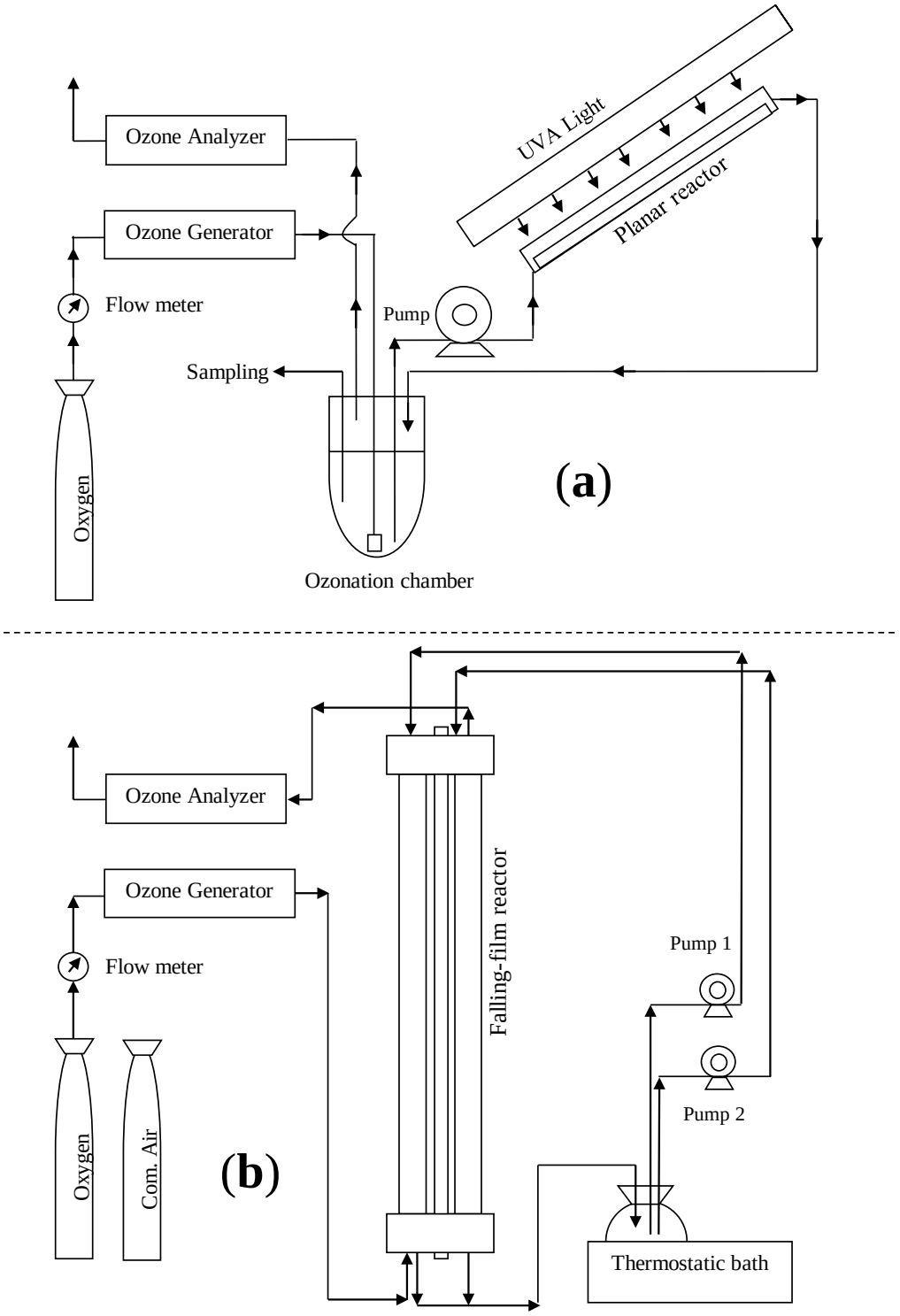

Fig. 2.4. Setup details for a) the planar reactor and b) the falling film reactor

2.5.1. Immobilisation on borosilicate glass

The coating process on the surface of borosilicate glass tubes was performed by an efficient and simple method in which a suspension of titanium dioxide nanoparticles in a mixture of ethanol and nitric acid was used to cover the glass surface. This technique was originally developed by scientists at the Netherlands Energy Research Foundation (ECN) for the deposition of titanium dioxide particles on quartz sheets of solar cells and was applied later with slight modifications for the immobilisation of this semiconductor on glass and fibreglass substrates [147], steel plates [148] and perlite granules [149].

The details of the preparation process of suspension and immobilisation using this method are given below:

First, the borosilicate glass tubes and plates were washed with acetone in order to remove organic and inorganic contaminants, then rinsed with deionised water and dried at 100°C for 30 min. After cooling, the tubes were fixed between two simple caps in a special structure similar to that of the falling film reactor. This facility (Fig. 2.5) was produced for coating purposes. The space between the two tubes was filled with the TiO_2 suspension, then the suspension was drawn out of the instrument at a rate of 10 $cm.min^{-1}$ to generate a thin film of photocatalyst nanoparticles on the surface of the tubes. In the case of coating on plates for the planar reactor, the plates were simply dipped and fixed in a special vessel containing the suspension and the slurry was purged from the bottom at a constant rate of 10 $cm.min^{-1}$.

A slurry of 1% solid TiO_2 content by mass was provided by dispersing 15 g of P-25 Degussa powder into 1125 g (1424 mL) of absolute ethanol and 375 g (357 mL) of diluted (10%) nitric acid. Acidification of the suspension by adding nitric acid has been described by many researchers [150, 151], and is necessary in order to obtain adequate dispersion with stabilised TiO_2 colloids. The suspension was processed in an ultrasonic device for 15 minutes and then immediately injected into the coating facility for the immobilisation process. After each loading (injection and suction) of the suspension into the instrument, the output slurry was re-ultrasonicated for 15 min to maintain the colloidal dispersion properties for the next loading. The loading process was repeated five times in order to obtain a proper thin film of the photocatalyst with a uniform surface capable for handling further photocatalytic activities.

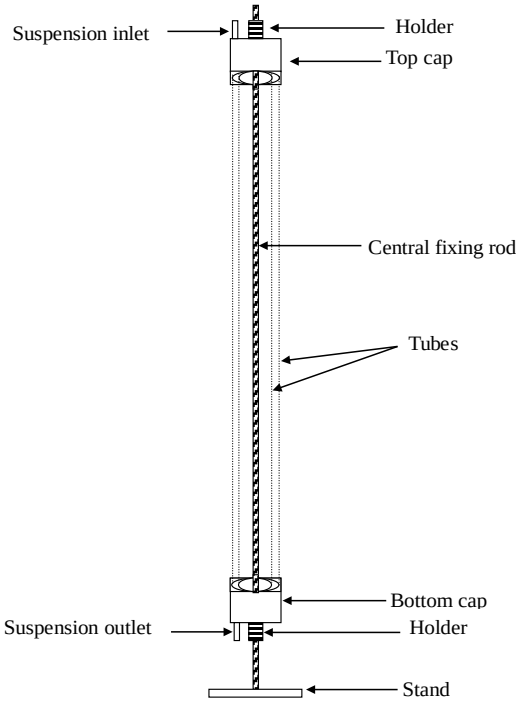

Fig. 2.5. Immobilisation (coating) facility

After the immobilised photocatalyst films were touch-dry (a few hours under laboratory temperature conditions), the tubes/plates were annealed at 450°C for 30 min, leading to the generation of hard and stable thin coatings of TiO_2 deposited on the wall of the glass tubes or plate surfaces. It is worth mentioning that, since only the anatase form is photocatalytically active and is transformed into rutile at about 600°C, any fixing process must be performed below this temperature.

In addition to this procedure, another relatively more complicated and long-process approach was also applied and assessed to generate more stable TiO_2 coatings on borosilicate glass plates using polysiloxane binder reagents, where 1 g of P-25 Degussa in addition to different amounts (1-10 g) of a polysiloxane reagent and 2 droplets of Triton X-100 as a non-ionic surfactant were added to 20 g of deionised water and processed ultrasonically for 15 minutes, then poured on borosilicate glass plates which were washed with a KOH/ethanol (5% KOH in ethanol) solution and dried prior to use. The coated plates were left in the laboratory air for 15 hours and then annealed at 200°C for 30 min. Due to low wettability, these coatings should pass an etching process using a KOH/ethanol solution before being used for treatment.

The immobilised coatings produced using this technique were assumed to be thicker, firmer and showed more adherence to their substrates compared with the coatings produced by applying the first method; however, the uniformity of these coatings was relatively worse and their photocatalytic activity was highly dependent on the content of the photocatalyst in suspension. The photocatalytic activities of these two types of catalytic coatings will be described later in the results and discussion section.

2.5.2. Immobilisation on Plexiglas (polymethylmethacrylate, PMMA)

Considering that the glass transition temperature (T_g) of polymethylmethacrylate ranges from 85°C to 165°C, the employment of methods dealing with high temperatures to prepare fixed TiO_2 thin films on Plexiglas surfaces was confined. Therefore, in order to achieve sticky thin layers with good adherence on the walls of the Plexiglas tubes and at the same time with a high level of photoactivity, the following procedure was used.

In the first step, 15 g of TiO_2 P-25 Degussa powder was added to 700 g of 1-methoxy-2-propanol as the solvent and ultrasonicated for 15 min. Later, 100 g of KASI ^{R}-GL component 1 and 50 g of KASI ^{R}-GL component 2 were added to the suspension, which was prepared in the first step and the complex was shaken well for 1-2 min. The PMMA tubes were rinsed with tap water, then deionised water and dried at a temperature of 80°C for 30 min. Next, the clean and dry tubes were fixed in the same structure described for immobilisation on borosilicate glass tubes. The coating was performed by the injection of the prepared suspension inside the structure and sucking it out at a rate of 10 $cm.min^{-1}$. The coating process was repeated until reaching a sufficient deposition of nanoparticles on the tube walls. After coating, the tubes were baked at 80°C for 2 h. Finally, after the PMMA tubes were cold, the surface of the deposited photocatalyst was washed with a solution of 5% KOH in ethanol for 5 min. The etching treatment with KOH/ethanol solution plays significant role in providing improved wettability of the surface of immobilised TiO_2.

2.6. Characterisation of the falling film reactor

In order to describe the quality and performance of the falling film reactor and to determine the optimised working conditions for it, elaborate assessments were performed with respect to some aspects involved in dealing with this kind of reactor. The following paragraphs present more

details about the operation of the membrane pumps engaged in recycling fluids through the reactor, the uniformity of the thickness of liquid falling films under different conditions, the gas washing effects of the falling films, ozone decomposition and adsorption of ozone in the liquid falling films, adsorption of model compound molecules on the surface of the photocatalyst and the influence of the movement direction of the gaseous stream through the reactor on the efficiency of the oxidation process and other practical aspects.

2.6.1. Evaluation of membrane pumps performance

A simple assessment was performed with the aim of plotting a correlation between the operation voltage of the membrane pumps and the solution recycling rates obtained at different pump voltages. The pumps did not work at voltages lower than 7 volts and their performance seemed to be constant at voltages higher than 22 volts. Fig. 2.6 shows how the solution recycling rate was enhanced as a result of pump voltage progress.

The persistency of membrane pumps was re-evaluated after about 300 working hours of recycling various ozonised solutions in order to check their suitability for further experiments. Their performance was found to be constant with deviations not more than 5% after this period of time.

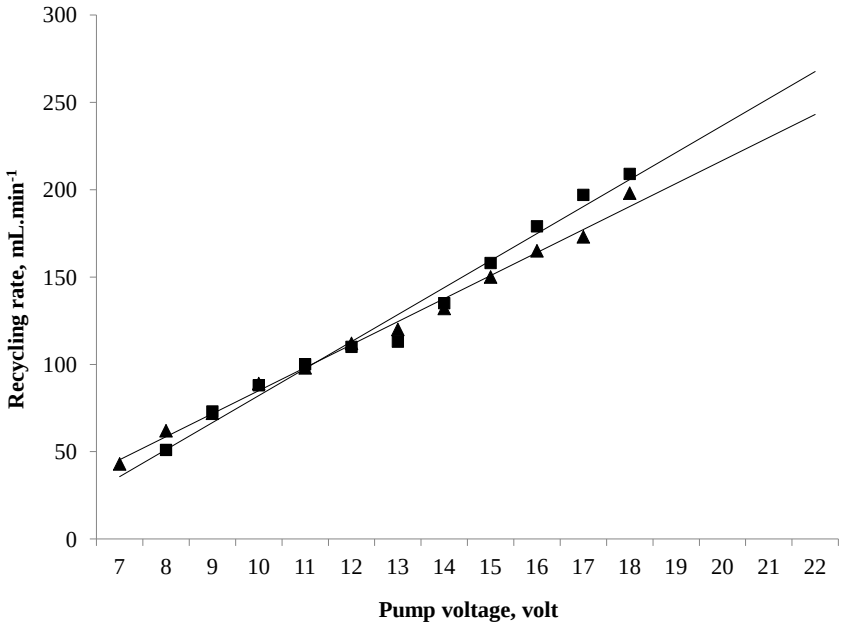

Fig. 2.6. Solution recycling rate vs. pump voltage for inner (■) and outer (▲) tubes

2.6.2. Distribution patterns of falling films

A simple technique was employed to determine the distribution patterns of liquid falling films or, in other words, to evaluate the thickness uniformity of falling films. In the beginning, a thin hypothetical transect (profile) was chosen in the middle of the falling film reactor to be the region of measurements. Four positions with similar distances from each other were determined and set on this transect around the outer tube from the outside. A particular sensor for UV light detection was connected to a volt meter fixed at each of these four positions at a right angle to the reactor wall. The sensor detected and reported the decrease in voltage when the falling film was running compared to the case when no falling film was present. The process was separately repeated for each of the four positions around the hypothetical transect. An ozonized saturated potassium iodide solution was used as falling liquid in this investigation. The colour of this solution was dark brown.

Data recording was performed three times for each tube separately by applying two different falling rates. The average numeric values of three repeated readings for each position were calculated and are presented in Fig. 2.7. In this figure, each point shows the decreased percentage of UV light intensity at each position after running the falling film. The farthest point from the graph centre reflects the thickest falling film at that point. It is clear that higher falling rates created thicker and more uniform films.

It is noteworthy that the first measurements exhibited improper thickness distributions for the falling films. Therefore, some basic modifications were made on the cap structure of the reactor, especially with regard to the quantity and orifice size of inputs in order to improve the quality of the falling films. Fig. 2.8 represents a simple comparison between the thickness distribution before and after the modification. According to this figure, the distribution pattern of falling films after this modification was considered to be satisfactory for handling the treatments.

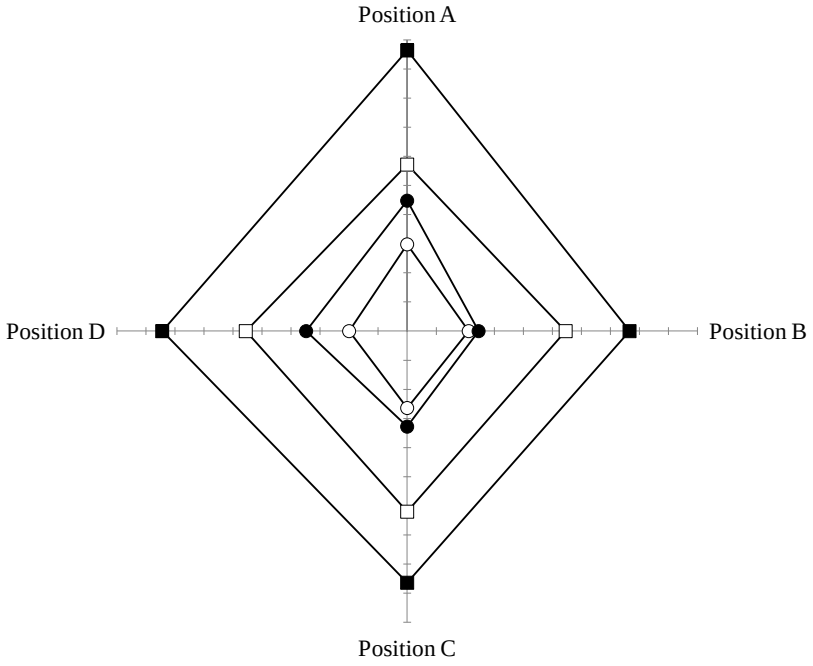

Fig. 2.7. Distribution pattern of liquid falling films on the outer tube (white) and inner tube (black) at solution recycling rates of 100 mL/min (○) and 200 mL/min (□)

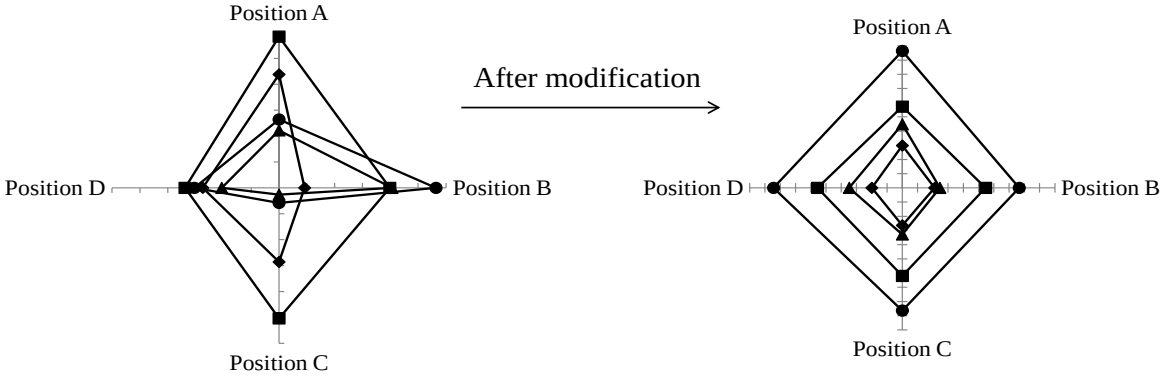

Fig. 2.8. Simple comparison between the distribution patterns of falling films before and after the modification

2.6.3. Thickness of falling films

The laminar thickness of liquid falling films was not constant along the horizontal tubes; this was described by Rogers [152] to be a function of the Reynolds number (Re) and Archimedes number (Ar) at any position on the tube. In this work, the average thickness of aqueous falling films formed on both the external wall of the inner tube and the internal wall of the outer tube were calculated roughly as follows:

a) Water recycling through the reactor was maintained for 5 minutes for each recycling rate (pump voltage) to reach steady state conditions of membrane pump performance.
b) After this time, the pump was switched off to interrupt solution injection into the reactor and, as soon as the pump was off, the out-coming water from the output point of the reactor was collected and its volume was determined by weighing.
c) This procedure was repeated three times for each recycling rate setup and the average volume was used as a result in the calculations of the next steps.
d) By plotting the average volumes vs. recycling rates, intercepts were computed and subtracted as remaining amounts of water in the connection pipes.
e) The average falling film thickness was obtained by dividing the average volumes of water which were calculated in step c by the appropriate active surface area (tubes walls) for each condition.

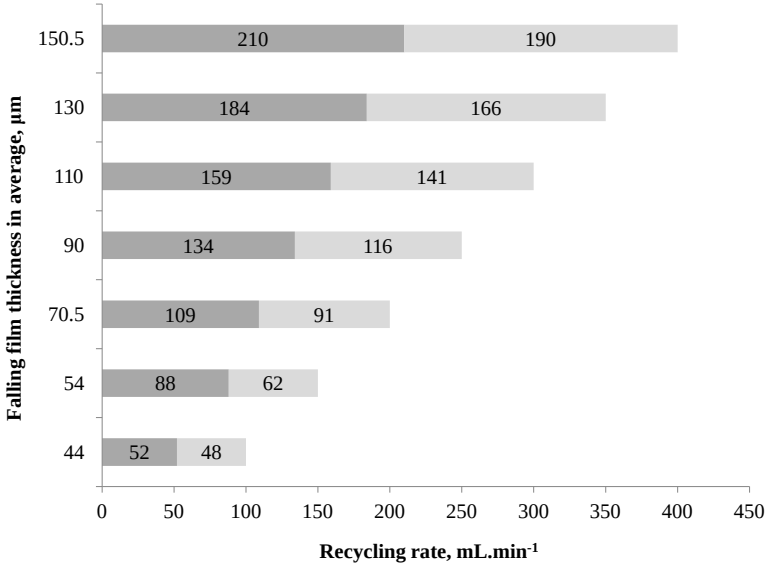

Fig. 2.9. The thickness of falling films in average vs. solution recycling rate over the wall of inner tube (light) and outer tube (dark)

The results are represented in Fig. 2.9 and were fitted to be used as a standard curve for the next experimental setup. The numerical data shown in the bars are the recycling rates for each pump individually and the sum of these is reported as the total recycling rate for each case. Considering the greater diameter of the outer tube, higher recycling rates were calculated and chosen for the pump connected to this tube compared to the inner tube to achieve almost similar thicknesses of falling films over the walls of both tubes.

2.6.4. Gas washing effect of falling films

Since the gas flow inside the reactor was considered to move from bottom to top, countering the falling liquid films, ozone molecules in the gaseous mixture would be absorbed into the liquid or be decomposed by the falling liquid streams. This investigation was planned in order to evaluate this effect for different falling rates. For this aim, the falling film reactor was first filled with an oxygen-ozone mixture with an ozone concentration of 130±5 $mg.L^{-1}$. The gas output of the reactor was connected to the ozone analyser to constantly measure the ozone concentration in the gas phase. After reaching a steady level of ozone at the output, the membrane pumps were switched on to recycle the deionised water through the reactor. Four different recycling rates between 100 $mL.min^{-1}$ and 400 $mL.min^{-1}$ were chosen for this investigation. The injection of the gaseous mixture of oxygen-ozone was maintained during water recycling. The experimental results illustrated in Fig. 2.10 show that an increase in the recycling rate of deionised water from 100 $mL.min^{-1}$ to 400 $mL.min^{-1}$ led to a decrease of about 16.5% in the ozone concentration in the gaseous phase after reaching equilibrium conditions.

These results could imply that increasing the recycling rate of water might lead to an increase in the absorption level of ozone in water. However, it will be clearly presented in the next section that increasing the recycling rate causes no considerable enhancement in the absorption level of ozone into the liquid phase. Therefore, other assumptions could be suggested, such that under recycling mode conditions, higher liquid recycling rates increase ozone decomposition by increasing turbulence. In other words, since the whole system is closed and fed continuously by a constant level of ozone under these conditions, a reduction in the ozone concentration in the gas phase, despite the lack of a reaction, could be explained only by the decomposition of ozone molecules because of shear stress of the falling liquid films.

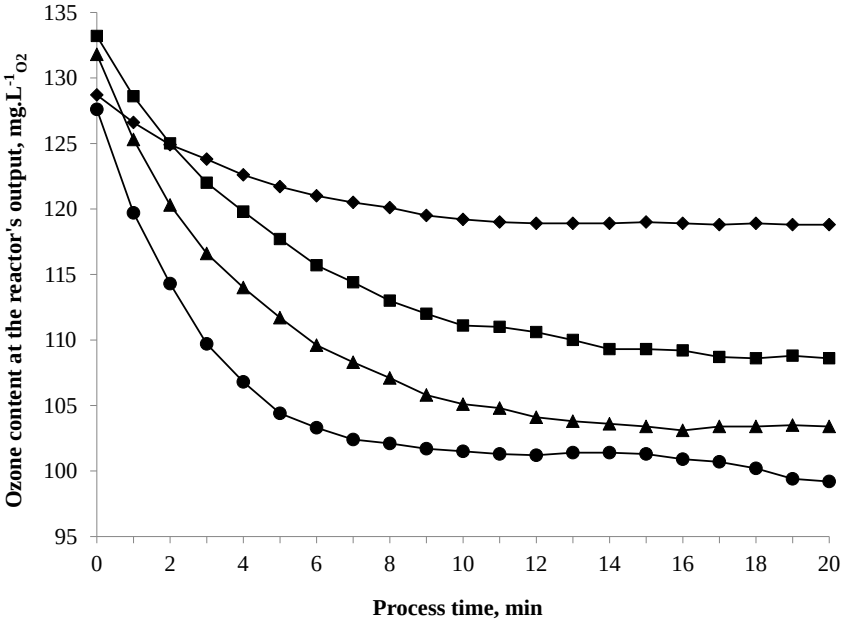

Fig. 2.10. Ozone content in the gas output of the reactor over the recycling time of deionized water at rates of 100 $mL.min^{-1}$ (♦), 200 $mL.min^{-1}$ (■), 300 $mL.min^{-1}$ (▲) and 400 $mL.min^{-1}$ (●), gas flow rate = 10 $L.h^{-1}$, T = 25° C

To summarise, it seems that applying lower falling rates during recycling-mode runs reduces the decomposition rate of ozone molecules. However, in the case of wastewater treatment by ozone or other advanced oxidation processes based on ozonation, since in addition to ozone decomposition there will be a reaction between ozone molecules and water pollutants, determining the optimum recycling rate for treatment is not easy. In order to assess this parameter when dealing with single-pass treatments, ozonation of three kinds of solutions was performed (Fig. 2.11).

The circumstances for the measurement of ozone concentrations were largely similar to those for the recycling mode with the difference that the falling liquids passed the reactor once and were not recycled again, which means that the gas stream was always affected by fresh falling liquids.

Fig. 2.11 shows that, not unexpectedly, the decreasing level of ozone in the gaseous mixture after contact with the falling liquid film mainly depended on the variety and concentration of substances in the falling liquid films as well as the reactivity of each substance inside the solution with ozone. While falling deionised water and an indigo solution over the reactor walls only caused a decrease in the ozone content of about 5 $mg.L^{-1}$ and 22 $mg.L^{-1}$ in the

gaseous mixtures, respectively, passing real pyrolysis wastewater through the reactor decreased the ozone content by about 100 $mg.L^{-1}$. This type of wastewater contained more than 30 organic and inorganic compounds. These behaviours, especially in the case of wastewater, indicate sufficient contact between the falling liquid films and ozone molecules for desirable treatment.

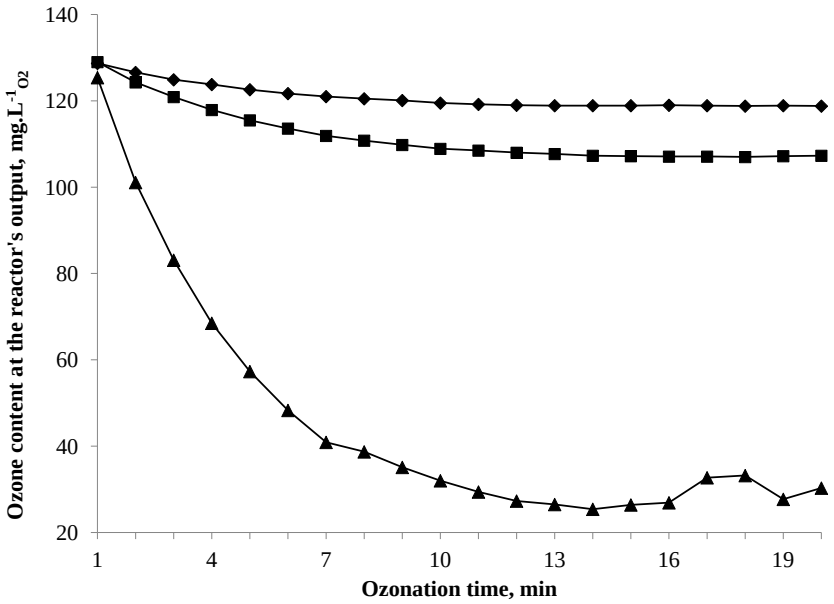

Fig. 2.11. Catalytic ozonation of deionized water (♦), Indigo solution, 0.03 M (■) and, pyrolysis wastewater (▲), falling film reactor, single-pass mode, falling rate = 100 $mL.min^{-1}$, gas flow rate = 10 $L.h^{-1}$, T = 25° C

2.6.5. Ozone absorption in the falling liquid films

The absorption level of ozone in the liquid phase was investigated under different process conditions. The indigo method [153] was employed for the measurement of ozone concentrations in water. Two initial attempts were arranged to assess the influence of the recycling rate on the ozone absorption level. For this purpose, 500 mL of deionised water were constantly recycled through the reactor, producing falling films in the presence of a counter-current flow of an ozone-oxygen gas mixture (C_{O3} = 135 $mg.L^{-1}{}_{O2}$) using two different recycling rates. The results presented in Fig. 2.12 show that increasing the recycling rate from 100 $mL.min^{-1}$ to 400 $mL.min^{-1}$ caused no remarkable enhancement in ozone absorption on average. Under these conditions, the ozone concentration in the liquid phase reaches a nearly constant value after a short period of time; however, it is clear that in the case of lower recycling rates, a relatively longer period of

time was expected to achieve the saturation level of ozone in water. The next two attempts were carried out under single-pass mode conditions such that appropriate amounts of fresh deionised water were injected into the reactor at similar rates mentioned above during the investigation. The ozone concentration in the output ozonised water was measured periodically and reported in Fig. 2.12. In the single-pass mode, a falling rate of 100 $mL.min^{-1}$ increased the ozone concentration in the liquid phase by about 3 $mg.L^{-1}$ compared with a rate of 400 $mL.min^{-1}$.

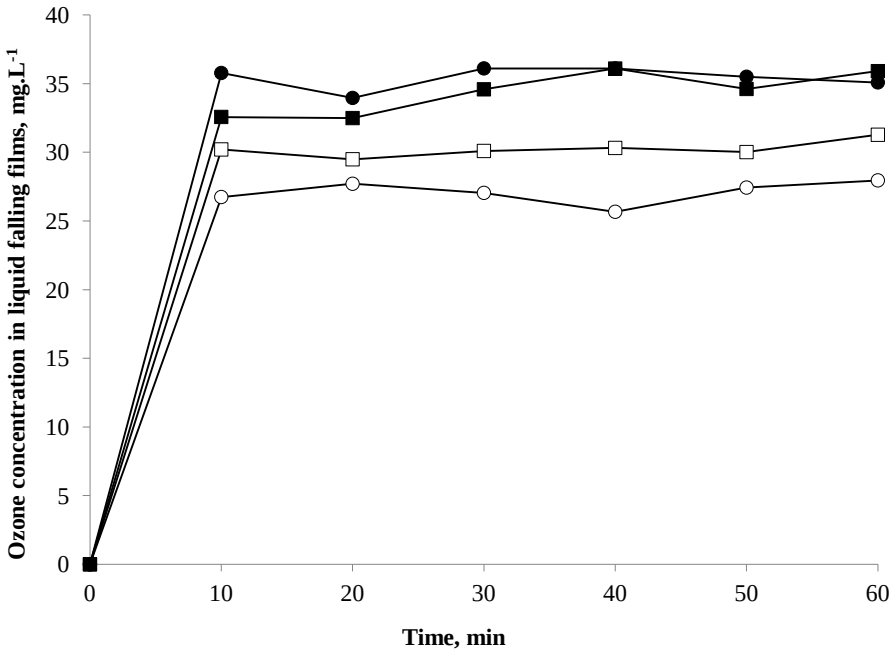

Fig. 2.12. Absorption level of ozone in the liquid falling films, recycling mode (black) and single-pass mode (white) for falling rates of 100 mL/min (□) and 400 mL/min (○), gas flow rate = 10 L/h, T = 25° C

Summarising, a high level of ozone absorption was observed in the single-pass mode and a slight difference was seen compared with the recycling mode, indicating that gas absorption in the falling liquid films occurs and rapidly reaches the saturation level under the setup conditions of the present study.

2.6.6. The effect of illumination on ozone decomposition

This set of experiments was performed in order to determine the influence of irradiation on the decomposition of different concentrations of ozone inside the falling film reactor. For this aim,

an ozone-oxygen gaseous mixture was injected continuously into the reactor and the ozone concentration in the gas phase was measured at the output of the reactor. After reaching steady state conditions of the gas phase ozone concentration, UVA irradiation was started. The measurement of the ozone concentration was done over a time period of 70 min under irradiation conditions, then the measurement was maintained in the dark. According to the results presented in Fig. 2.13, the decomposition of ozone molecules inside the reactor was accelerated by irradiation with UVA light. Fig. 2.13 shows that the level of ozone decomposition had a correlation with the initial content of ozone in the gas mixture entering the reactor such that a higher initial concentration led to higher ozone decomposition. However, for all concentrations of ozone, an almost constant ratio of the initial concentration (about 37±2%) was decomposed during illumination.

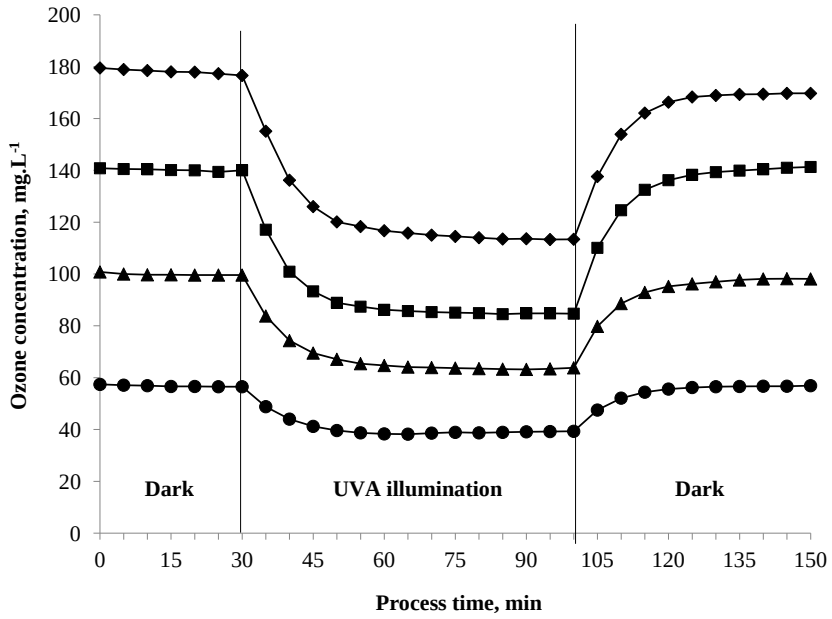

Fig. 2.13. The effect of UVA irradiation on ozone decomposition over TiO_2 surface, gas flow rate = 10 $L.h^{-1}$, T =25°C

The adsorption of ozone molecules on the surface of TiO_2 and their reaction with the photogenerated electrons thereon is the main reason for the decrease of ozone concentration in the gas phase during the irradiation time.

2.6.7. Adsorption of model pollutants on the photocatalyst surface

The adsorption level of pollutant molecules on immobilised TiO_2 nanoparticles in the falling film reactor was evaluated by applying two model compounds. For this aim, solutions of oxalic acid and dichloroacetic acid at two different concentrations (0.5 mM and 2.5 mM) were prepared at acidic pH (3-3.5) at 25°C. For these experiments, the surfaces of the falling film reactor were washed with 2 L of deionised water and dried using a hairdryer. After cooling down to ambient temperature, 500 mL of the appropriate solution were injected into the reactor and recycled for a duration of 4 h. The first sample was taken before the injection of the solution and subsequent samples were taken after 1, 2, 3 and 4 h of recycling. The adsorption level of each model compound for any situation was calculated by subtracting the concentration in the solution before and after the recycling process. All measurements were repeated three times and average values are reported as results in Table 2.2.

Table 2.2. Adsorption level of model compounds on the immobilized TiO_2 in the falling film reactor ($\mu g.cm^{-2}$)

	Oxalic acid		Dichloroacetic acid	
	C_0 = 0.5 mM	C_0 = 2.5 mM	C_0 = 0.5 mM	C_0 = 2.5 mM
After 1st hour	6.19	14.77	3.49	14.92
After 2nd hour	6.80	15.46	3.87	14.42
After 3rd hour	7.37	16.59	4.06	14.80
After 4th hour	7.85	17.64	4.43	15.55

Considering the results in Table 2.2, three points have to be highlighted. The first is that any enhancement in the concentration of model compounds will increase the level of their adsorption on the surface of the photocatalyst. The second point is that a simple comparison between the adsorption levels of these two model compounds at each concentration shows that the adsorbed amounts of oxalic acid were higher than those of dichloroacetic acid; however, the difference was relatively low at the concentration of 2.5 mM. This observation could be explained by the molecular size difference between these two carboxylic acids; compared to oxalic acid, the space occupied by bigger molecules of dichloroacetic acid could hinder the adsorption of more molecules on the surface of the photocatalyst. However, at a concentration of 2.5 mM, this effect seemed to be minimised by increasing the presence of molecules close to the

photocatalyst surface. The third point is the increase in the adsorbed amounts of model compounds over the process time. Two assumptions can explain this trend:

a) The first theory is that the descending trend of concentrations of model compounds in the solution over the duration of the process was simultaneous to the ascending concentration on the catalyst surface. In other words, the equilibrium between the adsorbed molecules on the photocatalyst surface and the molecules in the diffusion layer after 4 hours was not yet established, and a longer period of time was required to reach the equilibrium point.

b) The second theory is that equilibrium was established after the first hour and the further increase in the adsorbed amount of model compounds was due to the degradation of adsorbed molecules on the catalyst surface and the adsorption of new molecules of model compounds from the solution.

According to Fig. 2.14, plotting the adsorbed amounts of dichloroacetic acid versus chloride ions produced during the adsorption of this compound shows that a small increase in chloride ions as a degradation product was observed during the adsorption of dichloroacetic acid. These results indicate that some of the adsorbed dichloroacetic acid molecules decomposed slightly over the catalyst surface during the adsorption process.

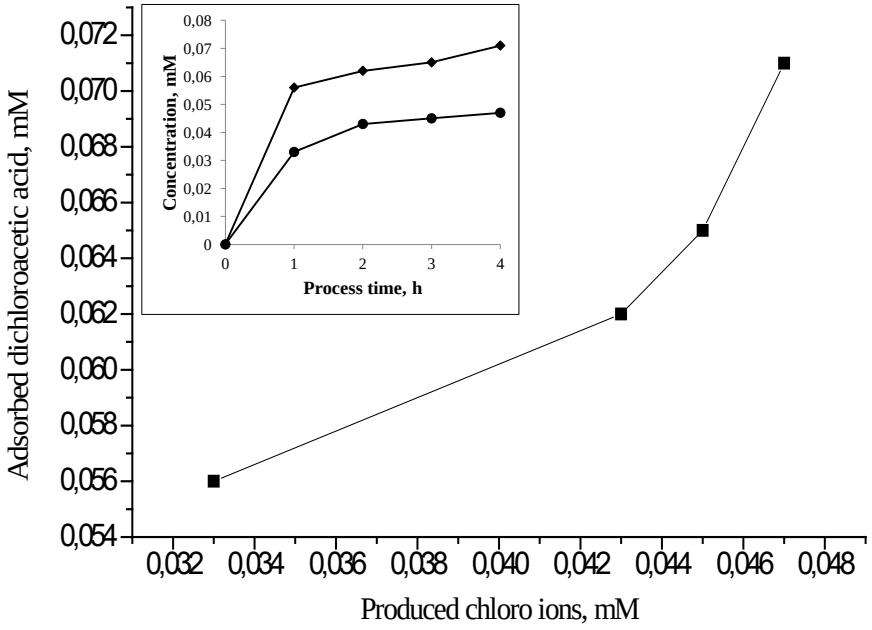

Fig. 2.14. Adsorption of dichloroacetic acid vs. generation of chlorine ions (inset graph: DCAA (♦) and Cl^- (●))

To conclude, a combination of both theories mentioned above seems to be reasonable, which means that the establishment of equilibrium between the molecules of model compounds in the solution and on the surface of the catalyst needs a longer period of time due to the slight degradation of model compounds on the surface of the catalyst.

2.6.8. The effect of direction of gas flow

This section of the present study was included in order to investigate the influence of the direction of movement of the gas stream beside the falling liquid films on the efficiency of the treatment process. For this aim, catalytic ozonation of a real sample of pyrolysis wastewater was performed under two different conditions related to gas flow. In the first setup condition, the gas flow was injected from the bottom inlet of the falling film reactor to move upward, countering the falling liquid films (counter-current) and exited at the top outlet of reactor, while in the second setup, the gas flow was inserted from the top inlet to move through the reactor with the same movement direction as the falling liquid films (co-current) and exited the reactor at the bottom outlet.

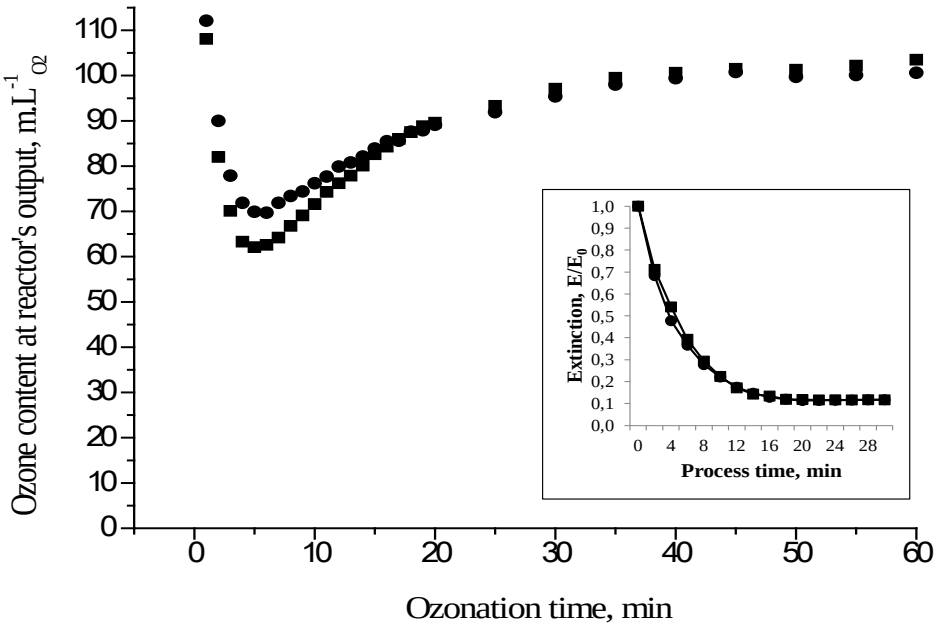

Fig. 2.15. Catalytic ozonation of pyrolysis wastewater in the falling film reactor with co-current (●) and counter-current (■) of ozone flow, wastewater recycling rate = 400 mL.min^{-1}, wastewater volume = 400 mL, gas flow rate = 10 L.h^{-1}, T = 25° C, pH = 8

Fig. 2.15 shows that, compared with the co-current setup conditions, under counter-current conditions, the concentration of ozone in the gaseous mixture at the output of reactor decreased by about 10% during the first 10 min of treatment, although the level of ozone consumption was similar for both setup conditions after 20 min. At the same time, the inset graph of Fig. 2.15 compares the colour removal of wastewater under these two conditions. It was clearly demonstrated that there was no significant difference between the efficiencies of colour removal under these two setup conditions. Therefore, in spite of the fact that counter-current gas flow caused slightly a greater decrease in ozone in the beginning due to more effective contact with the falling films, both setup conditions were in general considered to be similarly effective in the oxidation process.

2.7. Analytical methods

Based on need, different analytical methods were applied for the measurement of concentrations of the model compounds and for the evaluation of some other aspects of aqueous solutions or wastewaters.

2.7.1. Ion chromatography (IC)

Oxalic acid, dichloroacetic acid and citric acid concentration analyses as well as chloride ion concentration measurements in the case of dichloroacetic acid treatment were performed by ionic chromatography using a Dionex DX 500 apparatus with conductivity detection connected to an Ion Pac AG4A (guard column) and an AS14 anion exchange column with a 4 mm format (Dionex). The samples were pumped through a sample loop at a volume of 100 µL. The flow rate of the mobile phase, $NaHCO_3$ (1.7 mM)/Na_2CO_3 (1.8 mM), was fixed at 1.2 $mL.min^{-1}$.

2.7.2. High-performance liquid chromatography (HPLC)

The concentrations of p-benzoic acid and terephthalic acid were measured by the HPLC-MS technique. An Agilent 1100 HPLC series (Agilent Technologies, Germany) coupled to an Extended Capacity Trap (XCT) mass spectrometer were used for this purpose. Other parameters are briefly given in Table 2.3.

Table 2.3. HPLC and MS parameters

A. HPLC parameters

Column	Wicon Prontosil ACE-EPS column, 300x4.6 mm, 3-µm particle size (Heppenheim, Germany)
Column temperature	30° C
Mobile phase	A:Water and, B: Methanol both modified with formic acid, 0.1%; Gradient:0 min, A/B 10/90 (v/v); 20 min, A/B 0:100 (v/v); 30 min, A/B 0:100 (v/v)
Flow rate	0.7 $mL.min^{-1}$
Injection volume	10 µL

B. MS parameters

Source	ESI ion source; operating in positive and negative mode (alternating)
Nebulizer pressure	60 psi
Dry gas flow (N_2)	11 $L.min^{-1}$
Drying gas temperature	350° C

2.7.3. Headspace technique

This method was employed to measure the concentration of ethers and *tert*-butanol as model compounds on the basis of DIN 38407-F9-1. The heated headspace technique connected to gas chromatography or gas chromatography/mass spectrometry is a conventional measurement technique for oxygenates and their by-products [154]. The technical specifications of this determination technique are given in Table 2.4.

2.7.4. Total organic carbon analyses (TOC)

The evaluation of the mineralisation of model compounds was performed by means of a TOC-5000 Shimadzu (total organic carbon) analyser (Japan).

2.7.5. Chemical oxygen demand measurements (COD)

This analytical method was employed to quantify the quality of the real wastewater over the duration of treatment (DIN 38409-H41).

2.7.6. Spectrophotometery

A spectrophotometer (model Spekol 11, Carl Zeiss Jena) was used to determine the colour of the real pyrolysis wastewater. All samples were filtered using an E0 syringe filter (0.2 μm, Sartorius Stedim) before measurement to avoid light adsorption by the probable presence of suspended particles in the wastewater. This analytical method was also applied for measurements of the concentration of indigo solutions.

Table 2.4. Headspace and gas chromatography parameters

Combustion gases	Hydrogen 5.0 Air (hydrocarbon-free)	0.3bar 0.3 bar
Injector	splitless	
Injector temperature	280° C	
Detector	FID (flame ionization detector)	
Detector temperature	310° C	
Mobile Phase	Helium 5.0 Nitrogen 5.0	1bar 1bar
Stationary phase	SGE BP-624(Ciano-Methyl-Phenylsilicon) 30m x 0.32 mm 3μm film thickness	
Temperature program	5 min. at 40° C then, 10° C/min. up to 150° C, 0 min. then, 30° C/min. up to 180° C, 1 min.	
Injection volume	100 μL	

3. Results and discussion

An intensive study on a wide range of aspects relating to the oxidation and degradation of specific organic compounds as contaminants in water by means of different advanced oxidation processes is presented in this section. Immobilisation techniques used for fixing TiO_2 on borosilicate glass and Plexiglas are evaluated. The influences of some experimental variables such as solution temperature and pH, the initial concentration of model compounds, water/wastewater recycling rates, ozone content in the input gas mixture, the flow rate of the feed gas, as well as reactor design concepts and impact patterns on the efficiency of oxidation treatment are demonstrated. Appropriate results are illustrated in detail and discussed separately for each part. Moreover, an assessment of the performance of the falling film reactor in terms of colour removal and the treatment of a real wastewater sample produced by a thermal pyrolysis process is presented as a case study in this work.

3.1. Evaluation of immobilised photocatalysts

3.1.1. The photoactivity of immobilised photocatalysts

It was already mentioned that two techniques using suspensions of ethanol/nitric acid and polysiloxane/Triton X-100 were applied for the immobilisation of the photocatalyst on borosilicate glass. In terms of appearance, the surface of photocatalyst samples fixed by polysiloxane/Triton X-100 was non-uniform, but due to the existence of polysiloxane as a binder, the immobilised photocatalysts using this method were thicker and more stable than those produced by the ethanol/nitric acid method. The photocatalytic activity of fixed TiO_2

nanoparticles was assessed by photocatalytic degradation of indigo using the planar reactor. Fig. 3.1 shows that the efficiency of both photocatalyst samples in the photocatalytic oxidation of indigo seemed to be nearly equal. About 85%-90% of the initial concentration of indigo was similarly oxidised after 100 min of oxidation time using these two different photocatalysts. The trend of indigo degradation in the absence of the photocatalyst is also shown in Fig. 3.1.

Concerning the polysiloxane/Triton X-100 method, it is noteworthy that the ratio of TiO_2 to polysiloxane in the suspension used for the immobilisation procedure played an important role in the photoactivity of the prepared TiO_2 surfaces. It was observed that a ten-fold decrease in the TiO_2/polysiloxane ratio by maintaining the content of TiO_2 and increasing the polysiloxane content, led to a decrease in the photoactivity of the immobilised photocatalyst by about 50% (Fig. 3.2).

Polysiloxane was used as a binder to stabilise TiO_2 nanoparticles on the surface of borosilicate glass. Therefore, any excess of this material in the suspension will cover the fixed nanoparticles of TiO_2 and will consequently limit their availability for oxidation reactions.

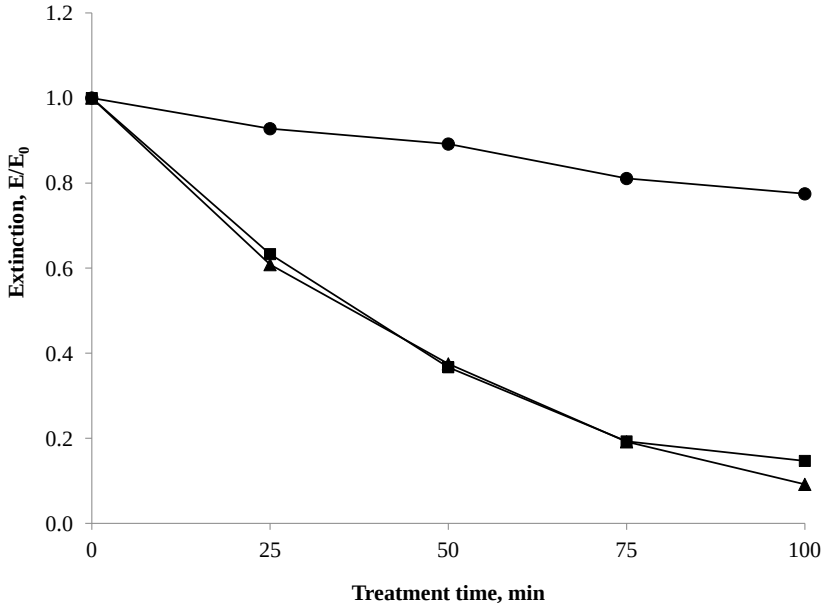

Fig. 3.1. Photocatalytic oxidation of indigo (0.01 mM) using immobilised TiO_2 by ethanol/nitric acid method (▲) and polysiloxane/triton X-100 method (■), as well as photolysis on borosilicate glass (●), planar reactor, recycling rate = 1 $L.min^{-1}$, solution volume = 400 mL, T = 25° C, pH = 2, , λ = 600 nm

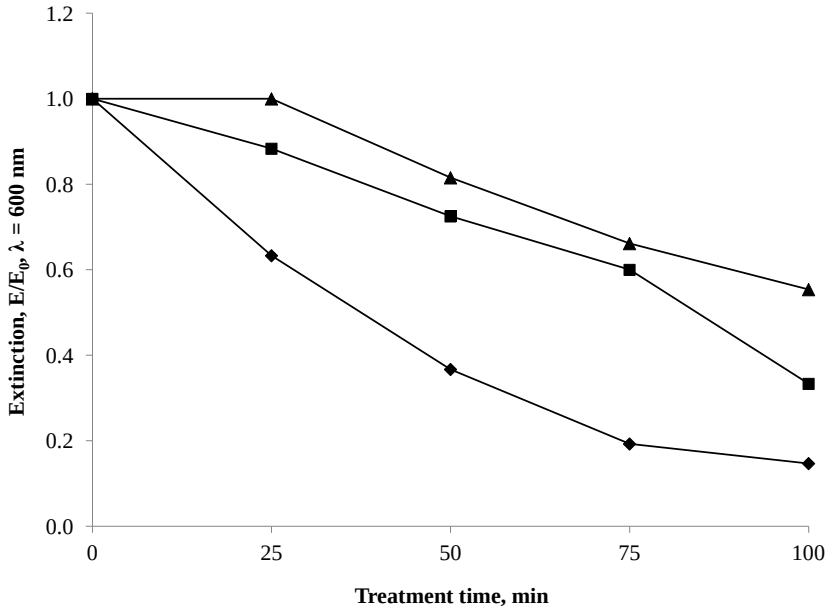

Fig. 3.2. Photocatalytic oxidation of indigo (0.01 mM) using immobilized TiO_2 by polysiloxane/triton X-100 method, TiO_2/polysiloxane ratios: 1 (♦), 0.5 (■) and 0.1 (▲), planar reactor, recycling rate = 1 $L.min^{-1}$, solution volume = 400 mL, T = 25° C, pH = 2, λ = 600 nm

To conclude, because of implementation difficulties with the polysiloxane/Triton X-100 method, especially for the immobilisation of TiO_2 on the surface of tubes in the falling film reactor on one hand, and due to the similar photoactive properties observed for samples obtained from both approaches on the other hand, the simple ethanol/nitric acid method was chosen for fixing the photocatalyst on the borosilicate glass tubes of the falling film reactor.

In this work, two different materials were selected as substrates for immobilised TiO_2 in the initial design of the falling film reactor: borosilicate glass (BSG) and polymethylmethacrylate (PMMA; Plexiglas). Considering the different physicochemical properties of these substrates, two different immobilisation techniques were applied for fixing TiO_2 on the surface of BSG and PMMA. The procedure of immobilisation was presented in detail in the experimental section. Despite the similar appearance of the two samples, an investigation of the photoactivity of photocatalysts immobilised on BSG and PMMA showed that the performance of TiO_2 particles fixed on BSG by means of the ethanol/nitric acid method using photocatalytic oxidation and photocatalytic ozonation was much better than that of immobilised TiO_2 on PMMA using the $KASI^R$-GL sol-gel method. Conversely, no difference was observed in the efficiencies of

catalytic ozonation for both photocatalysts (Fig. 3.3). According to the results in Fig. 3.3, the degradation of oxalic acid by photocatalytic ozonation over TiO_2-BSG was almost complete after 50 min, while it took 100 min to be complete over TiO_2-PMMA. Photocatalytic oxidation on TiO_2-BSG decomposed 76% of the initial concentration of oxalic acid after 100 min, but only 49% was decomposed on TiO_2-PMMA using the same oxidation method under similar conditions. This behaviour can be rationalised considering the low surface wettability of immobilised TiO_2 on PMMA. This effect decreases the effective contact between molecules of pollutants in the water and the surface of the photocatalyst and, as a consequence, it negatively influences the efficiency of oxidation.

The catalytic ozonation results in Fig. 3.3 indicate that the presence of a fixed catalyst in the ozonation medium and the adsorption of contaminant molecules on the catalyst surface provided no improvement in the efficiency of the ozonation process. Otherwise, the more hydrophilic surface properties of TiO_2-BSG compared to those of TiO_2-PMMA could lead to more effective catalytic ozonation treatment on TiO_2-BSG.

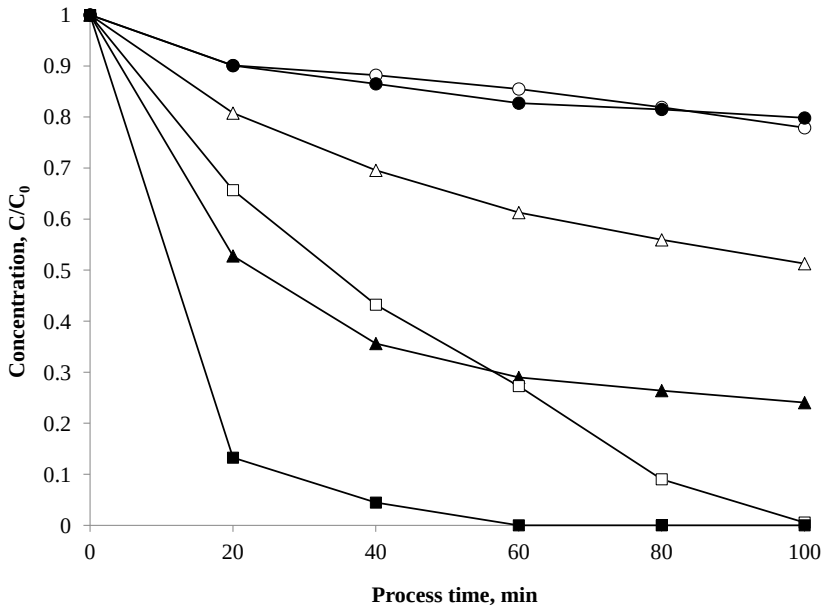

Fig. 3.3. Degradation of oxalic acid (1mM) by TiO_2/O_3 (○), $TiO_2/UVA/O_2$ (Δ) and $TiO_2/UVA/O_3$ (□) systems using immobilised TiO_2 on borosilicate glass (black) and polymethylmethacrylate (white), falling-film reactor, recycling rate = 150 $mL.min^{-1}$, solution volume = 500 mL, T = 25° C, pH = 2.8

However, the wettability in this case was modified by etching treatment, but it was significantly lower than that for the surface of the photocatalyst on borosilicate glass. This is considered as a significant disadvantage, thus hindering the utilisation of PMMA tubes for the falling film reactor. In order to overcome this issue, many advanced immobilisation approaches are suggested such as chemical vapour deposition (CVD), electron cyclotron resonance (ECR) plasma and chemical sputtering, which are outside the scope of this discussion.

Considering the observed results, the majority of the subsequent experiments on the falling film reactor were performed using TiO_2 immobilised on borosilicate glass by means of the ethanol/nitric acid method.

Looking back at Fig. 3.3, it is evident that the efficiency of TiO_2-based oxidation systems decreases over the duration of oxidation. This fact, which was observed for immobilised TiO_2 on borosilicate glass and Plexiglas, was probably due to two issues; first, the gradual poisoning of the catalyst surface [68] and second, the generation of some organic and inorganic substances over the duration of oxidation which react with hydroxyl radicals, forming secondary radicals which do not proceed in the oxidation process [11]. These substances, known as inhibitors or scavengers, terminate the chain reactions and reduce the efficiency of all oxidation processes involving hydroxyl radicals. Carbonate and hydrocarbonate are two well-known scavengers which react with OH radicals as described below (Reactions 3.1 and 3.2):

$$OH^{\bullet} + CO_3^{2-} \rightarrow OH^{-} + CO_3^{\bullet -} \qquad k = 4.2 \cdot 10^8\ M^{-1}s^{-1} \qquad (3.1)$$

$$OH^{\bullet} + HCO_3^{-} \rightarrow OH^{-} + HCO_3^{\bullet} \qquad k = 1.5 \cdot 10^7\ M^{-1}s^{-1} \qquad (3.2)$$

3.1.2. The durability of immobilised photocatalysts

Abrasion and gradual removal of fixed TiO_2 nanoparticles in addition to poisoning events likely occurred during the treatment of various types of polluted waters in the falling film reactor. The durability of the immobilised photocatalyst on the reactor walls was assessed by a comparison of the photoactivity of these photocatalysts before and after a certain period of time. For this aim, the performance of two different advanced oxidation processes in the decomposition of oxalic acid was investigated on a freshly immobilised photocatalyst (Fig. 3.4, t = 0). Later, after 10 months and handling approximately 200 h of several oxidation processes dealing with many compounds on the same immobilised photocatalyst, the oxidation of oxalic acid was repeated

under similar experimental conditions (Fig. 3.4, t = 200 h). The results in Fig. 3.4 indicate that after 200 h of fixed photocatalyst life, a decrease of about 17% on average was observed for the efficiency of the photocatalytic oxidation of oxalic acid. This reduction can be attributed to the removal and washing off of poorly fixed nanoparticles of TiO_2 from the surface as well as to the poisoning of fixed nanoparticles over time. However, this decrease in efficiency was much lower for photocatalytic ozonation, highlighting the considerable influence of ozone in the oxidation process which can effectively compensate for fatigue.

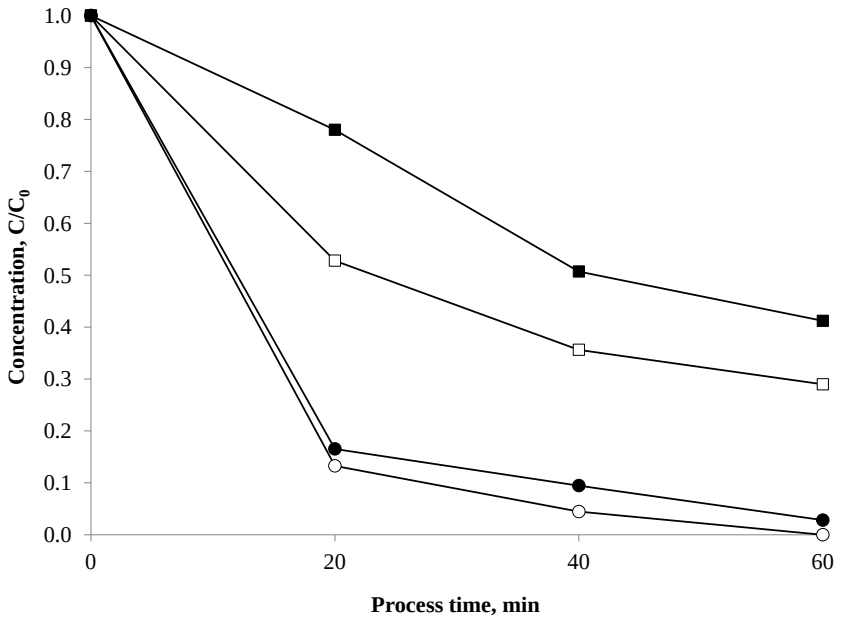

Fig. 3.4. Degradation of oxalic acid (1mM) using TiO_2/UVA/O_2 (□) and TiO_2/UVA/O_3 (○) oxidation systems at t= 0 (white) and t = 200 h (black) of the age of immobilised catalyst, falling film reactor, recycling rate = 100 mL.min^{-1}, solution volume = 400 mL, T = 25° C, pH = 2.8

3.2. The influence of reactor design

As far as TiO_2-based advanced oxidation processes are concerned, despite all the advantages mentioned for the immobilisation of photocatalysts on fixed beds for water and wastewater treatment, a great disadvantage of utilising fixed TiO_2 nanoparticles is the mass transfer problem which arises during the oxidation process, especially when the performance is compared with that of slurry applications. One important factor to solve this issue or at least to modify the conditions for better operation is the design of a reactor in which the fixed photocatalyst is

involved and can act under optimum conditions. The most significant parameter in this aspect is the ratio between the active surface of the photocatalyst and the volume of wastewater available on the surface for treatment. In order to evaluate this parameter, a simple comparison was performed between the efficiencies of two different reactors, the planar reactor and the falling film reactor in the oxidation of oxalic acid, dichloroacetic acid and citric acid. The results are presented in Fig. 3.5.

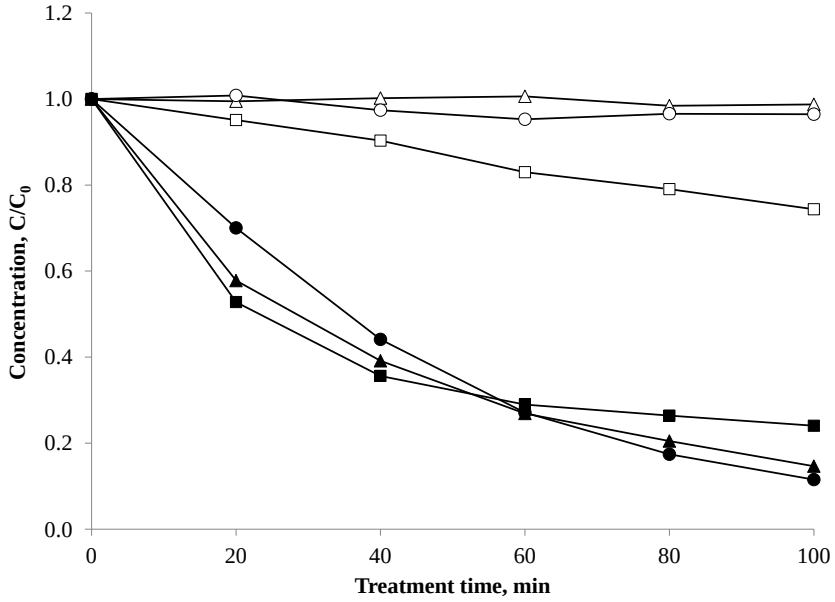

Fig. 3.5. Photocatalytic oxidation of oxalic acid, 1 mM (□), dichloroacetic acid, 1 mM (Δ) and, citric acid, 1 mM (○) in the falling film reactor (black) and planar reactor (white), solution volume = 400 mL, T = 25° C

It was clearly observed that increasing the surface to volume ratio from 500 $m^2.m^{-3}$ in the planar reactor to about 20000 $m^2.m^{-3}$ in the falling film reactor increased the oxidation rate of all model compounds; however, the increase in the oxidation rate in the falling film reactor compared with that of the planar reactor was highly dependent on the chemical structure and properties of the compounds.

3.3. Oxidation of model compounds

3.3.1. Oxidation of aliphatic carboxylic acids

In this section, the degradation of three aliphatic carboxylic acids, oxalic acid, dichloroacetic acid and citric acid as model compounds were evaluated under various oxidative atmospheres in the falling film reactor. For this aim, their decomposition rates were determined using simple ozonation and other five different advanced oxidation processes: catalytic ozonation, photo-ozonation, photo-oxidation (photolysis), photocatalytic oxidation and photocatalytic ozonation. Figs. 3.6-3.8 present a series of results in a comparative assessment for each model compound individually. It must be noted that besides all experimental variables, which can highly influence the oxidation rates, the chemical properties of model compounds which determine their reactivity with oxidising reagents as well as the adsorption level of their molecules on the catalyst surface are two fundamental aspects in TiO_2-based advanced oxidation processes that also play an important role in the manner of their degradation. Thus, due to the distinct chemical structures of these three carboxylic acids, their decomposition behaviours under oxidation conditions were expectedly different.

Photocatalytic ozonation (TiO_2/O_3/UVA) of oxalic acid in the falling film reactor led to a rapid decrease in the concentration of oxalic acid, such that about 90% of the initial concentration was removed after 40 min and complete degradation was achieved after 100 min (Fig. 3.6). Photocatalytic oxidation (TiO_2/O_2/UVA) as well as ozonation in the absence and presence of TiO_2 (O_3 and O_3/TiO_2) similarly caused a decrease of about 65% of the initial concentration of oxalic acid over the oxidation time, while UVA irradiation slightly increased the efficiency of ozonation (O_3/UVA) (Fig. 3.6). Photolysis (O_2/UVA) of oxalic acid was negligible over the duration of treatment.

Fig. 3.7 shows that dichloroacetic acid is more resistant than oxalic acid to ozone. Simple ozonation of this compound in the falling film reactor only decomposed 9% of the initial concentration over a similar treatment time; however, a combination of TiO_2 with ozone and UVA with ozone almost doubled the efficiency of ozonation. Like oxalic acid, the best degradation rate of dichloroacetic acid was observed using the TiO_2/O_3/UVA system, where no dichloroacetic acid molecules were detected in the reaction medium after 60 min of oxidation time. The TiO_2/O_2/UVA oxidation system also demonstrated effective performance in the

degradation of dichloroacetic acid, where about 75% of the initial concentration was removed after 100 min of treatment by this technique. Photolysis of dichloroacetic acid was very minor.

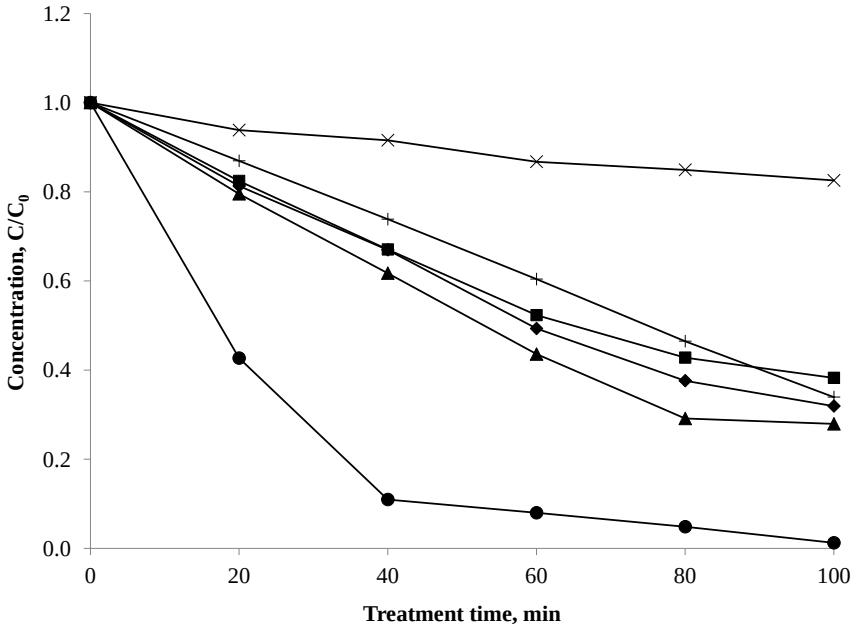

Fig. 3.6. Degradation of oxalic acid, 10 mM by ozonation, O_3 (♦), catalytic ozonation, TiO_2/ O_3 (■), photo-ozonation, O_3/UVA (▲), photo-oxidation, O_2/UVA (x), photocatalytic oxidation, TiO_2/UVA/O_2 (+) and photocatalytic ozonation, TiO_2/UVA/O_3 (●) in the falling film reactor, recycling rate = 100 mL.min^{-1}, solution volume = 500 mL, T= 25° C, initial pH = 2.5

Similar to the previous model compounds, photocatalytic ozonation was observed to be the most powerful oxidation method among all the investigated techniques for the decomposition of citric acid. Photocatalytic ozonation oxidised about 56 % of the initial concentration of citric acid after 100 min, almost twice the efficiency of the other advanced oxidation processes such as photocatalytic oxidation, catalytic ozonation and photo-ozonation (Fig. 3.8). In this case, no considerable differences were observed between ozonation, catalytic ozonation and photo-ozonation. Once again, compared with other techniques, simple UVA irradiation of citric acid solutions in the absence of TiO_2 (photolysis) could not remove this model pollutant to a considerable degree (Fig. 3.8).

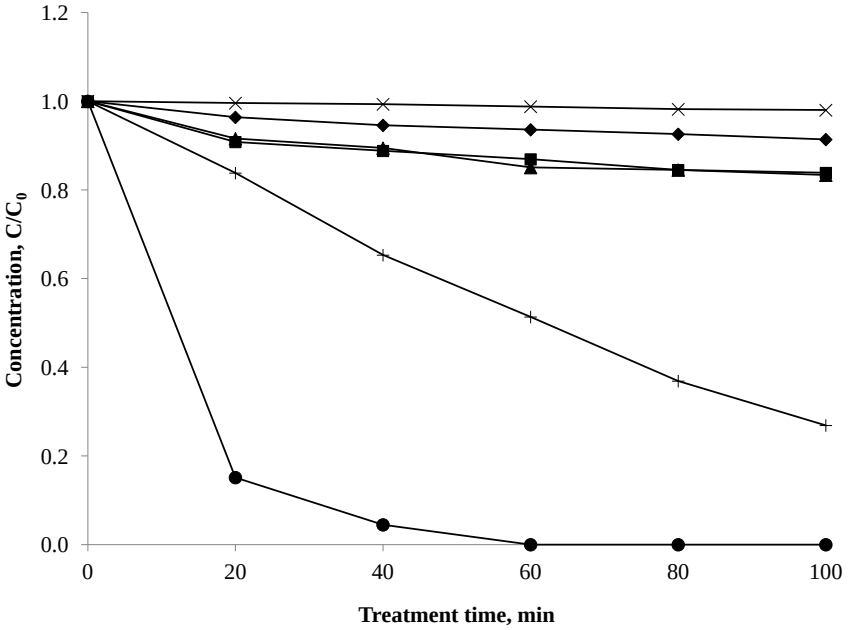

Fig. 3.7. Degradation of dichloroacetic acid, 1mM by ozonation (♦), catalytic ozonation (■), photo-ozonation (▲), photo-oxidation (x), photocatalytic oxidation (+) and photocatalytic ozonation (●) in the falling film reactor, recycling rate = 100 mL.min^{-1}, solution volume = 500 mL, T = 25° C, initial pH = 3

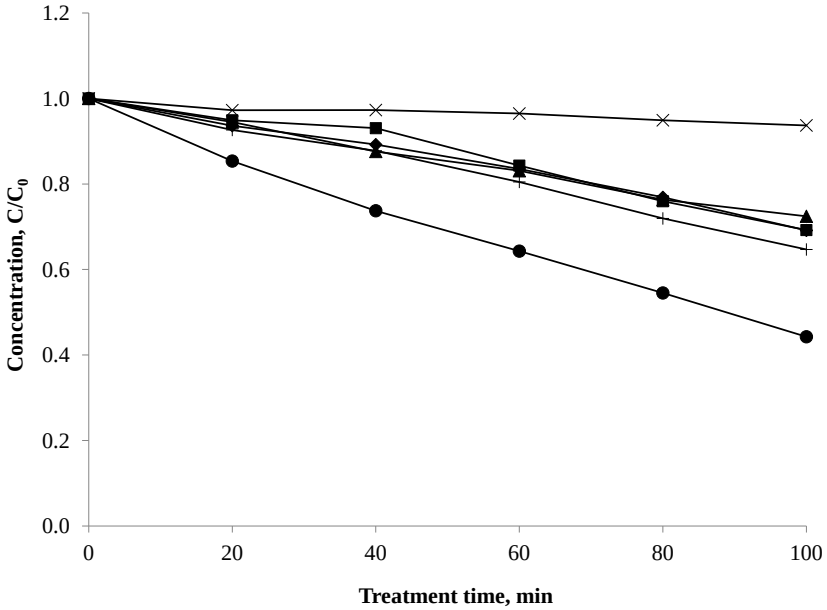

Fig. 3.8. Degradation of citric acid, 7 mM by ozonation (♦), catalytic ozonation (■), photo-ozonation (▲), photo-oxidation (x), photocatalytic oxidation (+) and photocatalytic ozonation (●) in the falling film reactor, recycling rate = 100 mL.min^{-1}, solution volume = 500 mL, T = 25° C, initial pH = 3.2

To summarise, some points must be highlighted. 1) The high rates of degradation of these aliphatic carboxylic acids by the TiO_2/UVA/O_3 oxidation system can be explained by a remarkable increase in the generation of free hydroxyl radicals using a combination of ozone and photoexcited TiO_2 particles. Considering the higher reaction rates between the molecules of the model compounds and hydroxyl radicals as the oxidising reagent compared to those of oxygen and ozone, these radicals handle the oxidation treatment more effectively. Thus, greater formation of hydroxyl radicals during the oxidation processes led to improved efficiency in the degradation of model compounds. 2) In the presence of TiO_2 and irradiation, oxygen and ozone can both act as traps for photogenerated electrons in order to avoid recombination. However, ESR studies by Hernandez-Alonso et al. [155] showed that ozone is more electrophilic than oxygen. Moreover, according to the mechanisms described by Addamo et al. [95], each electron trapped by ozone can proceed to generate a hydroxyl radical, while when oxygen acts as the electron trap, three photogenerated electrons are needed for the generation of a hydroxyl radical. For this reason, photocatalytic ozonation is more efficient than photocatalytic oxidation. 3) Under the setup conditions of the falling film reactor, the existence of TiO_2 in the dark reaction medium could not obviously improve the ozonation rate of these model compounds, although a poor effect was determined for the catalytic ozonation of dichloroacetic acid. 4) With the exception of citric acid, irradiation of ozonation media in the falling film reactor by near-UV wavelengths slightly increased the performance of ozonation. The effect of UVA could be attributed to the higher amount of hydroxyl radicals produced during the direct reaction of ozone with hydrogen peroxide molecules. Hydrogen peroxide molecules are generated as an intermediate in ozone decomposition chain reactions.

3.3.2. Oxidation of aromatic carboxylic acids

Decomposition of terephthalic acid (TFA) and *p*-chlorobenzoic acid (*p*CBA) using the falling film reactor was performed under two different advanced oxidation conditions, TiO_2/O_3 and TiO_2/O_2/UVA. Due to the poor solubility of these two substances in water, aqueous solutions with lower concentrations were prepared for the oxidation treatments. The heterogeneous catalytic ozonation of both compounds led to very fast degradation, such that neither TFA nor *p*CBA were detected in the reaction medium after the first sampling which was carried out 25 min after the treatment was started (Fig. 3.9). Meanwhile, the rate of photocatalytic oxidation

was found to be different for these substances. It can be seen in Fig. 3.9 that photocatalytic oxidation of *p*-chlorobenzoic acid decreased the initial concentration by about 78% after 100 min of treatment duration, while the same oxidation process completely removed terephthalic acid after 75 min.

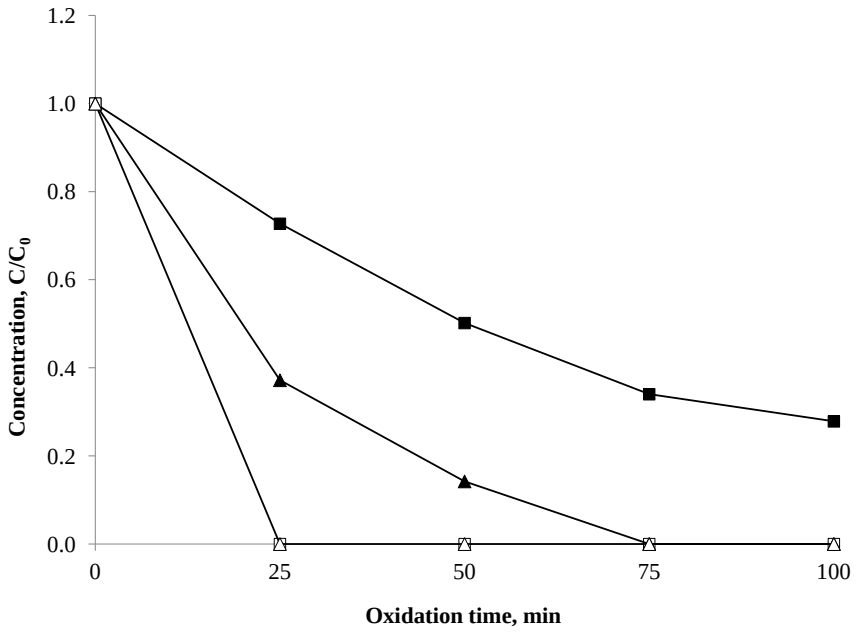

Fig. 3.9. Photocatalytic oxidation (black) and catalytic ozonation (white) of *p*-chloro benzoic acid, 0.1 mM (□) and terephthalic acid, 0.1 mM (Δ) in the falling-film reactor, recycling rate = 100 mL.min^{-1}, solution volume = 500 mL, T = 25° C, initial pH = 4 (pCBA) and pH = 3.5 (TFA)

It has been reported by Yao and Haag [126], Elovitz and Gunten [156] and Zang et al. [123] that the reaction rates between hydroxyl radicals and *p*-chlorobenzoic acid and terephthalic acid are $5{\cdot}10^{9}$ M^{-1}s^{-1} and $2.28{\cdot}10^{9}$ M^{-1}s^{-1}, respectively, whereas the oxidation rates of these two aromatic carboxylic acids by ozone molecules are considered to be negligible (≤0.2 M^{-1}s^{-1}). The rapid removal of TFA and *p*CBA under conditions of catalytic ozonation in the falling film reactor can be justified by three factors: 1) the low concentrations of these substances in the aqueous solution, 2) increased contact time between the contaminants and ozone molecules provided by the more effective design of the falling film reactor and 3) the generation of hydroxyl radicals which is promoted by presence of TiO_2 in an ozone atmosphere . It was clearly observed that under the operating conditions of the falling film reactor, the combination of TiO_2

and ozone in the dark could not increase the ozonation rate of the aliphatic oxalic acid model compounds. Therefore, it is assumed that the third factor mentioned above is not a major one causing the high degradation rates.

Even though similar initial concentrations were used for both model compounds, the decomposition of terephthalic acid using the photocatalytic oxidation system in the falling film reactor was faster than the decomposition of *p*-chlorobenzoic (Fig. 3.9). This observation could be explained by the characteristics of the chemical structures of these two molecules. The adsorption of contaminants on the surface of a photocatalyst is a fundamental step for photocatalytic oxidation treatments. Therefore, any repulsive event that inhibits adsorption can negatively affect the efficiency of treatment and vice versa. Compared with terephthalic acid which has two carboxylic acid groups, *p*-chlorobenzoic acid has just one carboxylic acid group and a larger chloro group as a substitution instead of the second carboxylic acid group. It seems that the greater steric hindrance of the chloro group in the *p*CBA molecule inhibits the adsorption of these molecules on the catalyst surface. Furthermore, if we accept that the acidic functional groups are the adsorption sites for this type of molecule, TFA has the ability to absorb at twice the rate of *p*CBA. Since the photocatalytic oxidation of TFA and *p*CBA was performed at slightly different pH levels, $pH_{TFA} = 3.5$ and $pH_{pCBA} = 4$, this difference in pH could also influence the isoelectric character of the immobilised photocatalyst and, as a consequence, could be a reason for the increased degradation rate of TFA under more acidic conditions.

3.3.3. Oxidation of ethers and their by-products

The low Henry's law constants reported in Table 1.4 for MTBE, ETBE and TBA indicate that even small amounts of these chemicals dissolved in water will evaporate. This feature caused some problems in precisely detecting these compounds during the treatment of their aqueous solutions in an open oxidation system where the gas stream passed the falling film reactor continuously. Therefore, unlike other model compounds, the degradation of this group of substances was investigated under conditions of a closed system by employing different advanced oxidation processes in the falling film reactor. To clarify, before the oxidation was initiated, the internal space of the falling film reactor was filled with oxygen and/or ozone on demand. At the same time, appropriate volumes of deionised water were recycled through the reactor and saturated with these gases. After 1 h, the gas flow was switched off and the model

compound (MTBE, ETBE, TAEE or TBA) was injected into the solution inside the reactor and mixed by a stirrer. The system was completely closed throughout the oxidation period.

Fig. 3.10 shows that the evaporation rate of MTBE while recycling the solution in the closed system was considered minor. Although ozonation, catalytic ozonation and photocatalytic oxidation gently decomposed 85%-90% of the initial concentration of MTBE in the aqueous solution after 50 min of oxidation, photocatalytic ozonation sharply decreased the initial concentration by about 91% after 10 min, and after 20 min, it was completely removed.

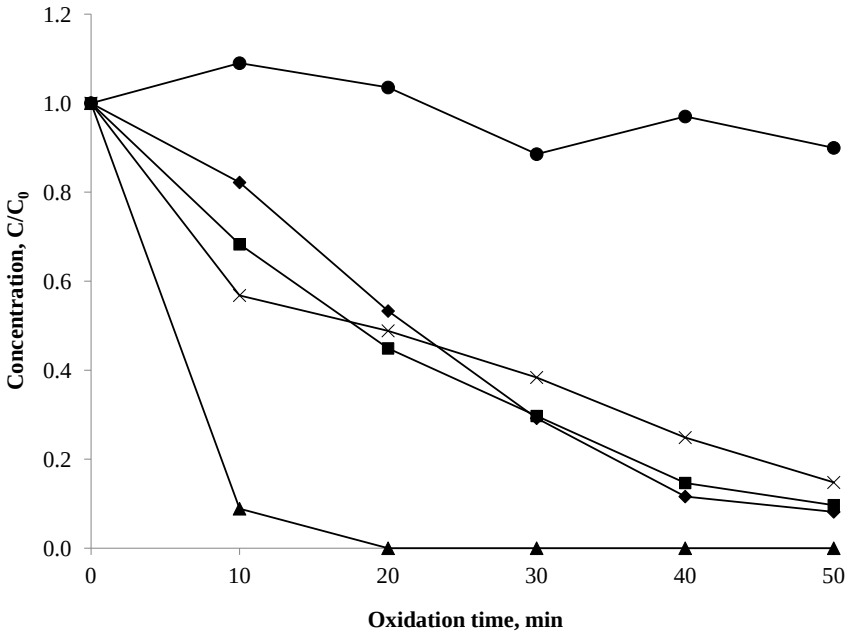

Fig. 3.10. Degradation of MTBE (0.01 mM) by means of different oxidation systems, simple recycling (●), Ozonation (♦), Catalytic ozonation (■), Photocatalytic oxidation (x), Photocatalytic ozonation (▲), falling film reactor, recycling rate = 100 mL.min^{-1}, solution volume = 500 mL, T = 25° C, pH = 6-7

It must be noted that, despite the fact that the reaction rate of ozone with MTBE has been reported by many researchers [137, 138] as being low, the high ozonation efficiencies observed in this study could be attributed to the design of the falling film reactor which provides better and longer contact time between molecules of ozone and MTBE in both the aqueous and gaseous phases.

According to the results reported in Fig. 3.11, compared with MTBE ozonation, catalytic ozonation of ETBE proceeded faster to complete removal after 50 min of oxidation time,

indicating that ETBE was less resistant than MTBE against the attack of ozone. At the same time, the efficiency of photocatalytic oxidation of ETBE was a little lower than that of MTBE. This effect can be explained by the larger size of ETBE molecules, such that less adsorption of these molecules occurred on the surface of the photocatalyst and, as a consequence, less photocatalytic oxidation occurred due to the steric hindrance of these larger molecules. Among all advanced oxidation techniques assessed for the degradation of ETBE, photocatalytic ozonation was again the most effective. This method almost removed ETBE from aqueous solution after just 10 min of treatment time.

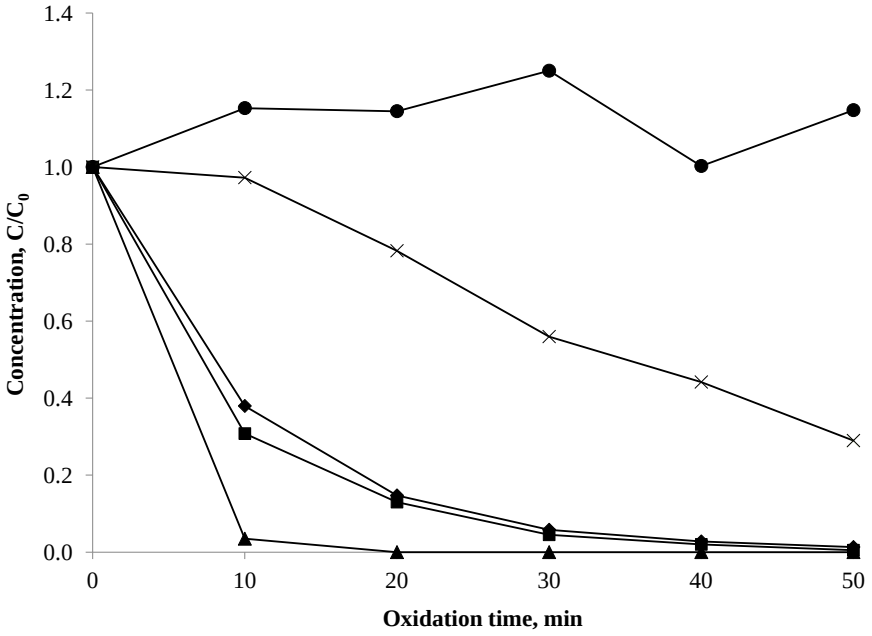

Fig. 3.11. Degradation of ETBE (0.01 mM) by means of different oxidation systems, simple recycling (●), Ozonation (♦), Catalytic ozonation (■), Photocatalytic oxidation (x), Photocatalytic ozonation (▲), falling film reactor, recycling rate = 100 mL.min^{-1}, solution volume = 500 mL, T = 25° C, pH = 6-7

The behaviour of TAEE under the conditions of different oxidation systems was very similar to that of ETBE (Figs. 3.11 and 3.12). However, the rate of photocatalytic oxidation of TAEE was slightly lower than that of ETBE, highlighting again the influence of the molecular structure of the pollutant on the level of its adsorption on the photocatalyst surface. In general, smaller and simpler molecular structures are adsorbed more readily on the surface and are consequently decomposed faster. In photocatalytic ozonation, the existence of ozone instead of

oxygen as the trap for photogenerated electrons and further generation of hydroxyl radicals will compensate for this difference in molecular structure. For this reason, the rates of photocatalytic ozonation of these ethers in the falling film reactor were nearly equal.

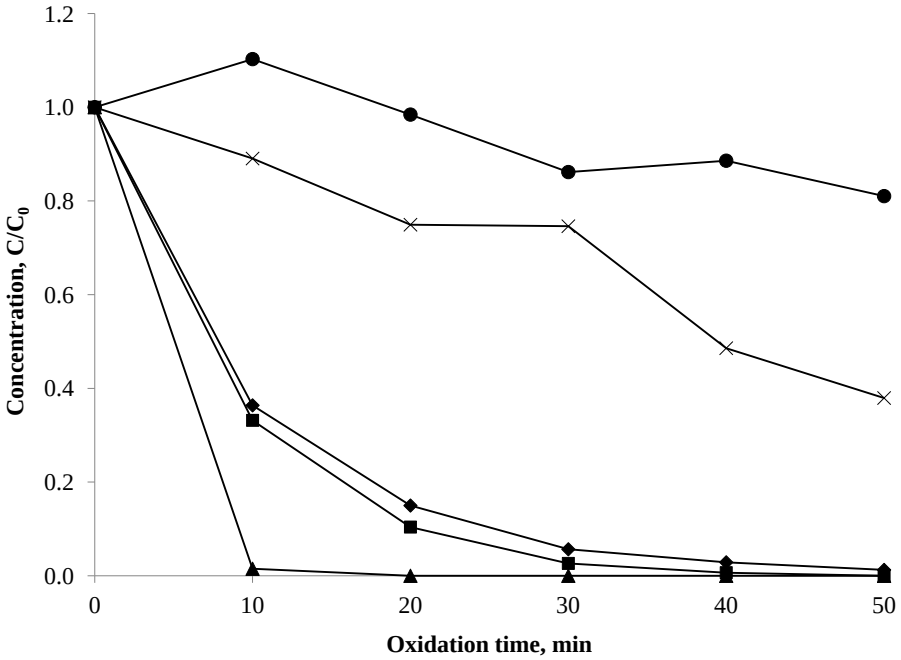

Fig. 3.12. Degradation of TAEE (0.01 mM) by means of different oxidation systems, simple recycling (●), Ozonation (♦), Catalytic ozonation (■), Photocatalytic oxidation (x), Photocatalytic ozonation (▲), falling film reactor, recycling rate = 100 mL.min^{-1}, solution volume = 500 mL, T = 25° C, pH = 6-7

3.3.3.1.Mineralisation of ethers: degradation of by-products

One of the major by-products identified during the degradation of MTBE and ETBE is TBA. It was noted that the toxicity of this substrate is not less than that of MTBE [144]. For this reason, the oxidation of TBA as an example of decomposition products of MTBE and ETBE was investigated using advanced oxidation processes in the falling film reactor. Fig. 3.13 shows that the photocatalytic oxidation system poorly decreased the initial concentration of TBA by 35% after 50 min of oxidation time, while the photocatalytic ozonation approach attained almost complete degradation after about 20 min. Expectedly, ozonation and catalytic ozonation showed a more or less similar influence on the degradation of TBA, where about 80% of the TBA on average was oxidised using these methods after 50 min of treatment time. Therefore, it can be

concluded that photocatalytic ozonation is the best oxidation method among all the assessed advanced oxidation methods, not just in the decomposition of model compounds, but it was also the most effective method for the mineralisation of these compounds.

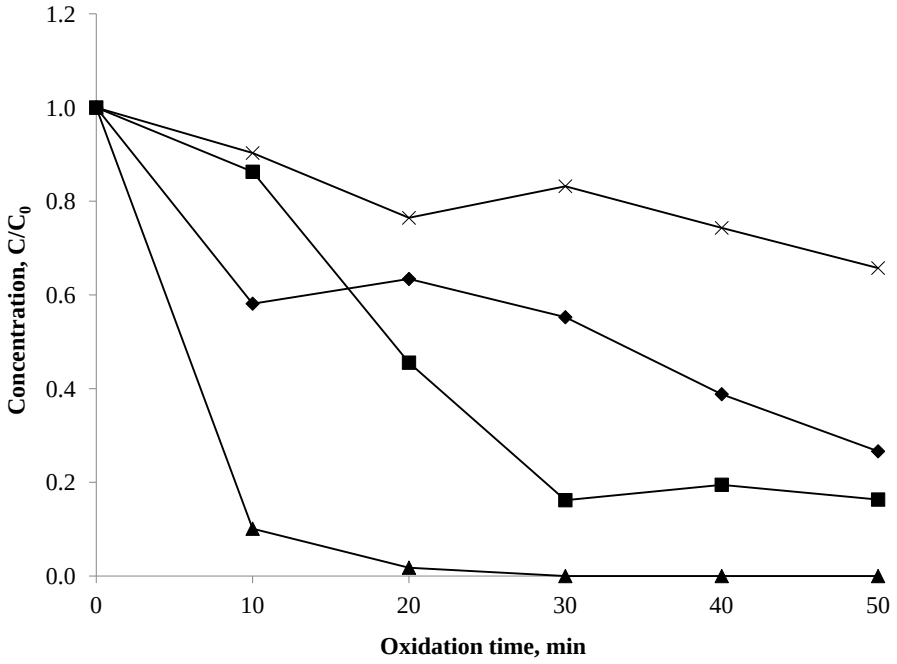

Fig. 3.13. Degradation of TBA (0.01 mM) by means of different oxidation systems, Ozonation (♦), Catalytic ozonation (■), Photocatalytic oxidation (x), Photocatalytic ozonation (▲), falling film reactor, recycling rate = 100mL.min^{-1}, solution volume = 500 mL, T = 25° C, pH = 6-7

In addition to TBA, *tert*-butyl formate (TBF) is another degradation product of MTBE and ETBE which was also highly decomposed by photocatalytic ozonation in the falling film reactor (Fig. 3.14). In this figure, it can be seen that over the degradation time of MTBE, the concentrations of by-products first increased because of the massive oxidation of MTBE and then the content in the reaction medium gradually decreased due to decomposition under these oxidative conditions.

Finally, in order to evaluate the potential of photocatalytic ozonation in the mineralisation of ether model compounds, a series of experiments was performed and the results are demonstrated in Fig. 3.15. It was clearly observed that the mineralisation rates of these ethers were nearly equal and that slight differences could be assigned to analytical mistakes.

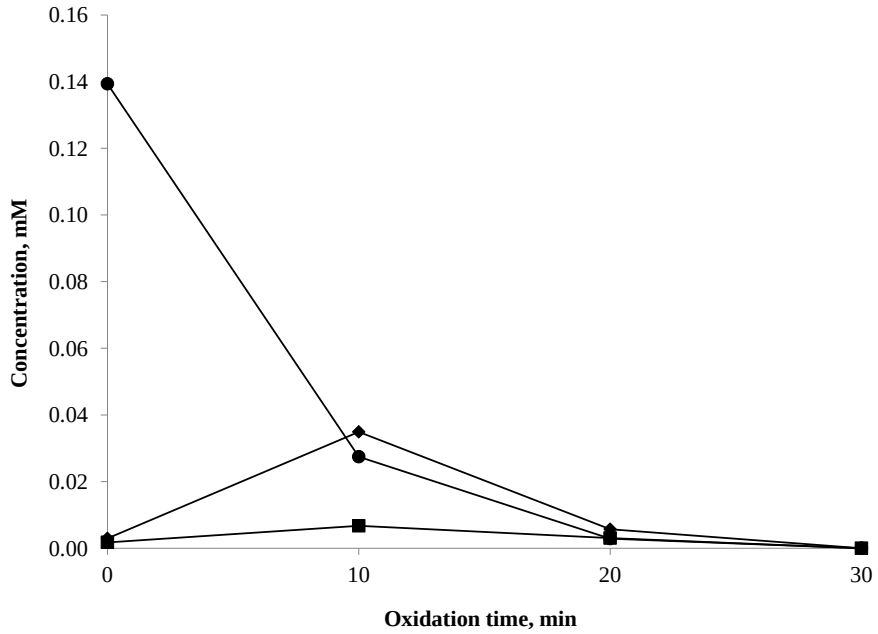

Fig. 3.14. Photocatalytic ozonation of MTBE (●) and its by-products TBA (■) and TBF (♦), in the falling film reactor, recycling rate = 100 mL.min^{-1}, solution volume = 500 mL, T = 25° C, pH = 6-7

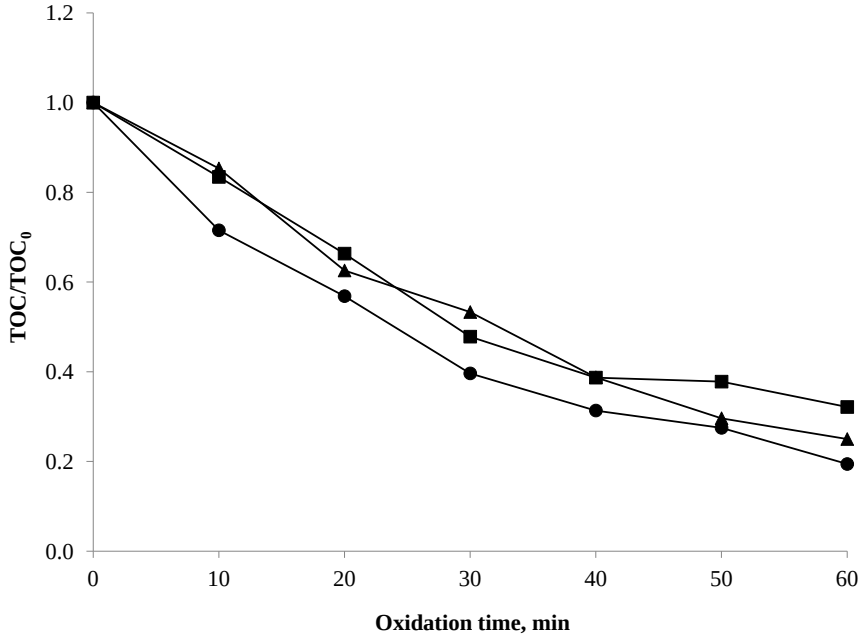

Fig. 3.15. Mineralisation of TAEE (●), ETBE (▲) and MTBE (■) by photocatalytic ozonation in the falling film reactor, initial concentration = 0.1 ±0.01 mM, recycling rate = 100 mL.min^{-1}, solution volume = 500 mL, T = 25° C, pH = 6-7

3.4. The influence of experimental variables on the oxidation process

In this section, the effects of variations in the experimental parameters on the degradation rate of model compounds in the falling film reactor are introduced and the results are discussed. Oxalic acid and dichloroacetic acid were chosen as the model compounds. Three TiO_2-based advanced oxidation processes were included in this investigation, $TiO_2/UVA/O_2$, $TiO_2/UVA/O_3$ and TiO_2/O_3. The influence of the initial concentration of model compounds, pH of the aqueous solution, solution temperature, ozone concentration and recycling rate of the solution inside the reactor were determined.

3.4.1. The importance of the presence of oxidants

As was already mentioned, the most significant disadvantage of photocatalytic treatments is the recombination of photogenerated electrons and holes. This event decreases the photonic efficiency and as a result it reduces the performance of photocatalytic oxidation methods. One solution for this problem is the utilisation of oxidant reagents as electron traps close to the surface of the photocatalyst. These electron traps react with photoexcited electrons, hindering the recombination process. In order to clarify the importance of the presence of oxidants for the promotion of photocatalyst-based oxidation processes, the photocatalytic decomposition of oxalic acid and dichloroacetic acid was studied in the presence of ozone, oxygen and nitrogen. The results in Fig. 3.16 indicate that the efficiency of photocatalytic oxidation of both model compounds in the presence of ozone as the electron trap was expectedly much higher than that in the presence of oxygen. The reason for this effect was extensively discussed in previous sections.

In this section, the results of photocatalytic oxidation in the absence of ozone and oxygen are shown. The two upper curves in Fig. 3.16 show that photocatalytic oxidation treatment in a nitrogen atmosphere inside the falling film reactor decreased the initial concentrations of dichloroacetic acid and oxalic acid by 6% and 12%, respectively, after 100 min of treatment time. Since the reactivity between an inert reagent like nitrogen and photogenerated electrons is considered negligible, this level of oxidation in the presence of nitrogen could be explained by the role of photogenerated holes in the formation of hydroxyl radicals. Depending on the solution pH, holes mostly react with adsorbed molecules of H_2O or OH^- anions on the catalyst surface to form free hydroxyl radicals; these radicals initiate the oxidation process. In fact, under conditions with the absence of ozone and oxygen in the falling film reactor, photo-produced holes are the

main initiator oxidant substances handling the degradation of oxalic acid and dichloroacetic acid. However, due to the high rate of hole-electron recombination under these conditions, the decomposition efficiency is very low.

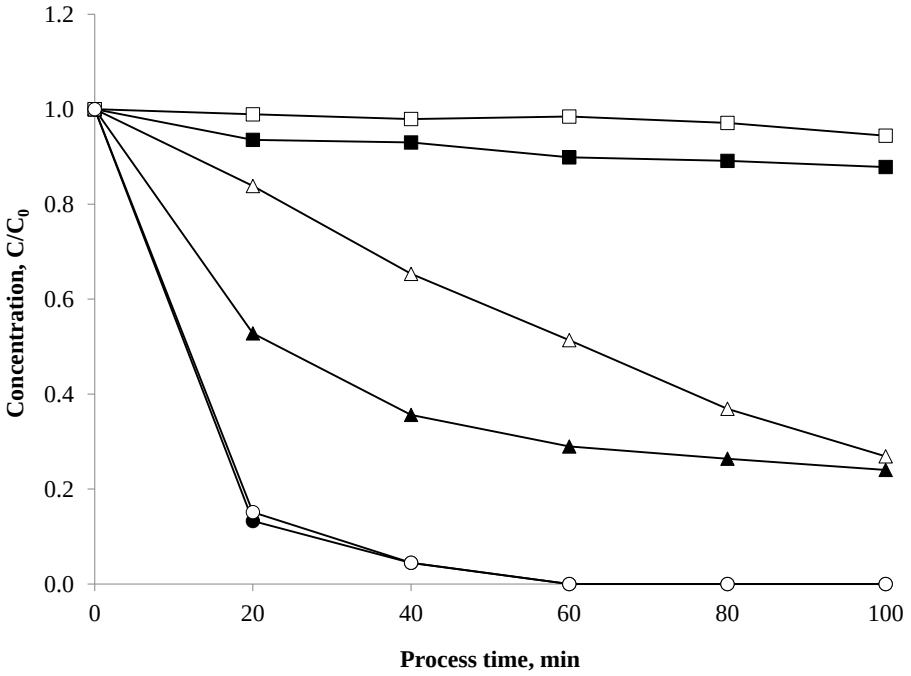

Fig. 3.16. Photocatalytic treatment of oxalic acid, 1 mM (black) and dichloroacetic acid, 1mM (white) in presence of nitrogen (□), oxygen (Δ) and ozone (○), falling-film reactor, recycling rate = 100 mL.min^{-1}, solution volume = 500 mL, T = 25° C, pH ≈ 3

3.4.2. The effect of the initial concentration of model compounds

For this investigation, oxalic acid was chosen as the model compound and was oxidised by three different advanced oxidation techniques. The relationship between the initial concentration of this substrate and its degradation rate over the range of 0.1 mM to 10 mM was studied. According to the results presented in Table 3.1, the oxidation rate increased with the concentration of oxalic acid. This increase was observed for all three oxidation methods.

As was already expressed in detail, the Langmuir-Hinshelwood (L-H) expression (Equation 1.1) can be used to describe the relationship between the degradation behaviour of many organic compounds and their concentrations in the solution under oxidation conditions. The decomposition of oxalic acid in the falling film reactor using photocatalytic oxidation and

photocatalytic ozonation systems was also represented well by the Langmuir-Hinshelwood (L-H) kinetic mechanism; the initial degradation rate increased almost linearly with an increase in the initial concentration of oxalic acid. This indicates that, over the range of concentrations chosen for this assessment, the degradation rate is assumed to be first-order with respect to the concentration of oxalic acid (Fig. 3.17). Nevertheless, the ascending slope of both graphs in Fig. 3.17 seems to be moderately decreased at concentrations higher than 5 mM, predicting that with higher initial concentrations of oxalic acid, after reaching a certain concentration, the degradation rate of oxalic acid will become independent of its initial concentration. The explanation for this event is that a saturation level is defined for each catalyst-based oxidation system, proportional to its circumstances, where all active sites on the surface of the catalyst are occupied by molecules of the degradable contaminant. After achieving this saturation level, any further increase in the concentration of the contaminant will not affect the adsorption of molecules on the surface of the catalyst and, as a result, will not increase the decomposition rate of the contaminants therein.

Table 3.1. Initial degradation rates of oxalic acid at different oxidation conditions and different initial concentrations

Concentration, mM	pH	Temperature, °C	Initial degradation rate, μM/min		
			$TiO_2/UVA/O_2$	TiO_2/O_3	$TiO_2/UVA/O_3$
0.1	3.7	25	1.65	0.15	6.15
0.5	3.1	25	5.50	5.45	19.70
1	2.8	25	9.05	6.20	40.15
5	2.1	25	41.70	29.65	182.10
10	1.8	25	70.45	88.3	301.3
1	5	25	1.75	6.95	17.40
1	7.5	25	<0.05	12.25	19.10
1	9.5	25	<0.05	12.55	16.00
1	2.8	40	13.70	13.05	37.25
1	2.8	55	17.45	16.35	32.40
1	2.8	70	20.10	24.60	30.90

A similar ascending trend was observed for the decomposition rate versus the initial concentration of oxalic acid using a catalytic ozonation system; however, the trend was not as regular as those of photocatalytic oxidation and photocatalytic ozonation (Table 3.1). It was

previously discussed that under the operating conditions of the falling film reactor, the presence of TiO_2 could not significantly improve the efficiency of ozonation of almost all model compounds investigated in this study. Therefore, photocatalytic ozonation of oxalic acid in the falling film reactor could be rewritten and discussed in terms of the ozonation of oxalic acid, where electrophilic attack of ozone or other oxidative substances, especially hydroxyl radicals produced during ozone decomposition, are responsible for the degradation of contaminants in water. Thus, under the condition of an excess of ozone in the reactor medium of the falling film reactor, any increase in the concentration of oxalic acid would simply increase the possibility of an efficient reaction between ozone or hydroxyl radicals and molecules of oxalic acid, which would consequently increase the degradation rate of oxalic acid.

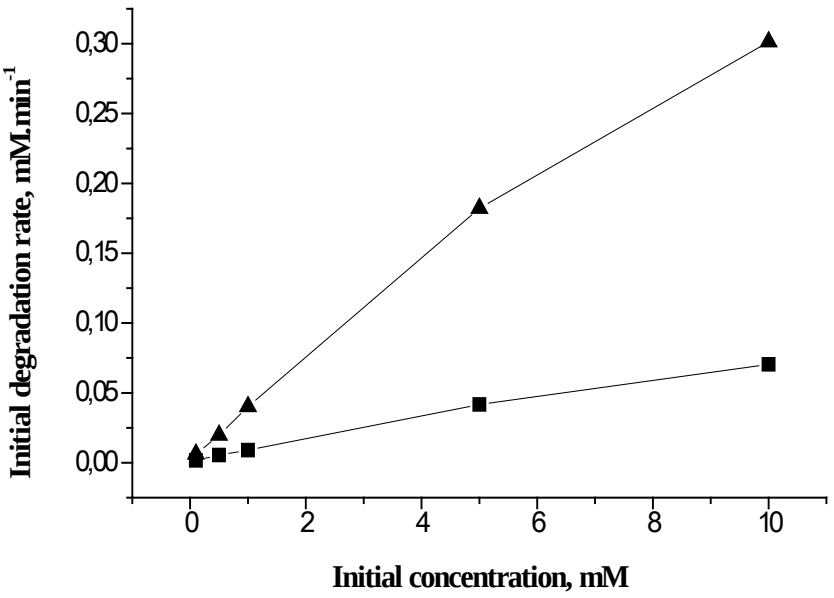

Fig. 3.17. Effect of concentration of oxalic acid on its initial degradation rate by photocatalytic oxidation (■) and photocatalytic ozonation (▲) systems, falling film reactor, recycling rate = 100 mL.min^{-1}, solution volume=500 mL, T = 25° C

3.4.3. The effect of solution pH

In order to understand the influence of solution pH on the degradation rate of oxalic acid as a model compound, a set of oxidation treatments using three TiO_2-based advanced oxidation

techniques was performed in the falling film reactor at four different pH levels. The results are presented in Fig. 3.18. It can be seen that, depending on the oxidation method, variation in the pH of the aqueous solution caused distinct influences on the rate of oxidation.

Fig. 3.18a shows that any increase in the pH level considerably decreases the rate of photocatalytic oxidation of oxalic acid; at the natural pH of the oxalic acid solution (C = 1 mM, pH 2.8), about half of the initial concentration of oxalic acid was decomposed after 1 h of treatment time, while only about 6% of the initial concentration was decomposed after 1 h when the same treatment was performed at pH 5. It must be added that shifting to pH values greater than pH 7 almost stopped the photocatalytic oxidation of oxalic acid under the setup conditions of the falling film reactor (Table 3.1). In order to determine the reason for this behaviour, the chemical properties of oxalic acid as well as the characteristics of the photocatalyst must be considered. Despite the fact that oxalic acid is a carboxylic acid, it is categorised among some relatively strong acids due to its pK_a value.

$$C_2O_4H_2 \rightleftarrows C_2O_4H^- + H^+ \qquad pK_{a_1} = 1.27 \qquad (3.3)$$

$$C_2O_4H^- \rightleftarrows C_2O_4^{2-} + H^+ \qquad pK_{a_2} = 4.28 \qquad (3.4)$$

On one hand, according to reactions 3.3 and 3.4, the pH value of an aqueous solution of a relatively powerful dicarboxylic acid determines the predominantly existing chemical species present therein. In this case, depending on the solution pH, oxalic acid could be present as a neutral molecule, as a hydrogen oxalate anion or as an oxalate anion. Under the experimental conditions of the present study, oxalic acid was mainly comprised of $C_2O_4H^-$ at pH 2.8, although $C_2O_4^{2-}$ was the main form of oxalic acid in solution at pH ≥5. On the other hand, the adsorption of oxalic acid molecules on the photocatalyst surface, as an essential step in photocatalytic oxidation treatment, is highly dependent on the interactions between the existing forms of these molecules in solution and the surface groups on the photocatalyst. In addition to the mentioned effect, proportional to the isoelectric point (pH_{iep}) of the photocatalyst used in this study, at different pH values, the surface of the photocatalyst can carry either a negative or positive charge. This parameter will also determine the interaction between the predominant

species of oxalic acid in the reaction medium and the active sites on the photocatalyst surface at each pH level.

To conclude, the low rate of photocatalytic oxidation of oxalic acid at pH ≥ 5 can be explained by the weaker adsorption of $C_2O_4^{2-}$, which is the main form of oxalic acid on the photocatalyst surface in this pH range.

As far as the influence of pH on catalytic ozonation of oxalic acid is concerned (Fig. 3.18b), the rates of degradation were definitely different for the two pH ranges, pH > 7 and pH < 7. Even though catalytic ozonation was generally observed as being poorly efficient for the decomposition of oxalic acid, alkalinising the reaction environment approximately doubled the initial degradation rate of this compound (Table 3.1) and increased on average the efficiency of degradation by about 20% over a treatment duration of 1 h. This enhancement in performance was attributed to the higher ozone decomposition rate and greater generation of hydroxyl radicals under alkaline conditions.

Fig. 3.18c shows that the pH of the aqueous solution significantly affects the degradation rate of oxalic acid using photocatalytic ozonation systems; at pH 2.8, about 90% of the initial concentration of oxalic acid was removed after 20 min of oxidation time, whilst at pH 9.5, only about 16% of the initial concentration was degraded. Between these two rates, moderate trends were similarly observed for the results of photocatalytic ozonation of oxalic acid at pH 5 and pH 7.5.

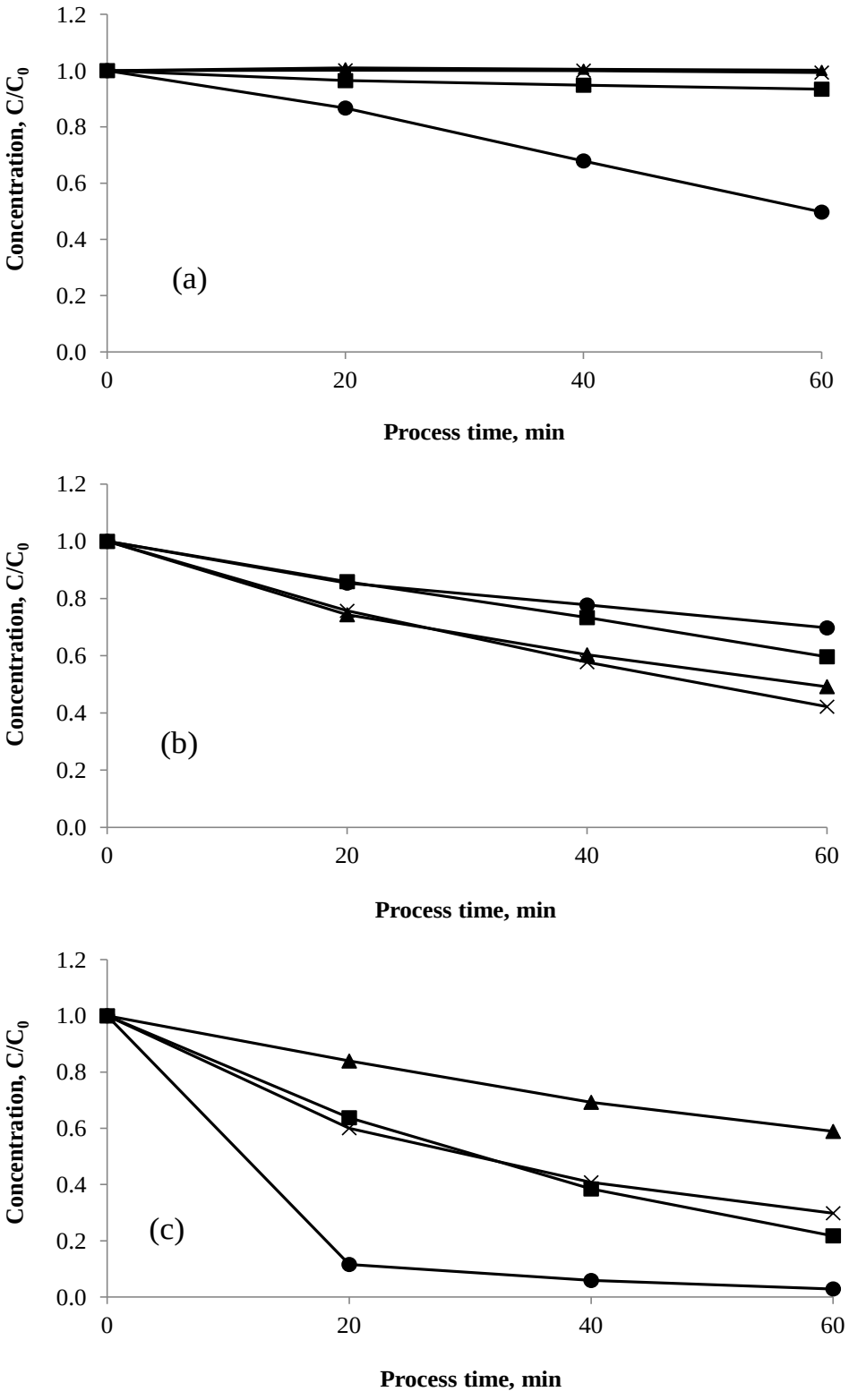

Fig. 3.18. The influence of solution pH on the degradation of oxalic acid (1 mM) using (a) photocatalytic oxidation, (b) catalytic ozonation and (c) photocatalytic ozonation at pH = 2.8 (●), pH = 5 (■), pH = 7.5 (x), pH = 9.5 (▲), falling-film reactor, recycling rate = 150 mL.min^{-1}, solution volume = 500 mL, T = 25° C

Reconsideration of the three sections of Fig. 3.18 indicates that, in the case of photocatalytic ozonation, the degradation rate at each pH level more or less equals the summation of the degradation rates of catalytic ozonation and photocatalytic oxidation. For example, at pH 9.5 where no adsorption of $C_2O_4^{2-}$ on the photocatalyst surface and no photocatalytic oxidation was consequently observed, the trend of photocatalytic ozonation was very similar to that of catalytic ozonation. This means that at pH 9.5, for both catalytic ozonation and photocatalytic ozonation, degradation of oxalic acid was initiated in the solution, not on the surface of the photocatalyst by OH radicals generated from ozone decomposition. The same pattern was established at pH 7.5; however, in this case, the rate of photocatalytic ozonation was a bit greater than that of catalytic ozonation (Table 3.1). Generally, due to the possibility of the adsorption of oxalic acid molecules on the catalyst surface at lower pH values and their reaction with hydroxyl radicals and other oxidising reagents therein, as we move to lower pH levels, the efficiency of photocatalytic ozonation seems to be more than the sum of the efficiencies of catalytic ozonation and photocatalytic oxidation. Considerable results highlighting the strong influence of photocatalytic ozonation on the degradation of oxalic acid were observed at pH 2.8. Under these pH conditions, the initial degradation rate of oxalic acid using photocatalytic ozonation was 40.1 $\mu M.min^{-1}$, while it was 6.2 $\mu M.min^{-1}$ and 9.0 $\mu M.min^{-1}$ using catalytic ozonation and photocatalytic oxidation, respectively (Table 3.1).

3.4.4. The effect of solution temperature

Another series of oxidation experiments were planned with the aim of studying the influence of the temperature of the aqueous solution in the falling film reactor on the degradation rate of pollutant molecules therein. Oxalic acid was chosen as the model compound in this section and the effect of temperature was studied for similar TiO_2-based advanced oxidation processes over the range of 25°C to 70°C. The results are shown in Fig. 3.19.

Fig. 3.19a and the information presented in Table 3.1 show that an increase in the temperature from 25°C to 70°C increased the initial degradation rate of oxalic acid by photocatalytic oxidation from 9.0 $\mu M.min^{-1}$ to 20.1 $\mu M.min^{-1}$, although this temperature increase could not affect the overall efficiency of oxalic acid degradation to a significant degree. This oxidation method removed 70%-75% of the initial concentration of oxalic acid at 25°C and 70°C, respectively, after 1 h of treatment time.

As with photocatalytic oxidation, a temperature increase from 25°C to 70°C led to a four-fold increase in the initial degradation rate of oxalic acid from 6.2 $\mu M.min^{-1}$ to 24.6 $\mu M.min^{-1}$ using catalytic ozonation (Table 3.1). However, unlike the case of photocatalytic oxidation, the overall treatment efficiency of this oxidation method at different temperatures was clearly different; the higher the solution temperature employed, the higher the observed overall oxidation efficiency. The overall oxidation efficiency in this series of experiments ranged from about 29% at 25°C to 66% at 70°C after 1 h of treatment (Fig. 3.19b).

Fig. 3.19c shows that the influence of increased temperature on the efficiency of the photocatalytic ozonation of oxalic acid was very small. Nonetheless, the initial degradation rate of oxalic acid using this technique decreased slightly with an increase in temperature from 25°C to 70°C (Table 3.1). After 1 h of treatment, about 97% and 92% of the initial concentration of oxalic acid was decomposed at 25°C and 70°C, respectively.

From a general point of view, temperature variations affect chemical oxidation systems in several ways, which are usually considered to be opposite to each other and act either to accelerate or to hinder the treatment. In other words, the observed influence of temperature in this study could be explained as a consequence of many co-current and/or counter-current functions. For instance, increasing temperature should lead to higher rates for all the chemical reactions involved in such heterogeneous oxidations and, moreover, it should decrease the thickness of the diffusion layer around the photocatalyst, providing better mass transfer conditions. On the other hand, increased temperature reduces the solubility of oxygen and ozone in an aqueous solution. It is obvious that any shortage in the concentration of these two important factors will negatively affect the output of advanced oxidation processes. Furthermore, according to the Freundlich adsorption isotherm (Equation 3.1), as the temperature increases at a constant pressure (or concentration), the adsorption rate is negatively reduced and the quantity adsorbed increases more slowly, leading, as a result, to a decrease in the degradation of adsorbed particles on the photocatalyst surface.

$$\frac{x}{m} = kP^{\frac{1}{n}} \qquad \text{(Equation 3.1)}$$

In this equation, x is the quantity adsorbed, m is the mass of the adsorbent, P is the pressure (or concentration) and k and n are empirical constants for each adsorbent-adsorbate pair at a given temperature.

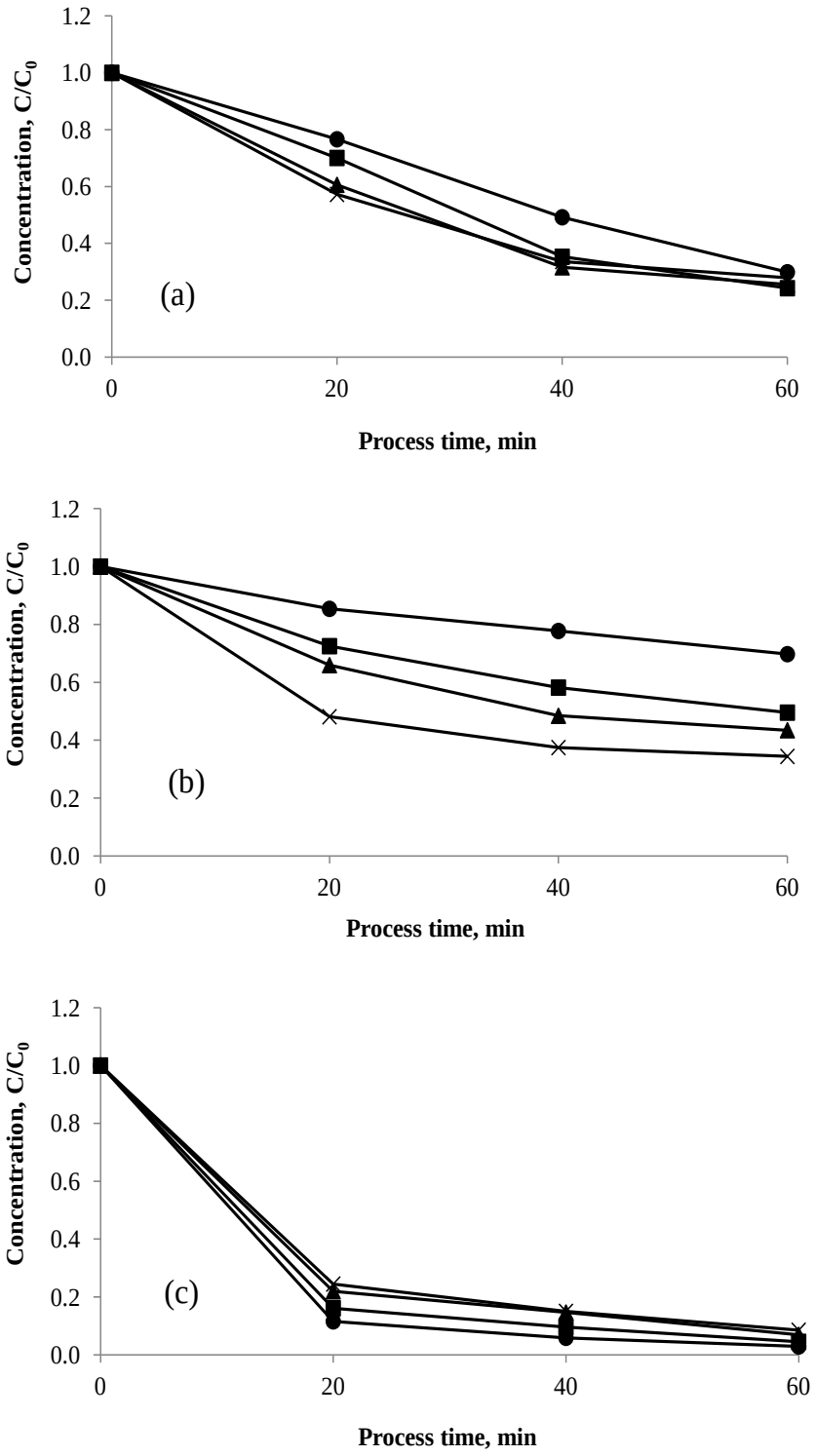

Fig. 3.19. The temperature effect on the degradation of oxalic acid (1 mM) using (a) photocatalytic oxidation, (b) catalytic ozonation and (c) photocatalytic ozonation at T = 25° C (●), T = 40° C (■), T = 55° C (▲), T = 70° C (x), falling-film reactor, recycling rate = 100 mL.min^{-1}, solution volume = 500 mL, pH = 2.8

To summarise, it seems that under the operating conditions of the falling film reactor, except for the case of catalytic ozonation, the performance of other advanced oxidation methods in the removal of oxalic acid from water was not significantly influenced by temperature variations. However, in such heterogeneous oxidation systems, where various simultaneous events occur, such as electron-hole pair generation on the irradiated semiconductor surface, their transfer and reaction with adsorbed molecules (ozone, oxygen and/or oxalic acid) or further recombination with each other, diffusion of oxalic acid, ozone and oxygen molecules into solution and their adsorption on the photocatalyst surface, ozone decomposition by irradiation, the direct attack of ozone on oxalic acid in the bulk of the solution or on the photocatalyst surface and the formation of hydroxyl radicals as stronger oxidants for indirectly attacking pollutants, to present a comprehensive and precise description of all events is very difficult. But, according to the observed results, it could be assumed that the inhibiting factor of increased temperature mentioned in the previous paragraph seemed to govern the photocatalytic ozonation runs, while photocatalytic oxidation and catalytic ozonation runs were mainly controlled by the promoting factor of increased temperature.

The overall activation energy of oxidation reactions in the falling film reactor is generally a reflection of both a homogeneous solute dissociation step and heterogeneous surface reaction steps. Many studies have reported that the activation energy of photocatalytic reactions is categorised by low activation energy values [157]. In order to evaluate this parameter under different oxidation conditions in the falling film reactor, Arrhenius plots were made for the three investigated oxidation techniques and presented in Fig. 3.20.

Considering the Arrhenius plot, the activation energies related to the degradation of oxalic acid using catalytic ozonation, photocatalytic oxidation and photocatalytic ozonation systems were 28.85 $kJ.mol^{-1}$, 13.55 $kJ.mol^{-1}$ and -6.07 $kJ.mol^{-1}$, respectively.

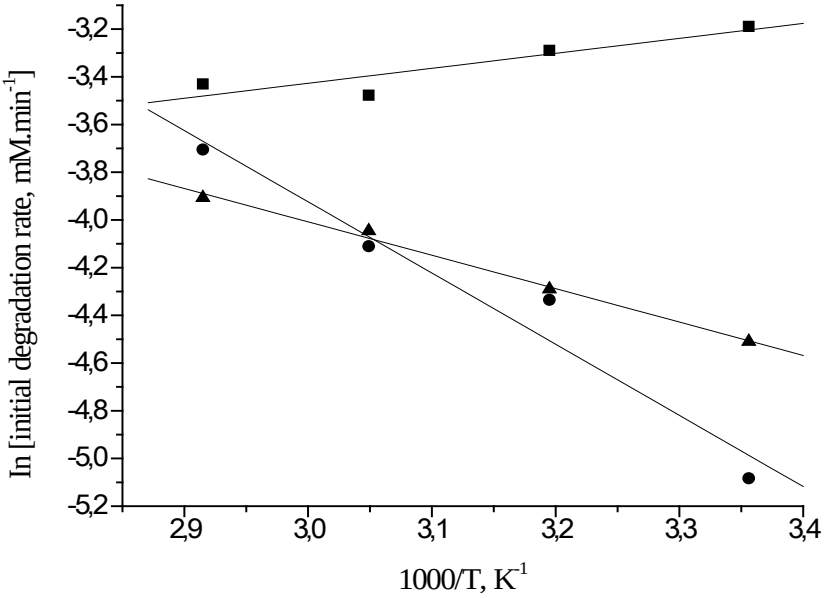

Fig. 3.20. Arrhenius' plot, photocatalytic oxidation (▲), catalytic ozonation (●), and photocatalytic ozonation (■) of oxalic acid (1 mM), falling-film reactor, recycling rate = 100 mL.min^{-1}, solution volume = 500 mL, pH = 2.8

3.4.5. The effect of ozone concentration

The ozone concentration is an important experimental variable in ozone-based advanced oxidation processes. A set of experiments was performed in order to investigate the influence of ozone concentration on the degradation of oxalic acid as a model compound using catalytic ozonation and photocatalytic ozonation in the falling film reactor. The degradation of oxalic acid was studied over a range of ozone concentrations from 0 mg.L^{-1} to 135 mg.L^{-1}; the results are presented in Figs. 3.21 and 3.22. Fig. 3.21 shows that an increase in the ozone concentration led to a tangible increase in the efficiency of the catalytic ozonation of oxalic acid. About 33% of the initial concentration of oxalic acid was removed after 1 h of treatment at [O_3] = 135 mg.L^{-1}, while within the same period of time, the removal efficiencies were 19%, 11% and < 1% at [O_3] = 70 mg.L^{-1}, 25 mg.L^{-1} and 0 mg.L^{-1}, respectively. Moreover, the internal diagram of Fig. 3.21 shows a linear trend for the initial degradation rate versus ozone concentration, indicating that the oxidation rate can be assumed to be first-order with respect to the ozone concentration under the conditions of catalytic ozonation. Table 3.2 shows that, under the operating conditions of the falling film reactor during the catalytic ozonation of oxalic acid, where a gaseous stream

of an ozone/oxygen mixture continuously passed through the reactor, the ozone concentration in the liquid phase was proportional to that in the gas phase. The numerical values reported in Table 3.2 are an average of values measured over the oxidation time. It was observed that the concentration of ozone in the gas phase decreased by about 5 mg/l after passing through the reactor.

Similar to the case of catalytic ozonation, the initial degradation rate and the efficiency of the photocatalytic ozonation of oxalic acid increased with an increased ozone content in the gaseous stream entering the falling film reactor. Due to the possibility of the photocatalytic oxidation process occurring even in the absence of ozone, about 56% of the initial concentration of oxalic acid was decomposed at $[O_3]$ = 0 mg.L^{-1} after 1 h (Fig. 3.22). However, the overall efficiency of degradation in the presence of ozone was determined as being between 86% and 97%, depending on the ozone concentration. Fig. 3.22 also shows that at $[O_3]$ = 25 mg.L^{-1}, the initial degradation rate was more sharply increased compared with that at $[O_3]$ = 0 mg.L^{-1}, highlighting the role of ozone in increasing the formation rate of hydroxyl radicals.

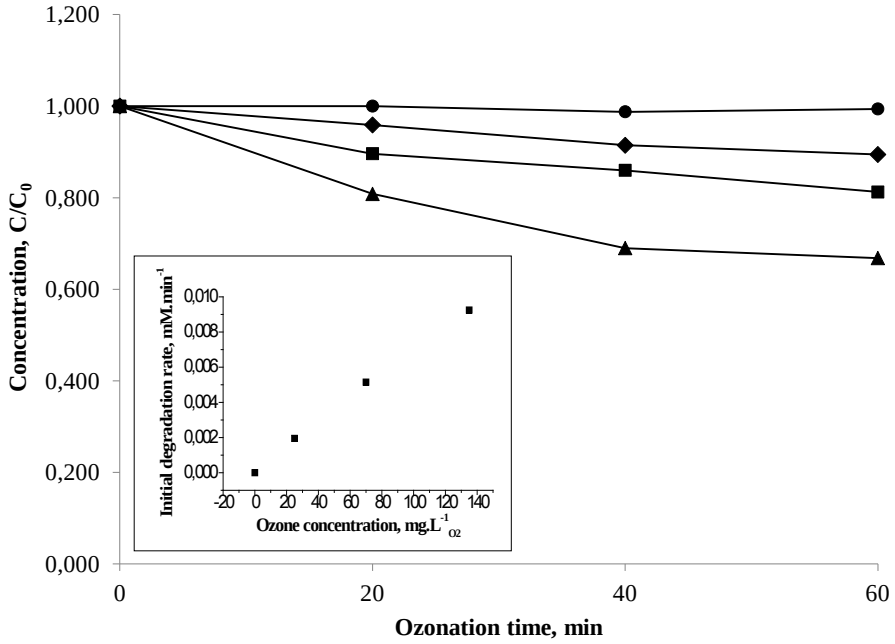

Fig. 3.21. Catalytic ozonation of oxalic acid, 1 mM using different ozone concentration; 0 mg.L^{-1} (●), 25±5 mg.L^{-1} (♦), 70±5 mg.L^{-1} (■) and 135±5 mg.L^{-1} (▲), falling film reactor, recycling rate = 100 mL.min^{-1}, solution volume = 500 mL, T = 25° C, pH = 2.8 (inside graph: initial degradation rate vs. ozone concentration)

For each concentration of ozone in the input gas phase, the relevant ozone concentration in the liquid phase inside the reactor over the time of photocatalytic ozonation was much less than that of catalytic ozonation (Table 3.2, a and b). In other words, the consumption rate of dissolved ozone under the conditions of photocatalytic ozonation was higher than the decomposition rate of dissolved ozone under catalytic ozonation conditions. Thus, the ozone concentration in the liquid phase was always lower in photocatalytic ozonation. This result again indicates the significantly higher rate of ozone decomposition and $OH^{\bullet}$ formation in TiO_2/O_3/UVA systems compared with those of TiO_2/O_3 systems.

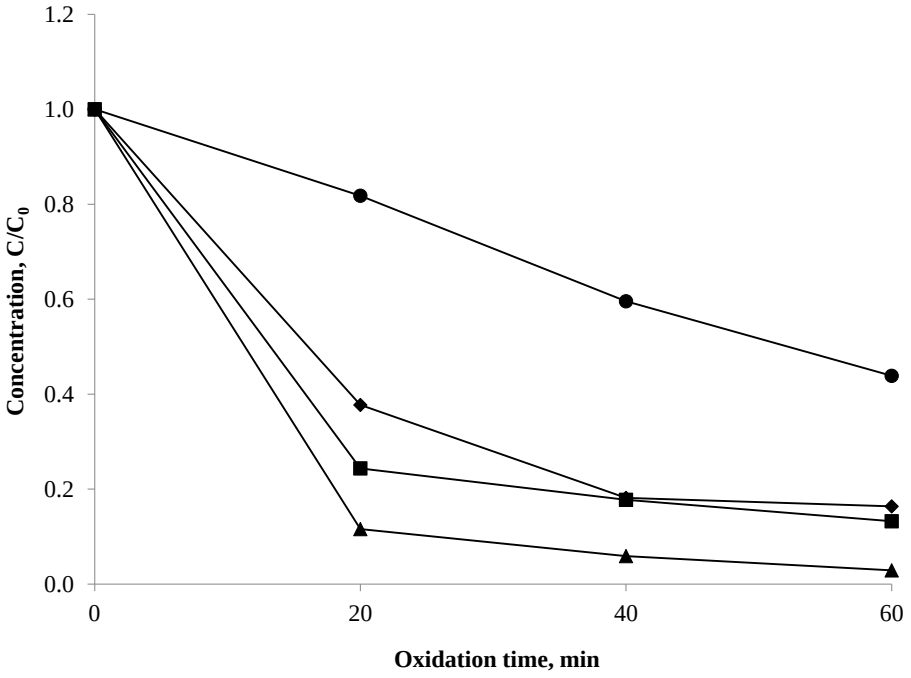

Fig. 3.22. Photocatalytic ozonation of oxalic acid, 1 mM using different ozone concentration; 0 $mg.L^{-1}$ (●), 25±5 $mg.L^{-1}$ (♦), 70±5 $mg.L^{-1}$ (■) and 135±5 $mg.L^{-1}$ (▲), falling film reactor, recycling rate = 100 $mL.min^{-1}$, solution volume = 500 mL, T = 25° C, pH = 2.8

For the same reason, the difference between the concentration of ozone in the gas phase at the input and output of the reactor was relatively higher under conditions of photocatalytic ozonation (Table 3.2).

Table 3.2. Variation of ozone concentration during degradation of oxalic acid, 1 mM using (a) catalytic ozonation and (b) photocatalytic ozonation

(a) Catalytic ozonation

C_{O3} in gas phase, $mg.L^{-1}$		C_{O3} in liquid phase, $mg.L^{-1}$
input	output	
25±5	20±5	9±0.5
70±5	65±5	18.5±0.5
135±5	130±5	29.5±0.5

(b) Photocatalytic ozonation

C_{O3} in gas phase, $mg.L^{-1}$		C_{O3} in liquid phase, $mg.L^{-1}$
input	output	
25±5	15±5	< 0.5
70±5	45±5	6.5±1
135±5	70±5	8.5±1

3.4.6. The influence of solution recycling rate (falling rate)

Regarding the effect of the recycling rate of the solution inside the reactor on the degradation rate, the photocatalytic oxidation of dichloroacetic acid as a model compound was performed in the falling film reactor at different recycling rates. The results are shown in Fig. 3.23. These results show that an increase in the recycling rate from 100 $mL.min^{-1}$ to 300 $mL.min^{-1}$ caused an increase in the initial degradation rate by about 32% from 11.58 $\mu M.min^{-1}$ to 15.30 $\mu M.min^{-1}$. At the same time, the overall degradation efficiency of dichloroacetic acid was increased moderately from 80.6% at 100 $mL.min^{-1}$ to 92.6% at 300 $mL.min^{-1}$. But, at recycling rates higher than 300 $mL.min^{-1}$, both the initial degradation rate and the degradation efficiency of dichloroacetic acid were negatively influenced; increasing the recycling rate from 300 $mL.min^{-1}$ to 400 $mL.min^{-1}$ led to small decreases in the initial degradation rate and degradation efficiency by about 4% and 3%, respectively (Fig. 3.23).

Generally, any enhancement in the recycling rate of the solution inside the falling film reactor is assumed to improve mass transfer in the bulk solution and to increase the thickness of the diffusion boundary layer associated with the surface of the catalyst. This effect should lead to an increase in the oxidation rate. On the contrary, due to existing liquid turbulence at high falling rates, increased recycling rates will negatively affect the adsorption of contaminant molecules on

the catalyst surface and their interaction with oxidising reagents therein. Moreover, as was described already in Fig. 2.9, increasing the recycling rate will increase the thickness of the falling liquid films over the walls of the reactor. Thickening of falling films at higher recycling rates could also be considered as a controlling parameter for oxidation rates.

To summarise, it seems that a gradual increase in the degradation rate of dichloroacetic acid in the falling film reactor at recycling rates from 100 mL.min^{-1} to 300 mL.min^{-1} could be attributed to improved mass transfer properties at 300 mL.min^{-1} compared with those at 100 mL.min^{-1}. The slight decrease in the degradation rate of dichloroacetic acid which was observed at 400 mL.min^{-1} in comparison with that at 300 mL.min^{-1} can be explained by the influence of turbulence caused by faster and thicker falling films at 400 mL.min^{-1}.

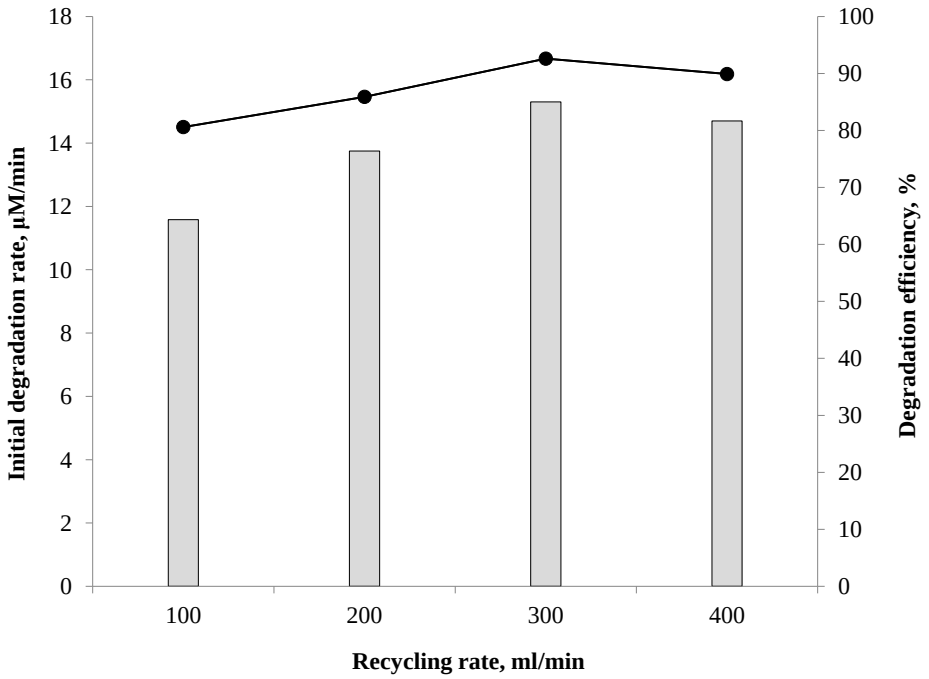

Fig. 3.23. Photocatalytic oxidation of dichloroacetic acid (1mM) under different recycling rates; initial degradation rate (column) and degradation efficiency (line), falling film reactor, volume = 400 mL, T = 25° C, initial pH = 3

3.5. Treatment and colour removal of pyrolysis wastewater (case study)

Treatment of a real wastewater sample produced in a thermal pyrolysis plant for plastic waste disposal was chosen as a case study for the assessment of the performance of the falling film reactor. In this study, a reduction in the level of chemical oxygen demand (COD) as well as

colour removal of this type of wastewater was evaluated by means of three different TiO_2-based advanced oxidation methods using the falling film reactor. In addition, the effect of acidification of this type of wastewater as well as the influence of the content of phosphate anions existing in the wastewater for biological treatment purposes on several treatment aspects were investigated and are discussed in subsequent sections.

As with most industrial sites, pyrolysis processes produce wastewaters. The wastewater was initially brown and shifted to darker brown over time until it became black after about three months. More than 30 organic and inorganic compounds were detected in these slightly basic (pH 7-8) wastewater samples [158], in addition to fine and mainly black particles, as a product of the combustion process, leading to an unfavourable appearance and odour with respect to the wastewater.

A quick check of the quality of water or wastewater is possible by an evaluation of colour and odour. Therefore, a first step in water and wastewater treatment is the removal of colour and odour. Depending on the characteristics of the wastewater, many contamination criteria or standards are defined for the quality of wastewaters, such as chemical oxygen demand (COD), biological oxygen demand (BOD), total organic carbon (TOC), total suspended solids (TSS), etc. The capability of any method for the treatment of wastewater is usually quantified by a decrease in the level of one or more of the criteria mentioned above by that method. In this study, the effectiveness of photocatalytic oxidation, catalytic ozonation and photocatalytic ozonation as three different oxidation methods on decreasing the level of COD and on the removal of colour and odour in pyrolysis wastewater was investigated. Light extinction measurements utilising a spectrophotometer were performed in order to determine colour removal in the wastewater. From our experience in dealing with such pyrolysis wastewaters, it has been shown that when the extinction value decreases to 20% over the process time, the wastewater is colourless.

3.5.1. Photocatalytic oxidation of wastewater

Fig. 3.24 shows that the photocatalytic oxidation of pyrolysis wastewater led to a slight decrease in colour extinction by about 31% after 5 h of treatment, while the decrease in the COD of this wastewater was negligible during the oxidation process, even after such a long treatment time. This indicates that photocatalytic oxidation of pyrolysis wastewater in the falling film reactor did not seem to be effective neither in improving the quality standards of this wastewater nor in

removing colour. It must be noted that the unpleasant odour of the wastewater was still detectable after treatment.

There are several reasons for the observed insufficient photocatalytic oxidation, such as the presence of different organic compounds in the wastewater which disturb the adsorption of each other on the photocatalyst surface, the existence of some inorganic ions blocking the active sites of the photocatalyst or scavenging the hydroxyl radicals produced over the photocatalyst surface, as well as the alkaline pH of the wastewater which reduces the effective adsorption of contaminants on the surface of the catalyst and consequently cause a decrease in the efficiency of the oxidation process.

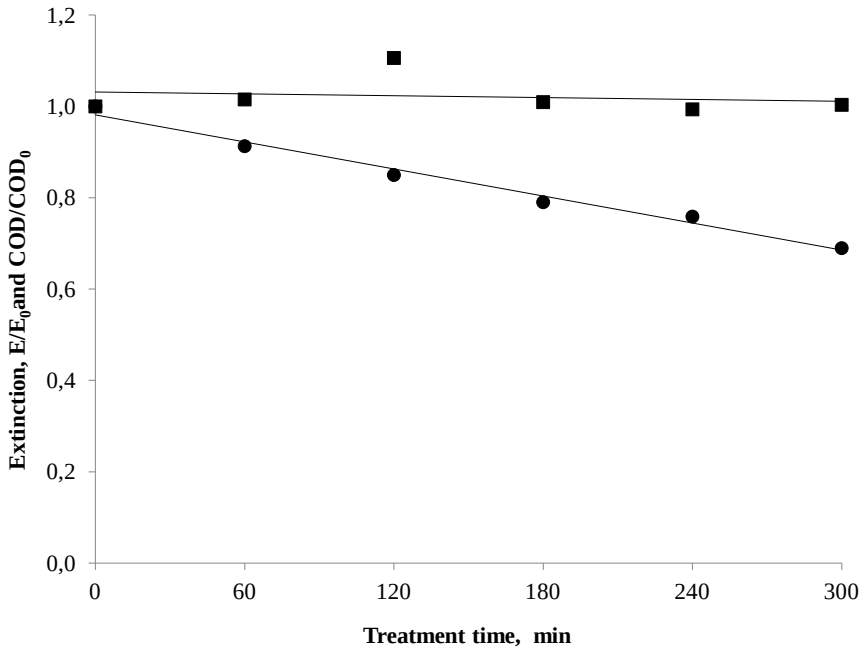

Fig. 3.24. Photocatalytic oxidation of pyrolysis wastewater; Extinction (●) and COD (■), falling film reactor, wastewater volume = 200 mL, initial COD level = 1900±100 mg.L^{-1}, recycling rate = 100 mL.min^{-1}, T = 25° C, pH = 7-8, λ = 340 nm

To better understanding the limiting parameters of the photocatalytic oxidation of pyrolysis wastewater, dichloroacetic acid was added to the wastewater and the degradation of this compound was investigated as a component of the wastewater. Two series of experiments were carried out. First, by adding nitric acid to the wastewater, the pH of the wastewater was decreased to pH 2-3. Then, dichloroacetic acid was mixed with the wastewater so that the

concentration of dichloroacetic acid in the wastewater was adjusted at 1 mM. Finally, the mixture of wastewater and dichloroacetic acid was treated by using the photocatalytic oxidation system in the falling film reactor. The degradation rate of dichloroacetic acid under these circumstances was individually determined over the treatment time. The obtained results of this treatment were compared with those of the degradation of pure solutions of dichloroacetic acid under similar conditions and are shown in Fig. 3.25.

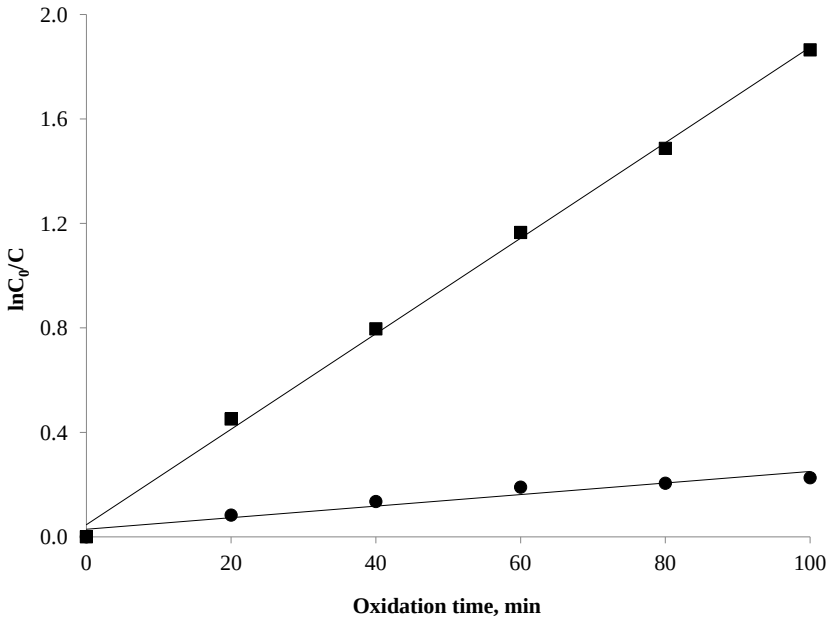

Fig. 3.25. Photocatalytic oxidation of pure dichloroacetic acid (■) and dichloroacetic acid as a component of pyrolysis wastewater (●) in the falling film reactor, solution volume = 200 mL, initial concentration of dichloroacetic acid = 1 mM, recycling rate = 100 mL.min^{-1}, T = 25° C, pH = 2-3

The second series of experiments was performed by adding dichloroacetic acid to the pyrolysis wastewater to prepare an initial concentration of 1 mM of dichloroacetic acid in the wastewater. The photocatalytic oxidation of this mixture was started at its natural pH (pH 7-8) and, after 1 h of treatment, nitric acid was added to the wastewater inside the reactor in order to decrease its pH value to about pH 2-3. Thus, the second hour of treatment was carried out at more acidic pH values. The degradation rate of dichloroacetic acid was continuously measured over the duration of treatment at different pH values and the results are shown in Fig. 3.26.

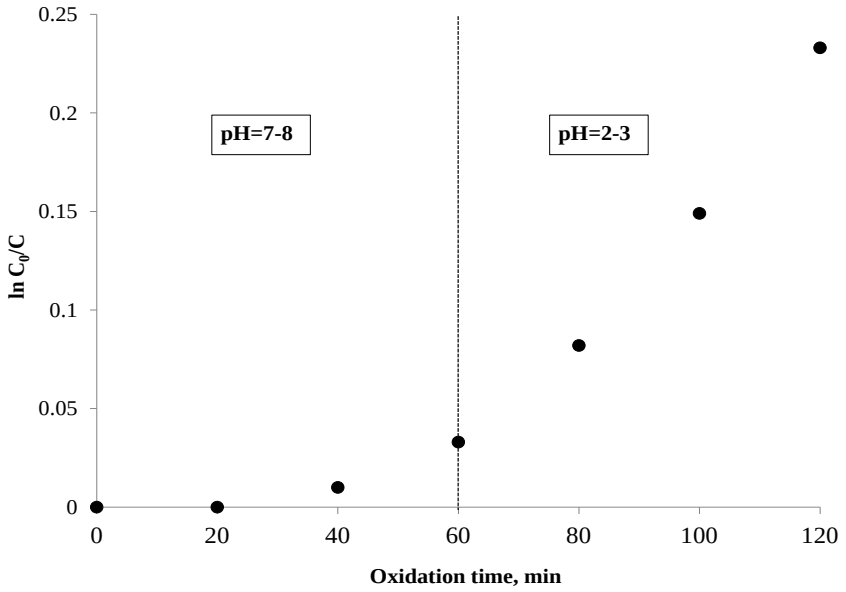

Fig. 3.26. Photocatalytic oxidation of dichloroacetic acid as a component of pyrolysis wastewater at pH = 7-8 (left side) and pH = 2-3 (right side), falling film reactor, wastewater volume = 200 mL, initial concentration of dichloroacetic acid = 1 mM, recycling rate = 100 mL.min^{-1}, T = 25° C

It is clearly shown in Fig. 3.25 that the degradation rate of dichloroacetic acid in clean water was significantly greater than that in wastewater. Likewise, according to the information presented in Fig. 3.26, the degradation rate of dichloroacetic acid as a constituent of pyrolysis wastewater was highly increased at acidic pH values, while it was very low at the natural alkaline pH of the wastewater. These observations indicate that the existence of various organic and inorganic compounds in the composition of pyrolysis wastewater, as well as the alkaline pH of the wastewater, could be responsible for decreasing the efficiency of the photocatalytic oxidation of this type of wastewater.

3.5.2. Catalytic and photocatalytic ozonation of wastewater

Although photocatalytic oxidation (TiO_2/O_2/UVA) was observed as being an unsuccessful procedure in the treatment of pyrolysis wastewater, the application of ozone as a more powerful oxidant instead of oxygen in the atmosphere of the falling film reactor combined with UVA irradiation as photocatalytic ozonation (TiO_2/O_3/UVA) and in the dark as catalytic ozonation (TiO_2/O_3) almost similarly led to considerable colour removal as well as a decrease in the COD level of the wastewater.

Fig. 3.27 shows that the COD level of pyrolysis wastewater was decreased by about 32% and 38% after 1 h of treatment using the catalytic ozonation and photocatalytic ozonation approaches, respectively. At the same time, the spectrophotometric measurements of colour extinction of wastewater, presented in the inset graph of Fig. 3.27, show that the dark colour of the wastewater was completely removed after 40 min of treatment under both oxidation conditions. The improved efficiencies of these oxidation methods for the treatment of pyrolysis wastewater were directly associated with the presence of ozone in the reaction medium and can be explained by the acceleration of ozone decomposition and the promotion of the generation of OH radicals at the alkaline pH of the wastewater.

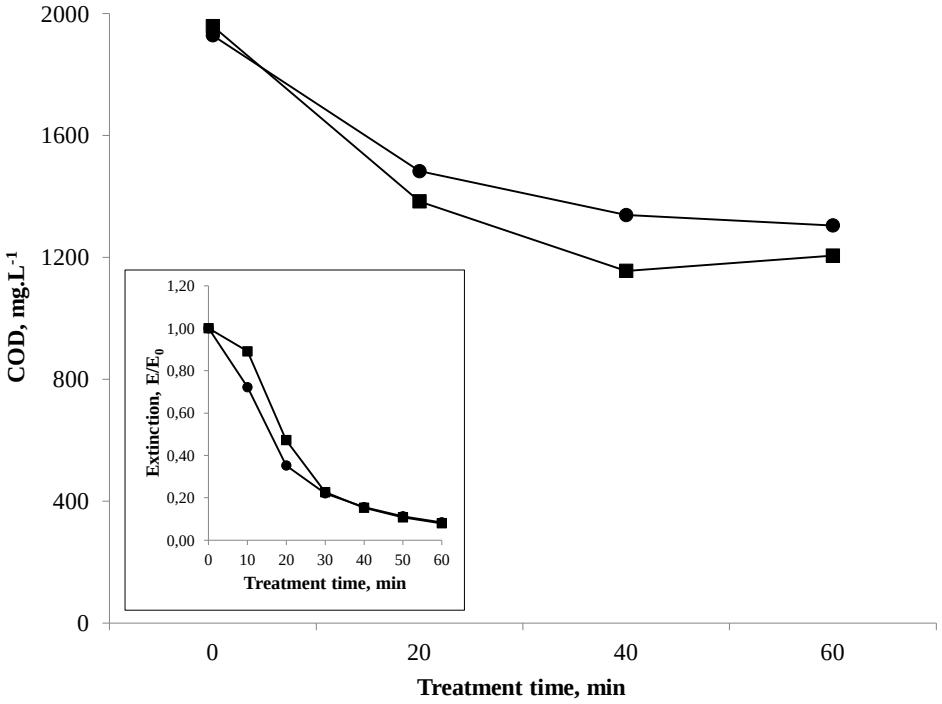

Fig. 3.27. Catalytic ozonation (●) and photocatalytic ozonation (■) of pyrolysis wastewater, falling film reactor, wastewater volume = 400 mL, recycling rate = 100 mL.min^{-1}, T = 25° C, pH = 7-8, (inset graph: colour removal over the time of treatment, λ = 340 nm)

3.5.3. The effect of acidification on the treatment of pyrolysis wastewater

As was already briefly described, the acidification of wastewater caused a remarkable increase in the degradation rate of dichloroacetic acid as a constituent of pyrolysis wastewater using the photocatalytic oxidation system. On the contrary, the positive influence of the natural alkaline

pH of pyrolysis wastewater in terms of increasing the efficiency of catalytic ozonation and photocatalytic ozonation was clearly shown in the previous section. In order to clarify the effect of acidification on the remediation conditions of pyrolysis wastewater, the treatment of this type of wastewater was performed at acidic pH conditions by means of three advanced oxidation processes in the falling film reactor; the results were compared with those under alkaline pH conditions. Nitric acid was added to the wastewater in order to decrease its pH level to pH 2.

On one hand, according to the results presented in Fig. 3.28, the acidification of pyrolysis wastewater led to an increase in the overall efficiency of colour removal by photocatalytic oxidation from about 12% to 26% after 1 h of oxidation time, while it was not effective in increasing the overall efficiency of catalytic ozonation and photocatalytic ozonation. The efficiencies of colour removal in pyrolysis wastewater by catalytic ozonation and photocatalytic ozonation were determined as being in the range of 85% to 92% under both pH conditions. However, the initial colour removal under acidic pH conditions was a bit higher than under alkaline pH conditions.

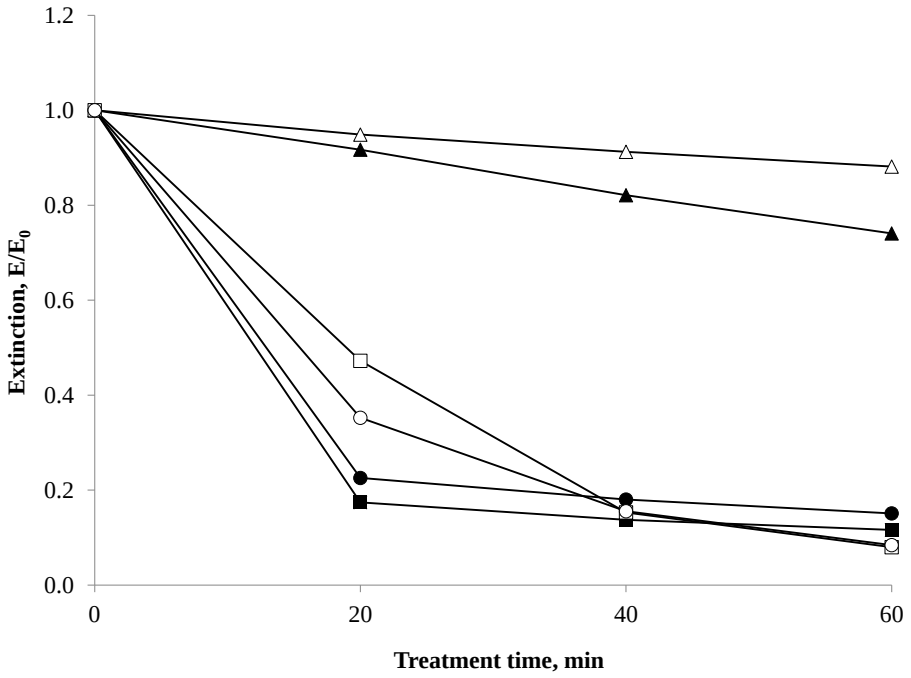

Fig. 3.28. Colour removal of pyrolysis wastewater using photocatalytic oxidation (Δ), catalytic ozonation (○) and photocatalytic ozonation (□) systems in the falling film reactor at pH = 2 (black) and pH = 8 (white), wastewater volume = 400 mL, recycling rate = 100 mL.min^{-1}, T = 25° C, λ = 340 nm

On the other hand, the treatment of pyrolysis wastewater at acidic pH levels caused no considerable change in the decrease of the COD level of the wastewater using photocatalytic oxidation and photocatalytic ozonation systems in the falling film reactor, while the acidification of wastewater led to a decrease in the efficiency of the catalytic ozonation system (Fig. 3.29).

As already explained, the higher performance of catalytic ozonation at alkaline pH values is attributed to the higher rate of ozone decomposition under these pH conditions (Fig. 3.29, middle graph).

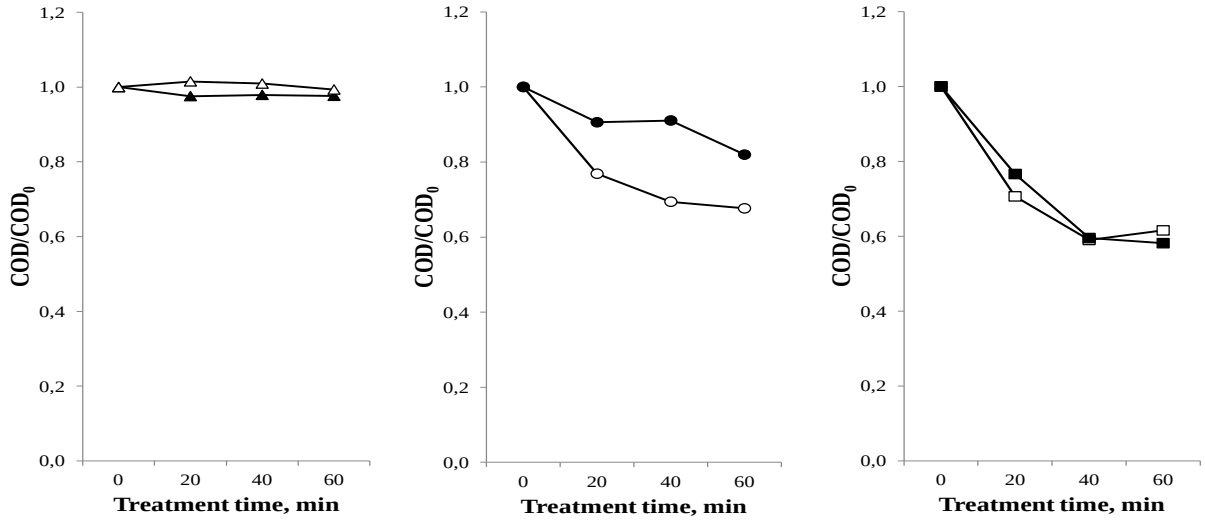

Fig. 3.29. Photocatalytic oxidation (Δ), catalytic ozonation (○) and photocatalytic ozonation (□) of pyrolysis wastewater at pH = 2 (black) and pH = 8 (white), falling film reactor, wastewater volume = 400 mL, recycling rate = 100 mL.min^{-1}, Initial COD level = 1800 ± 200 mg.L^{-1}, T = 25° C

In the case of photocatalytic ozonation of wastewater (Fig. 3.29, right graph), as was observed in the degradation of dichloroacetic acid as a component of wastewater (Fig. 3.26), it is generally supposed that the adsorption of contaminant molecules on the catalyst surface and consequently their degradation rate under acidic pH conditions are better than under alkaline conditions. On the other hand, ozone decomposition and the generation of OH radicals are reduced at low pH values which should conversely result in a decrease in the degradation rate under acidic conditions. Thus, the performance of the photocatalytic ozonation system in

decreasing the COD level of wastewater was not greatly improved at pH 2 compared with that at pH 8. Nevertheless, considering the complexity of the composition of this type of wastewater, to present a comprehensive and precise description of all the involved events is a complicated task that is beyond of the scope of the present study.

3.5.4. The effect of phosphate ions on the treatment of pyrolysis wastewater

As an elementary biological pre-treatment, mixed chemical substances which are commercially called "superphosphate" were added to the wastewater on the order of 1-2 $g.L^{-1}$ as nutritious additives for the microorganisms existing therein. This additive consisted of 34.7% phosphate and 17% sulphate anions. Therefore, all wastewater samples delivered for oxidation experiments contained lower or higher amounts of these inorganic ions.

Hordern et al. [32] have postulated that the great adsorption ability of metal oxides towards some inorganic ions such as phosphate or carbonate can cause permanent blockage of catalyst active surface sites and a decrease in their catalytic activity. In addition, Gottschalk et al. [11] have emphasised that phosphate, which is known to react slowly with hydroxyl radicals, can act as an efficient scavenger for these radicals when used in concentrations typically found in buffer solutions. These scavenging and inhibition effects were reported also by other researchers such as Liang et al. [159] and Chen et al. [160] in the photocatalytic degradation of dichlorophenol and dichloroethane, respectively.

In order to visualise and estimate the effect of superphosphate on the treatment of wastewater, photocatalytic oxidation of an indigo solution as a model compound was performed under more controlled conditions in the presence of superphosphate at two different concentrations of superphosphate in the planar reactor. The results in Fig. 3.30 show that the overall degradation efficiency of indigo by the photocatalytic oxidation system was decreased by about 20% and 60% in the presence of 0.01 $g.L^{-1}$ and 1 $g.L^{-1}$ of phosphate ions, respectively, highlighting the remarkable influence of these inorganic ions in hindering photocatalytic treatment. Therefore, the concentration of phosphate and other inorganic ions (sulphate, carbonate, chloride, etc.) could be considered as an important factor which disturbs the effective photocatalytic treatment of pyrolysis wastewater.

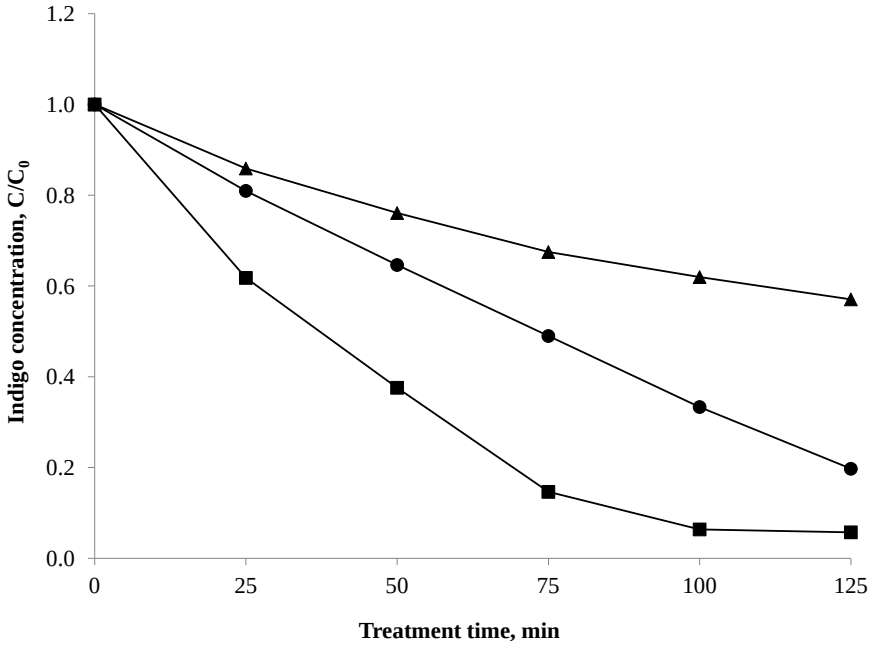

Fig. 3.30. Photocatalytic oxidation of indigo solution, 0.01 mM in the presence of 1 $g.L^{-1}$ (▲), 0.01 $g.L^{-1}$ (●) and 0 $g.L^{-1}$ (■) of superphosphate, planar reactor, solution volume = 400 mL, recycling rate = 1 $L.min^{-1}$, T = 25° C, pH =6

4. Conclusions and perspectives

The falling film reactor combines an immobilised photocatalyst as the solid phase, wastewater as the liquid phase and ozone/oxygen as the gas phase in an optimum design, providing various application possibilities for different oxidation systems. The unique design of the multi-phase falling film reactor greatly increased the ratio of active photocatalyst surface to wastewater volume. The increase in this ratio caused an improvement in the mass transfer properties inside the reactor.

The falling film reactor showed great potential and considerable benefits in the degradation of model compounds as contaminants in water as well as in the treatment of a real wastewater sample. Among the different investigated advanced oxidation methods, the highest degradation efficiencies were observed for photocatalytic ozonation systems where a combination of ozone, immobilised TiO_2 nanoparticles and UVA irradiation was employed for this aim. The photocatalytic ozonation systems were not only able to oxidise the model compounds, but they were also very effective in the mineralisation of these compounds. The photocatalytic oxidation systems were also able to sufficiently decompose some of the model compounds, but no considerable difference was observed between the performance of ozonation and catalytic ozonation systems under the setup conditions of this study. The significant effects of these advanced oxidation methods on the degradation of a wide range of organic and inorganic chemicals were mainly attributed to the formation of hydroxyl radicals. Unlike ozone, these powerful oxidising radicals attack and oxidise target molecules non-selectively. Therefore, advanced oxidation methods are especially considered as an important new approach for the decomposition of ozone-resistant compounds.

4. Conclusions and perspectives

The TiO_2 immobilisation techniques used in this study were simple but adequate; the photoactivity of immobilised photocatalysts did not decrease greatly after about 10 months of handling approximately 200 h of various oxidation processes. However, the performance of fixed TiO_2 nanoparticles on borosilicate glass tubes was better than on polymethylmethacrylate tubes.

Due to the physicochemical properties of oxalic acid, it was chosen as one of the model compounds for investigating the influence of experimental parameters on the degradation rate of pollutants in water. It was observed that any increase in the initial concentrations of oxalic acid (over the range between 0.1 mM and 10 mM) and ozone (from 0 $mg.L^{-1}$ to 135 $mg.L^{-1}$) increased the initial rate of catalytic and photocatalytic ozonation of this model compound. Similarly, the initial rate of photocatalytic oxidation was increased by increasing the initial concentration of oxalic acid.

The solution pH was an important parameter for controlling the efficiency of advanced oxidation processes on the degradation of oxalic acid in the falling film reactor. The pH level affects the charge of both the photocatalyst surface and the pollutant molecules as well as the rate of ozone decomposition in the reaction medium. The efficiency of photocatalytic oxidation and photocatalytic ozonation was decreased by increasing the solution pH. Inversely, any increase in pH caused an increase in the efficiency of catalytic ozonation.

The temperature also influences the oxidation rate of oxalic acid. The initial decomposition rate of oxalic acid by photocatalytic oxidation and catalytic ozonation was higher at high temperatures, while increased temperatures did not have a remarkable influence on the degradation rate and the efficiency of photocatalytic ozonation under the setup conditions of the falling film reactor.

Based on the results of this study and considering the high photoactivity of self-cleaning glasses, this kind of glass can be used as an active wall for the next generation of falling films. These glasses have a thin and stable layer of TiO_2 nanoparticles on their surface. Various trademarks of self-cleaning glasses are commercially available. A set of preliminary experiments were performed on one of these products called Pilkington Active^{TM} Glass (PAG) in order to investigate the ability of this material to handle the photocatalytic oxidation of contaminants in water. The results were promising. In addition to this type of immobilised photocatalyst, other commercial products of TiO_2 fixed on fibres or polymer granules are considered to be suitable alternatives for this aim.

In situ production of ozone using another advanced technique called dielectric barrier discharge (DBD) inside the falling film reactor could be considered as another source of ozone for ozone-based advanced oxidation processes.

The falling film reactor can be employed for the treatment of real wastewater samples such as agricultural wastewaters, pharmaceutical wastewaters, etc. For example, lindane is used as a pesticide worldwide. Therefore, this chemical is frequently found in agricultural wastewaters. The falling film reactor showed high performance in the removal of this compound from aqueous solutions.

To summarise, the application of advanced oxidation processes, especially photocatalytic ozonation using the falling film reactor, showed brilliant results in water treatment. Therefore, we believe that the new design of the falling film reactor introduced in this study can considerably promote the commercialisation process of advanced oxidation technologies.

5. Bibliography

1. Khan F.I. and Ghoshal A.K., "Review: Removal of volatile organic compounds from polluted air", Journal of Loss Prevention in the Process Industries, 13**,** 527-545 (2000).
2. Munoz I., Rieradevall J., Torrades F., Peral J., Domenech X., "Environmental assessment of different advanced oxidation processes applied to a bleaching Kraft mill effluent", Chemosphere, 62, 9-16 (2006).
3. Boulamanti A.K., Korologos C.A., Philippopoulos C.J., "The rate of photocatalytic oxidation of aromatic volatile organic compounds in the gas-phase", Atmospheric Environment, 42, 7844-7850 (2008).
4. Sanches S., Crespo M.T.B., Pereira V.J., "Drinking water treatment of priority pesticides using low pressure UV photolysis and advanced oxidation processes", Water Research, 44, 1809-1818 (2010).
5. Meijers R.T., Oderwald-Muller E.J., Nuhm P., Kruithof J., "Degradation of pesticides by ozonation and advanced oxidation", Ozone Science and Engineering, 17, 673-686 (1995).
6. Piera E., Caple J.C., Brillas E., Domenech X., Peral J., "2,4-Dichlorophenoxyacetic acid degradation by catalyzed ozonation: TiO_2/UVA/O_3 and Fe(II)/UVA/O_3 systems", Applied Catalysis B: Environmental, 27, 169-177 (2000).
7. Zhang L., Li P., Gong Z., Li X., "Photocatalytic degradation of polycyclic aromatic hydrocarbons on soil surfaces using TiO_2 under UV light", Journal of Hazardous Materials, 158, 478-484 (2008).
8. Ormad P., Cortes S., Puig A., Ovelleiro J.L., "Degradation of organochloride compounds by O_3 and O_3/H_2O_2", Water Research, 31, 2387-2391 (1997).

9. Saien J. and Nejati H., “Enhanced photocatalytic degradation of pollutants in petroleum refinery wastewater under mild conditions”, Journal of Hazardous Materials, 148, 491-495 (2007).
10. Glaze W.H., Kang J.W., “Advanced oxidation processes. Description of a kinetic model for the oxidation of hazardous materials in aqueous media with ozone and hydrogen peroxide in a semibatch reactor”, Industrial and Engineering Chemistry Research, 28, 1573-1580 (1989).
11. Gottschalk C., Libra J.A., Saupe A., “Ozonation of water and wastewater”, p.131, WILEY-VCH Verlag GmbH, Germany (2000).
12. Chong M.N., Jin B., Chow C.W.K., Saint C., “Recent development in photocatalytic water treatment technology: A review”, Water Research, 44, 2997-3027 (2010).
13. Almquist C.B., Sahle-Demessie E., Enriquez J., Biswas P., “The photocatalytic oxidation of low concentration MTBE on titanium dioxide from groundwater in a falling film reactor”, Environmental Progress, 22, 14-23 (2003).
14. Han F., Kambala V.S.R., Srinivasan M., Rajarathnam D., Naidu R., “Tailored titanium dioxide photocatalysts for the degradation of organic dyes in wastewater treatment: A review”, Applied Catalysis A: General, 359, 25-40 (2009).
15. Fujishima A., Rao T.N., Tryk D.A., “Titanium dioxide photocatalysis”, Journal of Photochemistry and Photobiology C: Photochemistry Reviews, 1, 1–21 (2000).
16. Hufschmidt D., Bahnemann D., Testa J.J., Emilio C.A. and Litter M.I, “Enhancement of the photocatalytic activity of various TiO_2 materials by platinisation”, Journal of Photochemistry and Photobiology A: Chemistry, 148, 223-231 (2002).
17. Bekbölet M., Lindner M., Weichgrebe D., Bahnemann D.W., “Photocatalytic detoxification with the thin-film fixed bed reactor (TFFBR): Clean-up of highly polluted landfill effluents using a novel TiO_2 photocatalyst”, Solar Energy, 56, 455-469 (1996).
18. Gorska P., Zaleska A., Kowalska E., Klimczuk T., Sobczak J.W., Skwarek E., Janusz W., Hupka J., “TiO2 photoactivity in vis and UV light: The influence of calcinations temperature and surface properties”, Applied Catalysis B: Environmental, 84, 440–447 (2008).
19. http://www.geocities.jp/ohba_lab_ob_page/structure6.html

20. Kopf P., Gilbert E., Eberle S.H., "TiO_2 photocatalytic oxidation of monochloroacetic acid and pyridine: influence of ozone", Journal of Photochemistry and Photobiology A: Chemistry, 136, 163–168 (2000).
21. Carp O., Huisman C.L., Reller A., "Photoinduced reactivity of titanium dioxide", Progress in Solid State Chemistry, 32, 33-177 (2004).
22. Lettmann C., Hildenbrand K., Kisch H., Macyk W., Maier W.F., "Visible light photodegradation of 4-chlorophenol with a coke-containing titanium dioxide photocatalyst", Applied Catalysis B: Environmental, 32, 215–227 (2001).
23. Chen M.l., Zhang F.j., Won-chun O., "Synthesis, characterization, and photocatalytic analysis of CNT/TiO_2 composites derived from MWCNTs and titanium sources", New Carbon Materials, 24, 159–166 (2009).
24. Litter M.I., "Review: Heterogeneous photocatalysis Transition metal ions in photocatalytic systems", Applied Catalysis B: Environmental, 23, 89–114 (1999).
25. Li L., Xu Z., Liu F., Shao Y., Wang J., Wan H., Zheng S., "Photocatalytic nitrate reduction over Pt–Cu/TiO2 catalysts with benzene as hole scavenger", Journal of Photochemistry and Photobiology A: Chemistry, 212, 113–121 (2010).
26. Fujishima A., Zhang X., Tryk D.A., "TiO_2 photocatalysis and related surface phenomena", Surface Science Reports, 63, 515-582 (2008).
27. Yoshida M.M., Flores W.A., Fierro K.G., Pando L.V., Morales R.S., Santiago P.S., Sanchez R.M., Yacaman M.J., "Groth and structure of TiO_2 thin films deposited inside borosilicate tubes by spray pyrolysis", Surface and Coating Technology, 200, 4111-4116 (2006).
28. Medina-Valtierra J., Reyes C.F., Ortiz J.R., Moctezuma E., Ruiz F., "Preparation of rough anatase films and the evaluation of their photocatalytic efficiencies", Applied Catalysis B: Environmental, 76, 264-274 (2007).
29. Ballari M.D.M., Brandi R., Alfano O., Cassano A., "Mass transfer limitation in photocatalytic reactors employing titanium dioxide suspensions I. Concentration profiles in the bulk", Chemical Engineering Journal, 136, 50-65 (2008).
30. Egerton T.A. and Mattinson J.A., "The influence of platinum on UV and visible photocatalysis by rutile and Degussa P25", Journal of photochemistry and photobiology A: Chemistry, 194, 283-289 (2008).

31. Langlais B., Reckhow D.A., Brink D.R., “Ozone in Water Treatment, application and engineering”, Chapter III, Lewis Publishers, Chelsea, Mich. (1991).
32. Hordern B.K., Ziolek M., Nawrocki J., “Catalytic ozonation and methods of enhancing molecular ozone reactions in water treatment”, Applied Catalysis B: Environmental, 46, 639–669 (2003).
33. Gunten U.V., “Ozonation of drinking water: Part I. Oxidation kinetics and product formation”, Water research, 37, 1443-1467 (2003).
34. Hoigne J., “Chemistry of aqueous ozone and transformation of pollutants by ozonation and advanced oxidation processes” in: J. Hubrec, editor. “The handbook of environmental chemistry, quality and treatment of drinking water”, Springer, Berlin (1998).
35. http://www.spartanwatertreatment.com/what-is-ozone.html
36. Broseus R., Vincent S., Aboulfadl K., Daneshvar A., Sauve S., Barbeau B., Prevost M., “Ozone oxidation of pharmaceuticals, endocrine disruptors and pesticides during drinking water treatment”, Water Research, 43, 4707-4717 (2009).
37. Chelme-Ayala P., Gamal El-Din M., Smith D.W., Adams C.D., “Oxidation kinetics of two pesticides in natural waters by ozonation and ozone combined with hydrogen peroxide”, Water Research, 45, 2517-2526 (2011).
38. Mehrjouei M., Müller S., Sekiguchi K., Möller D., “Decolorization of Wastewater Produced in a Pyrolysis Process by Ozone: Enhancing the Performance of Ozonation”, Ozone: Science & Engineering, 32, 5, 349-354 (2010).
39. Andreozzi R., Caprio V., Insola A., Marrota R., “Advanced oxidation processes (AOP) for water purification and recovery”, Catalysis Today, 53, 51-59 (1999).
40. Beltran F.J., Aguinaco A., Garcia-Araya J.F., Oropesa A., “Ozone and photocatalytic processes to remove the antibiotic sulfamethoxazole from water”, Water Research, 42, 3799-3808 (2008).
41. Rivas F.J., Beltran F.J., Gimeno O., Carbajo M., “Fluorene oxidation by coupling of ozone, radiation, and semiconductors: A mathematical approach to the kinetics”, Industrial and Engineering Chemistry Research, 45, 166-174 (2006).

42. Agustina T.E., Ang H.M., Vareek V.K., "A review of synergistic effect of photocatalysis and ozonation on wastewater treatment", Journal of Photochemistry and Photobiology C: Photochemistry Reviews, 6, 264-273 (2005).
43. Jing Y., Li L., Zhang Q., Lu P., Liu P., Lu X., "Photocatalytic ozonation of dimethyl phthalate with TiO_2 prepared by a hydrothermal method", Journal of Hazardous Materials, 189, 40-47 (2011).
44. Mehrjouei M., Müller S., Möller D., " Degradation of oxalic acid in a photocatalytic ozonation system by means of Pilkington Active™ glass" Journal of Photochemistry and Photobiology A: Chemistry, 217, 417–424 (2011).
45. Czili H. and Horvath A., "Photodegradation of chloroacetic acids over bare and silver-deposited TiO_2: Identification of species attacking model compounds, a mechanistic approach", Applied Catalysis B: Environmental 89, 342-348 (2009).
46. Turchi, C.S. and Ollis D.F., "Photocatalytic degradation of organic-water contaminants - Mechanisms involving hydroxyl radical attack", Journal of Catalysis, 122, 178-192 (1990).
47. Sisoev G.M., Matar O.K., Lawrence C.J., "Adsorption of gas into a wavy falling film", Chemical Engineering Science, 60, 827-838 (2005).
48. Akanksha, Pant K.K., Srivastava V.K., "Gas absorption with or without chemical reaction in a falling liquid film", Polymer-Plastic Technology and Engineering, 46, 957-964 (2007).
49. Faramarzpour M., Vossoughi M., Borghei M., "Photocatalytic degradation of furfural by titania nanoparticles in a floating-bed photoreactor", Chemical Engineering Journal, 146, 79-85 (2009).
50. Palominos R., Freer J., Mondaca M.A., Mansilla H.D., "Evidence for hole participation during the photocatalytic oxidation of the antibiotic flumequine", Journal of Photochemistry and Photobiology A: Chemistry, 193, 139-145 (2008).
51. Emeline A.V., Ryabchuk V.K., Serpone N., "Dogmas and Misconceptions in Heterogeneous Photocatalysis. Some Enlightened Reflections", Journal of Physical Chemistry: B, 109, 18515-18521 (2005).
52. Fogler H.S., "Elements of chemical reaction engineering", third ed., Prentice-Hall, Englewood Cliffs, NJ (1999).

53. Beltran F.J., Rivas F.J., Montero-de-Espinosa R., "A TiO_2/Al_2O_3 catalyst to improve the ozonation of oxalic acid in water", Applied Catalysis B: Environmental, 47, 101-109 (2004).
54. Brosillon S., Lhomme L., Vallet C., Bouzaza A., Wolbert D., "Gas phase photocatalysis and liquid phase photocatalysis: Interdependence and influence of substrate concentration and photon flow on degradation reaction kinetics", Applied Catalysis B: Environmental, 78, 232-241 (2008).
55. Tatsuma T., Tachibana S., Miwa T., Tryk D.A., Fujishima A., "Remote bleaching of methylene blue by UV-irradiated TiO_2 in the gas phase", The Journal of Physical Chemistry: B, 103, 8033-8035 (1999).
56. Zalazar C.S., Martin C.A., Cassano A.E., "Photocatalytic intrinsic reaction kinetics. II: Effects of oxygen concentration on the kinetics of the photocatalytic degradation of dichloroacetic acid", Chemical Engineering Science, 60, 4311-4322 (2005).
57. McMurray T.A., Byrne J.A., Dunlop P.S.M., Winkelman J.G.M., Eggins B.R. and McAdams E.T., "Intrinsic kinetics of photocatalytic oxidation of formic and oxalic acid on immobilized TiO_2 films", Applied Catalysis A: General, 262, 105-110 (2004).
58. Marugan J., Aguado J., Gernjak W., Malato S., "Solar photocatalytic degradation of dichloroacetic acid with silica-supported titania at pilot-plant scale" Catalysis Today, 129, 59-68 (2007).
59. Gassim F.G., Alkhateeb A.N., Hussein F.H., "Photocatalytic oxidation of benzyl alcohol using pure and sensitized anatase", Desalination, 209, 342-349 (2007).
60. John T., Yates J., "Photochemistry on TiO2: Mechanisms behind the surface chemistry", Surface Science, 603, 1605-1612 (2009).
61. Ishibashi K., Fujishima A., Watanabe T., Hashimoto K., "Quantum yields of active oxidative species formed on TiO2 photocatalyst", Journal of Photochemistry and Photobiology A: Chemistry, 134, 139-142 (2000).
62. Schneider M. and, Baiker A., "Review: Titania-based aerogels", Catalysis Today, 35, 339-365 (1997).
63. Dijkstra M.F.J., Buwalda H., de Jong A.W.F., Michorius A., Winkelman J.G.M., Beenackers A.A.C.M.," Experimental comparison of three reactor designs for photocatalytic water purification", Chemical Engineering Science, 56, 547-555 (2001).

64. Thakur R.S., Chaudhary R., Singh C., "Fundamentals and applications of the photocatalytic treatment for the removal of industrial organic pollutants and effects of operational parameters: A review", Journal of Renewable and Sustainable Energy, 2, 042701-37 (2010).
65. Chu W., Choy W.K., So T.Y., "The effect of solution pH and peroxide in the TiO_2-induced photocatalysis of chlorinated aniline", Journal of Hazardous Materials, 141, 86-91 (2007).
66. Kosmulski M., "The significance of the difference in the point of zero charge between rutile and anatase", Advances in Colloid and Interface Science 99, 255-264 (2002).
67. Nawrocki J., Hordern B.K., "Review: The efficiency and mechanisms of catalytic ozonation", Applied Catalysis B: Environmental, 99, 27-42 (2010).
68. Sanchez L., Peral J., Domenech X., "Aniline degradation by combined photocatalysis and ozonation", Applied Catalysis B: Environmental, 19, 59-65 (1998).
69. Beltran F.J., Rivas F.J., Gimeno O., Carbajo M., "Photocatalytic enhanced oxidation of fluorene in water with ozone. Comparison with other chemical oxidation methods", Industrial and Engineering Chemistry Research, 44, 3419-3425 (2005).
70. Witte B.D., Dewulf J., Demeestere K., Langenhove H.V., "Ozonation and advanced oxidation by the peroxone process of ciprofloxacin in water", Journal of Hazardous Materials, 161, 701-708 (2009).
71. Volk C., Roche P., Joret J.C., Paillard H., "Comparison of the effect of ozone, ozone-hydrogen peroxide system and catalytic ozone on the biodegradable organic matter of a fulvic acid solution", Water Research, 31, 3, 650-656 (1997).
72. Wu J., Doan H., Upreti S., "Decolorization of aqueous textile reactive dye by ozone", Chemical Engineering Journal, 142, 156-160 (2008).
73. Chu W., Chan K.H., Graham N.J.D., "Enhancement of ozone oxidation and its associated processes in the presence of surfactant: Degradation of atrazine", Chemosphere, 64, 931-936 (2006).
74. Beltran F.J., Garcia-Araya J.F., Acedo B., "Advanced oxidation of atrazine in water. I. Ozonation", Water Research, 28, 2153-2164 (1994).
75. Oguz E., Tortum A., Keskinler B., "Determination of the apparent rate constants of the degradation of humic substances by ozonation and modeling of the removal of humic

substances from the aqueous solutions with neural network", Journal of Hazardous Materials, 157, 455-463 (2008).

76. IUPAC Gold Book, web source, "http://goldbook.iupac.org/index.html".
77. Rosal R., Gonzalo M.S., Rodríguez A., Perdigón-Melón J.A., García Calvo E., "Catalytic ozonation of atrazine and linuron on MnO_x/Al_2O_3 and MnO_x/SBA-15 in a fixed bed reactor", Chemical Engineering Journal, 165 , 806-812 (2010).
78. Hordern B.K., Andrzejewski P., Dabrowska A., Czaczyk K., Nawrocki J., "MTBE, DIPE, ETBE and TAME degradation in water using perfluorinated phase as catalysts for ozonation process", Applied Catalysis B: Environmental, 51, 51-66 (2004).
79. Augugliaro V., Litter M., Palmisano L., Soria J., "Review: The combination of heterogeneous photocatalysis with chemical and physical operations: A tool for improving the photo process performance", Journal of Photochemistry and Photobiology C: Photochemistry Reviews, 7, 127-144 (2006).
80. Gracia R., Aragues J.L., Ovelleiro J.L., "Study of the catalytic ozonation of humic substances in water and their ozonation byproducts", Ozone Science and Engineering, 18, 195-208 (1996).
81. Sauleda R. and Brillas E., "Mineralization of aniline and 4-chlorophenol in acidic solution by ozonation catalyzed with Fe^{2+} and UVA light", Applied Catalysis B: Environmental, 29, 135-145 (2001).
82. Legube B., Karpel N., Leitner V., "Catalytic ozonation: a promising advanced oxidation technology for water treatment", Catalysis Today, 53, 61-72 (1999).
83. Beltran F., Rivas F.J., Montero-de-Espinosa R., "Ozone-enhanced oxidation of oxalic acid in water with cobalt catalysts. 1. Homogeneous catalytic ozonation", Industrial and Engineering Chemistry Research, 42, 3210-3217 (2003).
84. Pines D. and Reckhow D., "Effect of dissolved cobalt (II) on the ozonation of oxalic acid", Environmental Science and Technology, 36, 4046-4051 (2002).
85. Beltran F.J., Rivas F.J., Montero-de-Espinosa R., "Iron type catalysts for the ozonation of oxalic acid in water", Water Research, 39, 3553-3564 (2005).

86. Faria P.C.C., Orfao J.J.M., Pereira M.F.R., "Activated carbon and ceria catalysts applied to the catalytic ozonation of dyes and textile effluents", Applied Catalysis B: Environmental, 88, 341-350 (2009).
87. Faria P.C.C., Orfao J.J.M., Pereira M.F.R., "Activated carbon catalytic ozonation of oxamic and oxalic acids", Applied Catalysis B: Environmental, 79, 237-243 (2008).
88. Zhang T., Li C., Ma J., Tian H., Qiang Z., "Surface hydroxyl groups of synthetic α-FeOOH in promoting $OH^{\bullet}$ generation from aqueous ozone: Property and activity relationship", Applied Catalysis B: Environmental, 82, 131–137 (2008).
89. Roscoe J.M. and Abbatt J.P.D., "Diffuse reflectance FTIR study of the interaction of alumina surfaces with ozone and water vapor", Journal of Physical Chemistry A, 109, 9028-9034 (2005).
90. Cooper C. and Burch R., "An investigation of catalytic ozonation for the oxidation of halocarbons in drinking water preparation", Water Research, 33, 3695-3700 (1999).
91. Ma J. and Graham N.J.D., "Degradation of atrazine by manganese-catalyzed ozonation-influence of radical scavengers", Water Research, 34, 3822-3828 (2000).
92. Gracia R., Cortes S., Sarasa J., Ormad P., Ovelleiro J.L., "TiO_2-catalysed ozonation of raw Ebro river water", Water Research, 34, 1525-1532 (2000).
93. Beltran F.J., Rivas F.J., Montero-de-Espinosa R., "Catalytic ozonation of oxalic acid in an aqueous TiO_2 slurry reactor", Applied Catalysis B: Environmental, 39, 221-231 (2002).
94. Gilbert E., "Influence of ozone on the photocatalytic oxidation of organic compounds", Ozone Science and Engineering, 24, 75-82 (2002).
95. Addamo M., Augugliaro V., Garcia-Lopez E., Loddo V., Marci G., Palmisano L., "Oxidation of oxalate ion in aqueous suspensions of TiO_2 by photocatalysis and ozonation", Catalysis Today, 107-108, 612-618 (2005).
96. Ye M., Chen Z., Liu X., Ben Y., Shen J., "Ozone enhanced activity of aqueous titanium dioxide suspensions for photodegradation of 4-chloronitrobenzene", Journal of Hazardous Materials, 167, 1021-1027 (2009).
97. Li L., Zhu W., Chen L., Zhang P., Chen Z., "Photocatalytic ozonation of dibutyl phthalate over TiO_2 film", Journal of Photochemistry and Photobiology A: Chemistry, 175, 172-177 (2005).

98. Rajeswari R. and Kanmani S., "A study on synergistic effect of photocatalytic ozonation for carbaryl degradation", Desalination, 242, 277-285 (2009).
99. Müller T., Sun Z., Kumar M.P.G., Itoh K., Murabayashi M., "The combination of photocatalysis and ozonolysis as a new approach for cleaning 2,4-dichlorophenoxyacetic acid polluted water", Chemosphere,. 36, 2043-2055 (1998).
100. Obradovic, B.M., Kovacevic V., Kuraica M.M., and Puric J., "Electrical and Spectral Characteristics of Water Falling Film DBD in Nitrogen and Air", International Symposium on Non-Thermal/Thermal Plasma Pollution Control Technology & Sustainable Energy, ISNTP-7 June 21-25, 2010, St. John's, Newfoundland, Canada.
101. Kuraica M.M., Obradovic B.M., Manojlovic D., Ostojic D.R., and Puric J., "Ozonized water generator based on coaxial dielectric-barrier-discharge in air", Vacuum, 73, 705–708 (2004).
102. Xiao J.B., "Determination of nine components in Bayer liquors by high performance Ion Chromatography with conductivity detector", Journal of the Chilean chemical society, 51 (3), 964-967 (2006).
103. Kosanic M.M., "Photocatalytic degradation of oxalic acid over TiO_2 power", Journal of photochemistry and photobiology A: Chemistry, 119, 119-122 (1998).
104. Devipriya S. and Yesodharan S., "Photocatalytic degradation of pesticide contaminants in water", Solar Energy Materials and Solar Cells, 86 (3), 309-348 (2005).
105. Huston P.L. and Pignatello J.J., "Degradation of selected pesticide active ingredient and commercial formulations in water by the photo-assisted Fenton reaction", Water Research, 33 (5), 1238-1246 (1999).
106. Herrmann J.M., Tahiri H., Guillard C. and Pichat P., "Photocatalytic degradation of aqueous hydroxy-butandioic acid (malic acid) in contact with powdered and supported titania in water", Catalysis Today, 54, 131-141 (1999).
107. Hoigne J. and Bader H., "Rate constants of reactions of ozone with organic and inorganic compounds in water-II: Dissociating organic compounds", Water research, 17 (2), 185-194 (1983).
108. Komulainen H., "Experimental cancer studies of chlorinated by-products", Toxicology, 198, 239-248 (2004).

109. Hamidin N., Yu Q.J. and Connell D.W., “Human health risk assessment of chlorinated disinfection by-products in drinking water using a probabilistic approach”, Water research, 42, 3263-3274 (2008).

110. Kim H., Shim J., Lee S., “Formation of disinfection by-products in chlorinated swimming pool water”, Chemosphere, 46, 123-130 (2002).

111. World Health Organization, “Guidelines for drinking-water quality”, Volume 1, Recommendations, 3rd Edition, Electronic version for the Web.

112. Feitz A.J., Boyden B.H. and Waite T.D., “Evaluation of two solar pilot scale fixed-bed photocatalytic reactors”, Water research, 34, 16, 3927-3932 (2000).

113. Zalazar C.S., Labas M.D., Brandi R.J. and Cassano A.E., “Dichloroacetic acid degradation employing hydrogen peroxide”, Chemosphere, 66, 808–815 (2007).

114. Stacpoole P.W., Kurtz T.L., Han Z., Langaee T., “Role of dichloroacetate in the treatment of genetic mitochondrial diseases”, Advanced Drug Delivery Reviews, 60, 1478–1487 (2008).

115. Bonnet S., Archer S.L., Turner J.A., Haromy A., Beaulieu C., Thompson R., Lee C.T., Lopaschuk G.D., Puttagunta L., Bonnet S., Harry G., Hashimoto K., Porter C.J., Andrade M.A., Thebaud B., Michelakis E.D., “A mitochondria-K+ channel axis is suppressed in cancer and its normalization promotes apoptosis and inhibits cancer growth”, Cancer Cell, 11, 1, 37-51 (2007).

116. Ying-xue S. and Ping G., “Determination of haloacetic acids in hospital effluent after chlorination by ion chromatography”, Journal of Environmental Sciences, 19, 885–891 (2007).

117. Wang K., Guo J., Yang M., Junji H., Deng R., “ Decomposition of two haloacetic acids in water using UV radiation, ozone and advanced oxidation processes”, Journal of Hazardous Materials, 162, 1243–1248 (2009).

118. Quici N., Morgada M.E., Gettar R.T., Bolte M., Litter M.I., “Photocatalytic degradation of citric acid under different conditions: TiO_2 heterogeneous photocatalysis against homogeneous photolytic processes promoted by Fe (III) and H_2O_2”, Applied Catalysis B: Environmental, 71, 117–124 (2007).

119. Mazzarino I. and Piccinini P., “Photocatalytic oxidation of organic acids in aqueous media by a supported catalyst”, Chemical Engineering Science, 54, 3107-3111 (1999).

120. Kabra K., Chaudhary R., Sawhney R.L., “Solar photocatalytic removal of Cu (II), Ni (II), Zn (II) and Pb (II): Speciation modeling of metal–citric acid complexes”, Journal of Hazardous Materials, 155, 424–432 (2008).

121. Yang L., Xiao Y., Liu S., Li Y., Cai Q., Luo S., Zeng G., “Photocatalytic reduction of Cr(VI) on WO_3 doped long TiO_2 nanotube arrays in the presence of citric acid”, Applied Catalysis B: Environmental, 94, 142–149 (2010).

122. Pines D.S. and Reckhow D.A., “Solid phase catalytic ozonation process for the destruction of a model pollutant”, Ozone Science & Engineering, 25, 25-39 (2003).

123. Zang X.J., Tong S.P., Ma C.A., “ Kinetic and mechanism of ozonation of terephthalic acid”, Huan Jing Ke Xue, 30, 1658-1662 (2009).

124. Dionysiou D.D., Suidan M.T., Bekou E., Baudin I., Laıne J.M., “Effect of ionic strength and hydrogen peroxide on the photocatalytic degradation of 4-chlorobenzoic acid in water”, Applied Catalysis B: Environmental, 26, 153–171 (2000).

125. Magara Y., Aizawa T., Matumoto N., Souna F., “Degradation of pesticides by chlorination during water purification”, Water Science and Technology, 30, 119-128 (1994).

126. Yao C.C.D. and Haag W.R., “Rate constants for direct reactions of ozone with several drinking water contaminants”, Water Research, 25, 761-773 (1991).

127. Elovitz M.S. and Gunten U.V., “Hydroxyl radical/ozone ratios during ozonation processes. I. The R_{ct} concept”, Ozone: Science & Engineering, 21, 239-260 (1999).

128. Cui L., Shi Y., Dai G., Pan H., Chen J., Song L., Wang S., Chang H.C., Sheng H., Wang X., “Modification of N-Methyl-N-Nitrosourea initiated bladder carcinogenesis in Wistar rats by terephthalic acid”, Toxicology and Applied Pharmacology, 210, 24-31 (2006).

129. Dai G., Cui L., Song L., Gong N., Chen J., Zhao R., Wang S., Chang H.C., Wang X., “Terephthalic acid occupational exposure and its effect on organ functions in fiber workers”, Environmental Toxicology and Pharmacology, 20, 209-214 (2005).

130. Thiruvenkatachari R., Kwon T.O., Jun J.C., Balaji S., Matheswaran M., Moon I.S., “Application of several advanced oxidation processes for the destruction of terephthalic acid (TPA)”, Journal of Hazardous Materials, 142, 308-314 (2007).

131. Chandrasekara Pillai K., Kwon T.O., Moon I.S., "Degradation of wastewater from terephthalic acid manufacturing process by ozonation catalyzed with Fe^{2+}, H_2O_2 and UV light: Direct versus indirect ozonation reactions", Applied Catalysis B: Environmental, 91, 319-328 (2009).

132. ITRC, The Interstate Technology & Regulatory Council, "Overview of Groundwater Remediation Technologies for MTBE and TBA", Online version (2005).

133. Gregerson L.N., Siegel J.S., Baldridge K.K., "Ab Initio computational study of environmentally harmful gasoline additives: methyl tert-butyl ether and analogues", The Journal of Physical Chemistry, 104, 11106-11110 (2000).

134. Ahmed F.E., "Toxicology and human health effects following exposure to oxygenated or reformulated gasoline", Toxicology Letters, 123, 89–113 (2001).

135. Kane E.V. and Newton R., "Occupational exposure to gasoline and the risk of non-Hodgkin lymphoma: A review and meta-analysis of the literature", Cancer Epidemiology, 34, 516–522 (2010).

136. Mancini E.R., Steen A., Rausina G.A., Wong D.C.L., Arnold W.R., Gostomski F.E., Davies T., Hockett J.R., Stubblefield W.A., Drottar K.R., Springer T.A., Errico P., "MTBE ambient water quality criteria development: a public/private partnership", Environmental Science and Technology, 36, 125-129 (2002).

137. Acero J.L., Haderlein S.B., Schmidt T.C., Suter M.J.F., Gunten U.V., "MTBE oxidation by conventional ozonation and the combination ozone/hydrogen peroxide: efficiency of the processes and bromate formation", Environmental Science and Engineering, 35, 4252-4259 (2001).

138. Baus C., Sacher F., Brauch H.J., "Efficiency of ozonation and AOP for methyl-tert-butyl ether (MTBE) removal in waterworks", Ozone Science and Engineering, 27, 27-35 (2005).

139. Mezyk S.P., Hardison D.R., Song W., O'Shea K.E., Bartels D.M., Cooper W.J., "Advanced oxidation and reduction process chemistry of methyl tert-butyl ether (MTBE) reaction intermediates in aqueous solution: 2-Methoxy-2-methyl-propanal, 2-methoxy-2-methyl-propanol, and 2-methoxy-2-methyl-propanoic acid", Chemosphere, 77, 1352–1357 (2009).

140. Zang Y. and Farnood R., “Photocatalytic decomposition of methyl tert-butyl ether in aqueous slurry of titanium dioxide”, Applied Catalysis B: Environmental, 57, 275–282 (2005).

141. Gaffney J.S. and Marley N.A., “The impacts of combustion emissions on air quality and climate – From coal to biofuels and beyond”, Atmospheric Environment, 43, 23–36 (2009).

142. Obalı Z., Dogu T., “Activated carbon–tungstophosphoric acid catalysts for the synthesis of tert-amyl ethyl ether (TAEE)”, Chemical Engineering Journal, 138, 548-555 (2008).

143. Park S.J., Han K.J., Horstmann S., “ Liquid–liquid equilibria for binary systems of tert-amyl ethyl ether (TAEE), isopropyl tert-butyl ether (IPTBE) and di-sec-butyl ether (DSBE) with water and for ternary systems with methanol or ethanol”, Fluid Phase Equilibria, 260, 74-80 (2007).

144. Stupp H.D., Gass M., Lorenz D., “MTBE-Stoffeigenschaften und Verfahren zur Sanierung von Grundwasserschäden”, Web source.

145. Bakardjieva S., Subrt J., Stengl V., Dianez M.J., Sayagues M.J., “Photoactivity of anatase–rutile TiO_2 nanocrystalline mixtures obtained by heat treatment of homogeneously precipitated anatase”, Applied Catalysis B: Environmental, 58, 193–202 (2005).

146. Kawahara T., Konishi Y., Tada H., Tohge N., Nishii J., Ito S., “A Patterned TiO_2 (Anatase)/TiO_2 (Rutile) Bilayer-Type Photocatalyst: Effect of the Anatase/Rutile Junction on the Photocatalytic Activity”, Angewandte Chemie International Edition, 41, 15, 2811–2813 (2002).

147. Medina-Valtierra, J., Moctezuma E., Sanchez-Cardenas M., Frausto-Reyes C., “Global photonic efficiency for phenol degradation and mineralization in heterogeneous photocatalysis”, Journal of Photochemistry and Photobiology A: Chemistry, 174, 246–252 (2005).

148. Huang X. and Li N., “Structural characterization and properties of the TiO_2 film on tinplate”, Journal of Alloys and Compounds, 465, 317–323 (2008).

149. Hosseini S.N., Borghei S.M., Vossoughi M., Taghavinia N., “Immobilization of TiO_2 on perlite granules for photocatalytic degradation of phenol”, Applied Catalysis B: Environmental, 74, 53–62 (2007).

150. Marugan J., Christensen P., Egerton T., Purnama H., "Synthesis, characterization and activity of photocatalytic sol–gel TiO2 powders and electrodes", Applied Catalysis B: Environmental, 89, 273–283 (2009).

151. Kominami H., Kumamoto H., Kera Y., Ohtani B., "Immobilization of highly active titanium (IV) oxide particles; a novel strategy of preparation of transparent photocatalytic coatings", Applied Catalysis B: Environmental, 30, 329–335 (2001).

152. Rogers, J.T., "Laminar falling film flow and heat transfer characteristics on horizontal tubes", Canadian Journal of Chemical Engineering, 59, 213–222 (1981).

153. Bader H. and Hoigne J., "Determination of ozone in water by the indigo method", Water Research, 15, 449-456 (1981).

154. White H., Lesnik B., Wilson J., "Analytical Methods for Fuel Oxygenates" L.U.S.T. Line Bulletin 42. Lowell, Mass: New England Interstate Water Pollution Control Commission (2002).

155. Hernandez-Alonso M.D., Coronado J.M., Maira A.J., Soria J., Loddo V., Augugliaro V., "Ozone enhanced activity of aqueous titanium dioxide suspensions for photocatalytic oxidation of free cyanide ions", Applied Catalysis B: Environmental 39, 257-267 (2002).

156. Elovitz M.S. and Gunten U.V., "Hydroxyl radical/ozone ratios during ozonation processes: I. the R_{ct} concept", Ozone: Science & Engineering, 21, 239-260 (1999).

157. Bangun J. and Adesina A.A., "The Photodegradation kinetics of aqueous sodium oxalate solution using TiO2 catalyst", Applied Catalysis A: General, 175, 221-235 (1998).

158. Sieber, M., "Reaction engineering analysis for the pyrolysis of cellulose and plastic waste" (Reaktionstechnische Untersuchung zur Pyrolyse von Cellulose und Kunststoffabfällen). Degree dissertation (1999), info@kug-forst.de.

159. Liang H., Li X., Yang Y., Sze K., "Effects of dissolved oxygen, pH, and anions on the 2,3-dichlorophenol degradation by photocatalytic reaction with anodic TiO_2 nanotube films", Chemosphere, 73, 805–812 (2008).

160. Chen H.Y., Zahraa O., Bouchy M., "Inhibition of the adsorption and photocatalytic degradation of an organic contaminant in an aqueous suspension of $Ti0_2$ by inorganic ions", Journal of Photochemistry and Photobiology A: Chemistry, 108, 37-44 (1997).

5. Bibliography

List of figures

List of figures

List of figures

List of figures

List of tables

Acknowledgements

First of all, I would like to thank my wife for all her kindness and affection. Likewise, I would like to express my appreciation for my parents. I am grateful to Professor Dr. Detlev Möller for his gentle guidance in the development of my study. Also, my hearty thanks to him and his spouse, Madam Ursula Möller, for all their help to me and my family toward easing our life abroad.

Also, I would like to thank Professor Busch, Professor Martienssen, Professor Ay and Dr. Schöpke, who accepted refereeing the present study.

My deepest gratitude goes to Dr. Siegfried Müller, who always supported me scientifically and promoted my work. I thank him for all of his suggestions, opinions and comments toward improving the quality of my work.

I am deeply thankful to Dr. Karin Acker for her support with the analytical measurements and to Mr. Dieter Kalass and Mr. Jürgen Hofmeister for supporting my technical requirements.
Last but not least, I appreciate the friendly support of my colleagues Dr. Siegfried Gantert and Dr. Wolfgang Wieprecht for me and my work.